THE EFFECTS OF BODY SIZE ON SOFT-BODIED BURROWERS

Jessica Anne Kurth

A dissertation submitted to the faculty at the University of North Carolina at Chapel Hill in partial fulfillment of the requirements for the degree of Ph.D in the Department of Biology in the University of North Carolina at Chapel Hill.

Chapel Hill
2015

Approved by:

William Kier

Louise Roth

Joel Kingsolver

Tyson Hedrick

Kenneth Lohmann

ABSTRACT

Jessica Kurth: The effects of body size on soft-bodied burrowers
(Under the direction of William M. Kier)

Burrowing is a difficult form of locomotion due to the abrasive, heterogeneous, and dense nature of many substrates. Despite the challenges, many vertebrates and invertebrates spanning multitudes of taxa and body sizes burrow in a variety of terrestrial and aquatic substrates. Unlike terrestrial burrowers and modern digging equipment, many invertebrate burrowers lack rigid elements, and instead possess a fluid-filled hydrostatic skeleton. Soft-bodied burrowing invertebrates range in size from several hundred micrometers in length (e.g. nematodes) to several meters in length (e.g. earthworms), and burrow in environments ranging from muds to sands to soils. However, relatively little of the burrowing literature available has focused the effect of size on burrowing mechanics, and it is possible that the physical characteristics of soil may impose size-dependent constraints on burrowers. My research has found significant changes in morphology, soil stiffness, and burrowing behavior in *Lumbricus terrestris* earthworms during ontogeny. My results suggest that many aspects of the hydrostatic skeleton may change shape during growth to compensate for the ecological context of the organism. Specifically, I found that soil stiffness and resistance may become a significant challenge for soft-bodied burrowers as they increase in size, and must strain a greater volume of soil in order to form a burrow.

To my family. Sorry I drove you crazy, Mom.

ACKNOWLEDGEMENTS

I would like to thank my advisor and committee members for providing key intellectual contributions that were vital to the creation and implementation of many of the experiments performed over the course of my graduate career. I would also like to thank many of the invaluable staff at UNC who helped me to meet deadlines, properly use equipment, and perform relevant statistics. Particularly, I would like to thank Julie Lawrence, Tony Perdue, and Jack Weiss. Lastly, I would like to thank the professors from separate institutions who took time out of their schedules to help with my dissertation projects. In particular, I would like to thank Dr. Brina M. Montoya for her insights into soil properties, Karen Osborn for access to the annelid collections at the Smithsonian Institute, Dr. Christopher Rahn at Penn State for providing us with Mckibben actuators, and Dr. Daniel Goldman for his input on my projects and for access to his X-ray cinematography equipment and software. Lastly, I would like to thank my undergraduate adviser, Mike Kennish, for helping me get into grad school in the first place.

PREFACE

Burrowing can be abrasive against the body, energetically costly, and physically taxing, but many animals across species can effectively burrow in a variety of terrestrial and aquatic environments. Furthermore, many of these burrowing species lack rigid elements, instead possessing a flexible, fluid-filled hydrostatic skeleton. My research aims to understand how the soil imposes physical constraints on soft-bodied burrowers, how changes in body size alter these constraints, and how the hydrostatic skeleton has adapted to overcome these challenges.

TABLE OF CONTENTS

LIST OF TABLES

LIST OF FIGURES

LIST OF ABBREVIATIONS AND SYMBOLS

A	Area
a	Scaling Constant
b	Scaling Exponent
C	Projected coelomic area
CM	Circumferential muscle fibers
D	Diameter
d	Displacement
DA	Distance Advantage
F	Force
L	Body length
L/D	Length to diameter ratio
LM	Longitudinal muscle fibers
M	Body mass
MA	Mechanical Advantage
P_m	Pressure due to muscle contraction
V	Volume
σ_m	Muscle stress

CHAPTER 1: RESEARCH OVERVIEW

Introduction

Burrowing can be a taxing form of locomotion; soil can be compact, coarse, and resistant to deformation. Despite the challenges, many vertebrates and invertebrates spanning multitudes of taxa and body sizes burrow in a variety of terrestrial and aquatic substrates. Their burrowing actions alter the physical characteristics of their soil environment and have important ecological and economic consequences across habitats and ecosystems (Darwin, 1881; Edwards and Bohlen, 1996).

Many invertebrate burrowers lack rigid elements. Instead, these invertebrates possess hydrostatic skeletons, consisting of liquid-filled internal cavities surrounded by muscular body walls (Chapman, 1958; Kier, 2012). When the muscles in the body wall contract, the fluid pressurizes allowing for skeletal support, muscle antagonism, skeletal leverage, locomotion, and numerous other skeletal functions (Chapman, 1950, 1958; Alexander, 1995). The hydrostatic skeleton can also accommodate shape changes in the body during various muscle contractions. Earthworms, for example, possess two sets of muscles, the circumferential and longitudinal muscles. Circumferential muscle contraction elongates the worm, allowing it to move forward and excavate a new burrow; the longitudinal muscle shortens and expands the worm, allowing for anchorage, burrow consolidation, and stress relief in the soil ahead of the worm. Such shape changes allow soft-bodied burrowers to simply dilate the soil away laterally during burrowing,

avoiding the need to scrape soil out of the burrow and to bring it to the surface as many hard-bodied burrowers do.

Soft-bodied burrowing invertebrates range in size from several hundred micrometers in length (e.g. nematodes) to several meters in length (e.g. earthworms), and burrow in a variety of terrestrial and marine environments. Relatively little of the burrowing literature available has focused on the effects of body size on burrowing mechanics, however (e.g. Piearce, 1983; Quillin, 2000; Chi and Dorgan 2010). There has been concern and study on the impacts of anthropogenic changes in soil properties from chemicals and heavy machinery on subterranean organisms, yet it is not known if there are size-dependent effects on burrowers. This research may also provide useful information for the design and modification of soft robots for surface locomotion and burrowing (e.g. Trimmer, 2008; Trivedi et al., 2008; Daltorio et al., 2013).

It is possible that the physical characteristics of soil may impose size-dependent constraints on burrowers (Dorgan et al., 2008; Che and Dorgan, 2010; Kurth and Kier, 2014). For example, many soils exhibit strain hardening, in which the modulus of compression or stiffness of the soil increases with increasing strain (Chen, 1975; Yong et al., 2012; Holtz et al., 2010). As burrowers grow they must displace a greater volume of soil, which may result in an increase in the stiffness of the soil surrounding the burrow. There could be morphological adaptations burrowers employ (e.g. becoming relatively thinner) to reduce this strain hardening effect, but such adaptations are not currently known (Piearce, 1983; Kurth and Kier, 2014).

My research has found significant changes in morphology, burrowing mechanics, and soil resistance as *L. terrestris* earthworms grow (Kurth and Kier, 2014). I have also found significant morphological differences between burrowing and surface dwelling earthworm ecotypes that are likely linked to differences in ecology. My research suggests that strain

hardening poses a significant challenge for growing soft-bodied burrowers, and that burrowers compensate via size-dependent changes in musculoskeletal form and function.

The Burrowing Cycle in Soft-Bodied Invertebrates

Previous research has provided a foundational understanding of the principles of burrowing in animals with hydrostatic skeletons (Piearce 1983; Quillin, 1998; Quillin, 1999; Quillin, 2000; Che and Dorgan, 2010; Lin et al., 2011). Despite their diversity, soft-bodied burrowers such as holothurians, bivalves, annelids, and cnidarians all use a dual anchoring system to burrow (Trueman, 1975). In order to move into the soil, every soft-bodied animal first dilates the posterior of its body to anchor itself while it extends its anterior section forward to excavate the burrow. Once this occurs, the burrower then dilates the anterior portion of the body to anchor itself, and withdraws the posterior portion to draw it into the burrow. In some species, including earthworms, burrowing can also involve ingestion of soil particles to "eat" through the substrate if the substrate is sufficiently dense that displacing soil using the dual anchoring system proves ineffective (McKenzie and Dexter, 1988)

The way in which the dual anchoring system is achieved varies widely, however. Some animals, such as bivalves, use a hydraulic system in order to move their muscular foot into the soil, shunting blood from one location to another (Trueman, 1975). Others, including *Arenicola marina* and many other polychaete species, use direct peristaltic waves, which travel from the posterior of the body to the anterior (Trueman, 1975). Many oligochaetes, including earthworms, use retrograde peristaltic waves that travel the opposite direction from direct waves and require hair-like setae to brace the worm and to prevent blackslip (Gray and Lissman, 1938).

Known Adaptations to Burrowing

There are many challenges soft-bodied burrowers must overcome in order to burrow effectively. Although these challenges are shared among soft-bodied burrowers, invertebrates across many taxa have developed numerous ways to compensate. Known adaptations to burrowing in such animals include: high pressure production, a stiff body wall, the presence of septa, an eversible proboscis, and friction-reducing mucus production.

High Pressure Production

Pressurization of the hydrostatic skeleton allows for sufficient force production and turgor pressure to burrow (McKenzie and Dexter, 1988). Burrowing animals must overcome greater resistance to movement than their surface dwelling counterparts, and thus burrowers generally have more well developed musculature and higher pressure production. (McKenzie and Dexter, 1988). Both terrestrial and aquatic burrowing is challenging for soft-bodied invertebrates; high pressure production is found in both marine and terrestrial burrowers (Trueman, 1966; Seymour, 1969).

Body Wall Stiffening

Hydrostatic skeletons are flexible, and must become sufficiently stiff and rigid to displace soil effectively (Seymour, 1969). Achieving rigidity in the body wall can be achieved using both passive and active mechanisms. Passive mechanisms are inherent features of the hydrostatic skeleton, while active mechanisms require muscle contraction. A common way burrowers passively increase body wall rigidity is through an outer cuticle, extensive connective tissue reinforcement, and/or the use of septa (see below) (Elder, 1973). Conversely, burrowers may actively stiffen the body through muscle contraction. The effectiveness of passive and active stiffening mechanisms vary widely from species to species. Terrestrial earthworms, for example,

rely heavily on passive mechanisms to keep the body rigid during burrowing, while many marine polychaetes such as the lugworm *Arenicola marina* depend on active muscle contractions to achieve rigidity (Clark, 1967; Trueman, 1966). The prevalence of passive or active stiffening mechanisms is largely environment-dependent; terrestrial soft-bodied invertebrates often use passive body wall stiffening to counteract gravitational effects, while marine soft-bodied invertebrates are supported by the surrounding water column and do not require passive stiffening.

Septae

In addition to keeping the body wall rigid, the use of septa is also adaptive for burrowing for a number of other reasons. These muscular divisions between segments act as bulkheads within an animal's body, allowing for the isolation of fluid between segments. While the presence of septa does not appear to be a prerequisite for burrowing, it can assist soft-bodied burrowers by allowing different areas of the body to act independently from one another (Newell, 1950; Clark, 1967). Because fluid pressurization from muscle contraction cannot pass down the body while the septa are contracted, muscular contraction in one part of the body does not pressurize or contract segments further down the body (Clark, 1967). Such abilities can be useful while burrowing; if some segments become impeded underground, other segments can continue functioning normally. In addition, damage to several segments will not debilitate the entire animal. In fact, septa allow earthworms to perform autotomy (tail loss when threatened) without excessive fluid leakage (Maginnis, 2006).

Robust Dilator Muscles

The muscles responsible for radial expansion of the body are so powerful in burrowers that they can be used to distinguish surface-dwelling and burrowing earthworm ecotypes

(Bouché, 1977). This is because a majority of soil displacement occurs during radial expansion and dilation of the body (Barnett et al., 2009). By shortening and thereby expanding their bodies and forcing soil aside, burrowers effectively enlarge the sides of the burrow to a sufficient diameter to allow the remainder of the body to enter. Radial expansion of the animal also tends to break up soil particles ahead of the animal, making forward progression into the soil easier (Seymour, 1969; Keudel and Schrader, 1999). It may also open new voids in the soil for the earthworm to enter and progress forward (Barnett et al., 2009). Another important function of radial dilation is anchorage. Radial expansion also allows burrowers to secure themselves in the soil and prevent backslip during burrow excavation (Trueman, 1975).

Mucus

Friction can severely impede locomotion in soil (Dorgan et al., 2013). Soil particles can attach to burrowing organisms, forcing the animal to drag soil along with it as it moves (personal observation). In order to lubricate the body and reduce friction with the soil, some burrowers have mucus producing cells (Edwards and Bohlen, 1996; Gibson et al., 2006). In addition to reducing friction, production of mucus can also serve as a kind of adhesive that binds soil particles together to form the burrow's walls (Gibson et al., 2006).

Proposed Size-Dependent Adaptations to Burrowing

While the aforementioned adaptations are of great importance in burrowing for soft invertebrates, the list is likely not exhaustive. Below, I propose several additional burrowing adaptations in animals possessing hydrostatic skeletons. These adaptations consider the possibility that burrowing mechanics and interactions with the soil will differ depending on the body size of the organism. Hypotheses testing and further discussion can be found in Chapters 2-5.

Small Diameter

Thin bodies may be a key adaptation in a soft-bodied burrower to mitigate strain hardening in soils as the animal becomes larger. Strain hardening occurs when the modulus of compression or stiffness of the soil increases with increasing strain, which occurs in granular soils and consolidated clays (Chen, 1975; Holtz et al., 2010; Yong et al., 2012). As an earthworm grows in cross-section, it must displace more soil radially, which may result in an increase in the stiffness of the soil surrounding the burrow. Thus, strain hardening may be negligible in small burrowers but could pose significant challenges in large burrowers. By growing disproportionately thin, the animal's cross-sectional area is reduced. In turn, less soil must be radially displaced and strain hardening would be reduced compared with an animal that maintains its proportions.

Allometric Force Production

If soil indeed becomes disproportionately resistant for larger burrowers due to strain hardening, then I predict the ontogenetic development of muscle area and force production to also grow disproportionately to match the soil resistance. Prior research has noted the importance of robust dilator muscles to displace soil for burrow formation, break up soil particles ahead of the burrower, and anchor burrowers to prevent backslip (Chapman, 1950; Bouché, 1977; Keudel and Schrader, 1999). I thus expect dilator muscle force to increase rapidly with body size to overcome strain hardening.

Robust Anterior Segments

Bouché 1977 noted that the anterior musculature of burrowing earthworms is well developed, but it is not clear how muscular development and force production varies along the length of a burrower's body. The retrograde peristaltic waves of contraction that travel down the

body of the earthworm often dissipate about halfway down the length of the worm (Yapp, 1956). In burrowing, I have observed that approximately the first 30 segments appear to be involved in the formation of the burrow in the earthworm *Lumbricus terrestris*; contraction of the remaining segments appear to draw the body into the burrow and consolidate the burrow's walls. Thus I believe that earthworms would need the anterior portion of their body to be more powerful relative to the rest of their body in order to exert sufficient force to create a new burrow. I predict that the muscle cross-sectional area and forces in the anterior segments will be large relative to the middle and posterior segments.

Study System

L. terrestris is an ideal species for scaling and burrowing research as it is a deep terrestrial burrower that grows 3 orders of magnitude in mass during development (Fig. 1.1) (Quillin, 1998). The adults of this species can excavate permanent vertical burrows as deep as 1-2 meters below the soil surface, while the hatchlings and juveniles are generally found in the first few centimeters of soil (Arthur, 1965; Gerard, 1967; Piearce, 1986). This species is also commercially available, can be bred in the lab, and is of environmental and commercial interest in soil amelioration (Butt et al., 1992).

Earthworms have a segmented hydrostatic skeleton (Clark, 1967). In *L. terrestris*, the number of segments remains constant during development (Quillin, 1998). Each segment contains coelomic fluid that is largely isolated from the fluid of adjacent segments by muscular septa, allowing segments to act as essentially independent hydraulic units (Seymour, 1969). Two orientations of muscle fibers are present, the circumferential and longitudinal muscles. The circumferential fibers act to thin the worm and elongate it, while the longitudinal muscles shorten the worm and cause radial expansion. Earthworms crawl and burrow using alternating

waves of circumferential muscle and longitudinal muscle contraction typically involving approximately 30 segments that pass from anterior to posterior down the length of the body

Figure 1.1: **Comparison of adult and hatchling *L. terrestris* earthworm.** The adult is approximately 8g in mass, and the hatchling is approximately 0.3g in mass.

(Gray and Lissman, 1938; Sims and Gerard, 1995). During burrowing, circumferential muscle contraction allows earthworms to excavate a new burrow. Contraction of the longitudinal muscles displaces soil laterally, enlarges the burrow, anchors the worm, and pulls the posterior segments into the burrow (Gray and Lissman, 1938; Trueman, 1975, Quillin, 2000). There are typically 1 to 2 simultaneous waves of circumferential and longitudinal muscle contraction along the length of the worm during locomotion (Gray and Lissman, 1938; Quillin, 1999).

1.6 Thesis Overview

The overall goal of my work is to understand soil/animal interactions in soft-bodied invertebrates, how changes in body size might alter these interactions, and how the hydrostatic skeleton has adapted to burrowing locomotion. Past work was limited by the ability to visualize subterranean animals in natural soil, an inability to differentiate tissue types in the smallest burrowers, and limited knowledge of terrestrial soil behavior during burrowing (e.g. Quillin, 1998, Quillin, 2000; Dorgan et al., 2005). I used alternative methods such as glycol methacrylate histology, x-ray cinematography, and robotics in order to explore these topics and move the field forward. Below, I briefly outline the content and relevance of the chapters that follow.

Chapter 2: I measured the ontogenetic scaling of the hydrostatic skeleton of *Lumbricus terrestris* using glycol methacrylate histology to predict changes in skeletal function with size. I then related the scaling of the skeleton to size-related changes in burrowing mechanics and soil interactions. This allowed me to form testable predictions concerning the effects of body size on burrowing mechanics and kinematics.

Chapter 3: I compared the ontogenetic and interspecific scaling of burrowing and surface-dwelling lumbricid earthworms to determine if the allometric scaling relationships found in *L. terrestris* earthworms are adaptations to burrowing constraints. I predicted that surface-dwelling earthworms would scale differently from burrowing earthworms due to constraints imposed by the soil.

Chapter 4: To explore if soil stiffness varies with burrower size, I measured the scaling of burrowing kinematics using x-ray cinematography and characterized the mechanical properties of topsoil using a size range of inflatable worm robots. I then related the scaling of burrowing kinematics to changes in soil resistance and stiffness with burrower size.

Chapter 5: If soil properties indeed change with burrower size, burrowers likely alter their burrowing behavior as they grow. To determine the effects of body size on burrowing mechanics, I measured the scaling of pressure generation in the hydrostatic skeleton during burrowing locomotion. I then empirically tested for size-related differences in burrowing pressures and forces.

Implications and Significance

Burrowers are found in nearly every environment on earth. Their actions aid in soil de-compaction, nutrient recycling, and air and water infiltration. Ultimately, these ecosystem engineers improve soil quality for agriculture and ecosystems alike (Darwin, 1881).

Soft-bodied burrowers displace the soil laterally during burrowing, avoiding the need to remove soil from the burrow and bring it to the surface as in many hard-bodied burrowers (e.g. crabs, moles, ants). No burrowing robots interact with soil in this manner, though crawling soft-bodied robots exist (e.g. Trimmer, 2008; Trivedi et al., 2008). I hope that my research provides new insights into the application of worm-like robots for burrowing. Such a machine may prove useful for irrigation, soil amelioration, and tunnel construction, since earthworms are capable of making numerous deep, complex, and unobstructed burrows.

There is also concern and study on the impacts of anthropogenic changes in soil properties from chemicals and heavy machinery on subterranean organisms (e.g. Ehlers, 1975; Roberts and Dorough, 1985; Chan and Barchia, 2007), yet it is not known if there are size-dependent effects on burrowers. Machinery could detrimentally affect certain life history stages more than others, but I am aware of relatively little research on this issue (Gerard, 1967).

My research also examines a constraint on burrowing in terrestrial soils, strain hardening, that has not been investigated previously, as well as adaptations of the hydrostatic skeleton to

overcome it. I then demonstrate how this effect impacts the scaling of terrestrial burrowing kinematics and mechanics. The resulting scale effects are vastly different from other forms of locomotion, and show interesting reversals and exceptions that are likely unique to burrowing.

I believe that my research provides interesting insights for academic study, conservation, and practical applications. Burrowing locomotion is relatively understudied compared with other forms of animal locomotion, yet burrowers are extremely important in maintaining soil quality across species and across body sizes.

CHAPTER 2: SCALING OF THE HYDROSTATIC SKELETON IN THE EARTHWORM, *LUMBRICUS TERRESTRIS*[1]

Summary

The structural and functional consequences of changes in size or scale have been well studied in animals with rigid skeletons, but relatively little is known about scale effects in animals with hydrostatic skeletons. I used glycol methacrylate histology and microscopy to examine the scaling of mechanically important morphological features of the earthworm *Lumbricus terrestris* Linnaeus, 1758 over an ontogenetic size range from 0.03-12.89 g. I found that *L. terrestris* becomes disproportionately longer and thinner as it grows. This increase in the length to diameter ratio with size means that, when normalized for mass, adult worms gain approximately 117% mechanical advantage during radial expansion, compared with hatchling worms. I also found that the cross-sectional area of the longitudinal musculature scales as body mass to the ~0.6 power across segments, which is significantly lower than the 0.66 power predicted by isometry. The cross-sectional area of the circumferential musculature, however, scales as body mass to the ~0.8 power across segments, which is significantly higher than predicted by isometry. By modeling the interaction of muscle cross-sectional area and mechanical advantage, I calculate that the force output generated during both circumferential and longitudinal muscle contraction scales near isometry. I hypothesize that the allometric scaling of earthworms may reflect changes in soil properties and burrowing mechanics with size.

[1] This chapter previously appeared as an article in the *Journal of Experimental Biology*. The original citation is as follows: **Kurth, J. A. and Kier, W. M.** (2014). Scaling of the hydrostatic skeleton in the earthworm *Lumbricus terrestris*. *J. Exp. Biol.* **217**, 1860-1867.

Introduction

Body size plays a pivotal role in the structure and function of all organisms. Size affects how an organism interacts with its environment as well as the processes needed for survival (Vogel, 1988). Size also imposes physical constraints on organisms, with fundamental effects on organismal design (Schmidt-Nielson, 1997). A range of important traits change as a function of body size, including: geometry, metabolic rate, kinematics, mechanics, and even lifespan. As a consequence, almost every facet of an organism's life may be influenced by its size, including its physiology, morphology, ecology, and biomechanics (Schmidt-Nielson, 1984; Quillin, 1999; Vogel, 2013; Biewener, 2005; Hill et al., 2012). Scaling, the changes in form and function due body size, has been studied primarily in the vertebrates and in some arthropods (e.g. Schmidt-Nielson, 1997; Biewener, 2005; Nudds, 2007; Chi and Roth, 2010). The effects of scaling on soft-bodied animals have, however, received relatively little attention. The aim of this study was to use histological and microscopic techniques to examine the effects of size and scale on components of the hydrostatic skeleton of an iconic soft-bodied animal, the earthworm.

Many soft-bodied organisms or parts of organisms (e.g. terrestrial and marine worms, cnidarians, echinoderms, bivalves, gastropods, nematodes) possess a hydrostatic skeleton. Hydrostatic skeletons are characterized by a liquid-filled internal cavity surrounded by a muscular body wall (Kier, 2012). Because liquids resist changes in volume, muscular contraction does not significantly compress the fluid and the resulting increase in internal pressure allows for support, muscular antagonism, mechanical amplification, and force transmission (Chapman, 1950, 1958; Alexander, 1995; Kier, 2012).

Animals supported by hydrostatic skeletons range in size from a few millimeters (e.g. nematodes) to several meters in length (e.g. earthworms), yet little is known about scale effects

on their form and function. Indeed, many individual cephalopods, which rely on a type of hydrostatic skeleton termed a muscular hydrostat, may grow through this entire size range and larger. In addition, many of these animals burrow, and the scaling of burrowing mechanics is also poorly understood compared with other forms of locomotion. We also know little about the effects of the physical properties of the soil on burrowing organisms, or how changes in body size impact soil-animal interactions. Further, this work is of interest because these animals are taxonomically diverse, they live in many environments, and are ecologically and economically important in bioturbation, ecosystem engineering, and soil maintenance. Human-induced changes in soil properties from chemicals and heavy machinery could impose size-dependent effects on burrowers that can only be predicted by understanding the scaling of the morphology and mechanics of burrowers. Finally, this research may provide insights useful for the design of biomimetic soft robots for surface locomotion and for burrowing (e.g. Trimmer, 2008; Trivedi et al., 2008; Daltorio et al., 2013).

Previous research on scaling in soft-bodied animals has provided a foundation for our understanding of the scaling of hydrostatic skeletons (Piearce 1983; Quillin, 1998; Quillin, 1999; Quillin, 2000; Che and Dorgan, 2010; Lin et al., 2011). A number of important issues remain unexplored, however. Prior studies did not sample the smallest specimens in the size range, and were unable to measure several mechanically relevant aspects of the morphology (e.g. circumferential muscle cross-sectional area) (Quillin, 1998; Quillin, 2000). The results of several previous studies were also contradictory. Some experiments indicate that the hydrostatic skeleton maintains geometric and kinematic similarity with change in body size (e.g. Quillin, 1998; Quillin, 1999), while others suggest disproportionate scaling in both shape and force production (e.g. Piearce, 1983; Quillin, 2000). In addition, many hypotheses on the scaling of the hydrostatic

skeleton have not yet been tested, including possible size dependent changes in muscle stress, muscle cross-sectional area, skeletal leverage, burrowing kinematics, respiration, and soil properties (Pearce, 1983; Quillin, 2000).

In this study, I investigated the scaling of functionally relevant aspects of hydrostatic skeleton morphology, using an ontogenetic size range of the earthworm *Lumbricus terrestris*. The results provide new insights into the effects of scale on hydrostatic skeletons and allow me to make testable predictions about the implications of body size for distance and mechanical advantage, force output, and internal pressure production.

The Hydrostatic Skeleton of *Lumbricus terrestris*

Earthworms have a segmented hydrostatic skeleton. In *L. terrestris*, the number of segments remains constant during development (Piearce, 1983; Quillin, 1998). Each segment contains coelomic fluid that is largely isolated from the fluid of adjacent segments by muscular septa, allowing segments to act as essentially independent hydraulic units (Seymour, 1969). Two orientations of muscle fibers, circumferential and longitudinal, are present. The circumferential fibers act to radially thin the worm and elongate it, while the longitudinal muscles shorten the worm and cause radial expansion. Earthworms crawl and burrow using alternating waves of circumferential muscle and longitudinal muscle contraction that pass from anterior to posterior down the length of the body and typically involve approximately 30 segments (Gray and Lissman, 1938; Sims and Gerard, 1985). When the circumferential muscles contract, the segments thin and are thrust forward, excavating a new burrow in the soil. Contraction of the longitudinal muscles expands the segments radially, enlarging the burrow, anchoring the worm, and pulling the more posterior segments forward. There are typically 1 to 2 simultaneous waves

of circumferential and longitudinal muscle contraction along the length of the worm during locomotion (Gray and Lissman, 1938; Quillin, 1999).

Scaling of Functionally Relevant Morphological Features

Rather than maintaining similar relative proportions with change in body size, termed isometric growth, many animals show allometric growth, in which the relative proportions change with body size (Huxley and Tessier, 1936; Schmidt-Nielsen, 1997). Allometry is common in animals with rigid skeletons, which must increase disproportionately in relative cross-section to avoid buckling due to increase in mass. Hydrostatic skeletons lack rigid elements loaded in compression and have been hypothesized to scale isometrically (Quillin, 1998). Thus my null hypothesis is isometric scaling, which can be tested as follows. Since the density of an animal does not change significantly with size, the mass (M) is proportional to the volume (V). If an earthworm scales isometrically, linear dimensions such as length (L) or diameter (D) are predicted to scale to the animal's $V^{1/3}$ and thus $M^{1/3}$ and any area, such as surface area or muscle cross-sectional area, will scale as $V^{2/3}$ and thus $M^{2/3}$ (see Table 2.1 below for terms).

Alternatively, I hypothesize that the hydrostatic skeleton may scale allometrically in response to selective pressures and constraints on the animal as it grows. Such factors are potentially diverse and include, for example, burrowing mechanics, internal hydrostatic pressure, respiration, heat exchange, evaporation, predation, competition, or fecundity.

Symbol	Variable	Isometric Scaling Exponent (b_o)
V	Volume	αM
M	Body mass	αV
L	Body length	$\alpha M^{1/3}$
D	Diameter	$\alpha M^{1/3}$
A	Cross-sectional muscle area	$\alpha M^{2/3}$
C	Projected coelomic area	$\alpha M^{2/3}$
P_m	Pressure due to muscle contraction	αM^{0}
σ_m	Muscle stress	αM^{0}
F	Force output to environment	$\alpha M^{2/3}$

Table 2.1: Definition of variables used and their isometric scaling exponents.

Scaling of Linear Dimensions

The scaling of the linear dimensions and muscle cross-sectional areas have important implications for the mechanics of the organism, including its kinematics, force production, mechanical advantage, and internal coelomic pressure. For hydrostatic skeletons, a change in the length-to-diameter (L/D) ratio affects the leverage provided by the skeletal support system. This can be understood by first referring to animals with rigid skeletons in which levers may amplify force (force output > force input from muscle contraction and thus positive mechanical advantage) or amplify distance (distance output > distance input from muscle contraction and thus positive distance advantage) (Kier and Smith, 1985; Vogel, 1988). Mechanical advantage and distance advantage are reciprocal. Although cylindrical hydrostatic skeletons lack rigid levers, they still allow mechanical advantage or distance advantage, depending on the orientation

of the musculature in question and the length/diameter (*L/D*) ratio of the body (Kier and Smith, 1985). For instance, if two cylindrical bodies have identical volume, but one is more elongate and thus has a larger *L/D* ratio, the body with the larger *L/D* ratio will show greater distance advantage during elongation (due to shortening by circumferential muscle) and greater mechanical advantage during lateral expansion (due to shortening by the longitudinal muscle), compared with a hydrostatic skeleton with a smaller *L/D* ratio (Fig. 2.1) (Vogel, 2013)\

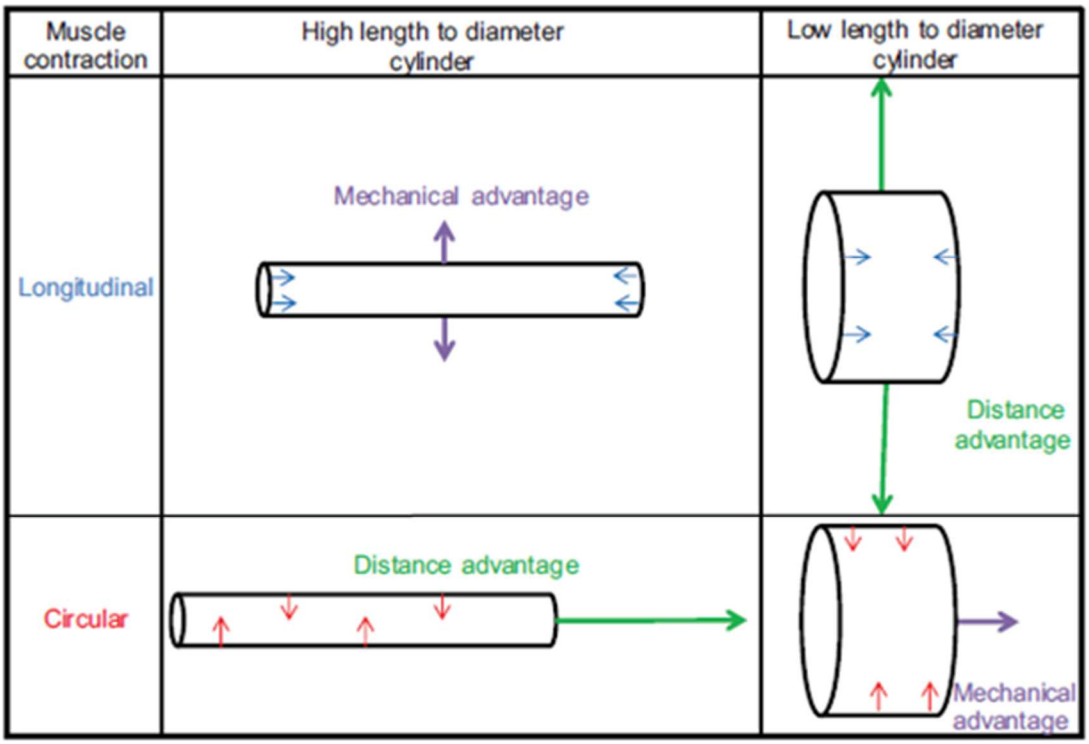

Fig. 2.1. Schematic comparing skeletal leverage between a high length to diameter cylinder and a low length to diameter cylinder.

If *L. terrestris* scales isometrically, the *L/D* ratio will not change with size because both *L* and *D* are linear dimensions and should scale as $M^{1/3}$. Allometry in the overall dimensions of *L. terrestris*, however, could affect the relative force and displacement of the musculature during growth. For instance, an increase in the *L/D* ratio during growth would mean that for a given relative shortening of the circumferential muscle fibers, the elongation of a large worm would be

relatively greater (an increase in distance advantage for the circumferential muscle). From the standpoint of the longitudinal muscles, an increase in the *L/D* ratio would result in an increase in mechanical advantage of this musculature in radial expansion of the worm. Since mechanical advantage and distance advantage are reciprocal, an increase in the *L/D* ratio would decrease the mechanical advantage of the circumferential musculature and decrease the distance advantage of the longitudinal musculature.

Scaling of Muscle Cross-Sectional Areas and Force Output

The scaling of muscle physiological cross-sectional area (*A*) determines how relative force production by the musculature changes with size, because force due to muscle contraction is proportional to cross-sectional area. If the circumferential and the longitudinal musculature scale isometrically, the cross-sectional area of each will be proportional to $M^{2/3}$. The final force output the animal exerts, however, depends not only on the force producing muscles, but also the force transmitting skeleton.

The force transmitted by the skeleton to the environment is a product both of the force generated by the muscles and the mechanical advantage produced by the skeleton itself:

$$F \alpha A(MA) \quad (1)$$

Where *F* is the force output to the environment, *A* is the muscle cross-sectional area, and *MA* is the mechanical advantage from the skeleton. As stated above, mechanical advantage in hydrostatic skeletons will remain constant unless the *L/D* ratio of the animal changes. If *L. terrestris* grows isometrically and thereby maintains a constant *L/D* ratio, the mechanical advantage of the two muscle groups will not change and thus the final force output would also scale as $M^{2/3}$.

Scaling of Coelomic Pressure

The internal pressure due to muscle contraction is a function of the stress in the muscles, the cross-sectional areas of the muscles, and the projected coelomic area over which the muscles act (equation 3 from Quillin, 1998):

$$P_m = (\sigma_m A) C^{-1} \quad (2)$$

Where P_m is the pressure in the coelomic fluid due to muscle contraction, σ_m is the muscle stress, A is the cross-sectional area if the muscle, and C is the area of the coelom. If *L. terrestris* grows isometrically and the peak isometric stress in the muscle (σ_m) remains constant with body size, the internal coelomic pressure from muscle contraction (P_m) will be constant since the ratio of the cross-sectional area of the muscle (A) and the coelomic area (C) would be unchanged. If the worm scales allometrically in either muscle area (A) or coelomic area (C), then pressure will change with body size.

Materials and Methods

L. terrestris Collection and Maintenance

Juvenile (1-3g) worms were supplied by Knutson's Live Bait (Brooklyn, MI USA) as well as raised from hatchlings bred in a colony maintained in the laboratory. Adult worms (3-10g) were purchased locally, raised from purchased juveniles, and raised from colony hatchlings. Hatchlings were raised from cocoons deposited by adults bred in the laboratory colony. All worms were housed in plastic bins filled with moist topsoil (composed of organic humus and peat moss) at 17ºC (Berry and Jordan, 2001) and fed dried infant oatmeal (Burch et al., 1999).

Anesthetization, Length Measurements, and Dissection

Each worm was anesthetized in a 10% ethanol solution in distilled water (v/v) until quiescent, patted dry, and weighed. The length was obtained after pulling the worm by the anterior end along the bench surface in order to straighten the body and extend the segments to a consistent resting length. Because *L. terrestris* does not add segments with growth, I measured the length of the entire body (Piearce, 1983; Quillin, 1998). The worm was then sacrificed and three blocks of tissue containing 20 segments each were removed (segments 1-20, 21-40, and 41-60, numbering from anterior). I examined these three areas to document potential variation along the length of the worm, although particular attention was paid to segments in the anterior half of the worm since it is of greatest importance in locomotion (the posterior half of the worm is often passively dragged along) (Yapp, 1956).

The tissue blocks were fixed in 10% formalin in distilled water (v/v) for 24-48 hours. After fixation, the blocks were further dissected for embedding (segments 9-14, 29-34, and 49-54). I refer to segments 9-14 as "anterior", segments 29-34 as "middle", and segments 49-54 as "posterior". The anterior, middle, and posterior segments were then cut in half transversely so that both transverse and sagittal sections could be obtained from each location (Fig. 2.2).

Histology and Morphometrics

The tissue blocks were partially dehydrated in 95% ethanol and embedded in glycol methacrylate plastic (Technovit 7100, Heraeus Kulzer GmbH, Wehrheim, Germany) to minimize tissue distortion. Sections of 3-7 μm thickness were cut with a glass knife. I used a Picrosirius/Fast Green stain in order to differentiate muscle from connective tissue (López-DeLeón and Rojkind, 1985). I adapted the protocol to glycol methacrylate by staining at 60 °C

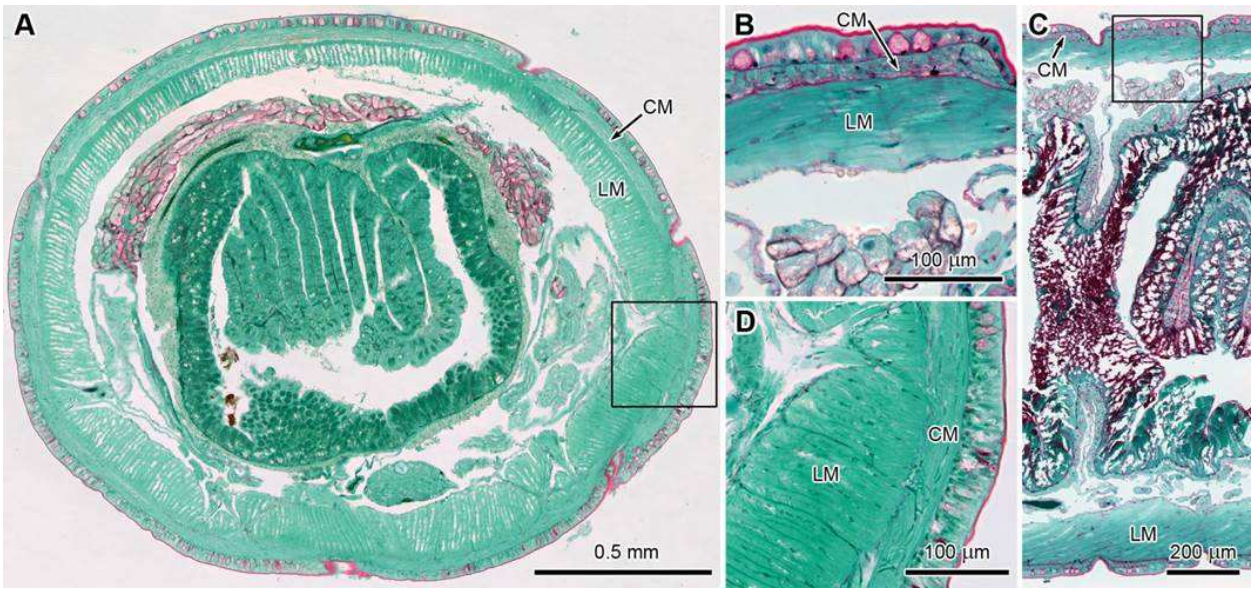

Fig. 2.2: Photomicrographs (bright field microscopy) of 7-µm-thick sections of *Lumbricus terrestris* stained with Picrosirius/Fast Green. **A.** Transverse section through the anterior segments. **B**. Inset of sagittal section shows higher magnification view of cross-section of the circumferential musculature. **C**. Parasagittal section through the anterior segments. **D**. Inset of transverse section shows higher magnification view of cross-section of the longitudinal musculature. L M, longitudinal muscle; C M, circumferential muscle.

for 1-2 hours followed by a distilled water rinse, drying, and mounting of coverslips. I used Sigma Scan (Systat Software, Inc., San Jose, CA, USA) to make morphological measurements on micrographs. Longitudinal muscle cross-sectional area (A_l), projected area of application in the coelom during longitudinal muscle contraction (C_l), and diameter (D) were measured using transverse sections. Circumferential muscle cross-sectional area (A_c) and projected area of application in the coelom during circumferential muscle contraction (C_c) were measured using sagittal sections. The earthworms prepared in this way were flattened slightly and thus had elliptical cross-sections. To determine an equivalent diameter of a circular cylinder, I used measurements of the major and minor axes to calculate the area of the ellipse and then calculated the diameter of a circle of the same area.

I estimated the scaling of internal pressure produced by muscle contraction using Equation 2 and measurements of coelomic area from transverse and sagittal sections, with the assumption of no change with size in the peak isometric stress of the muscle σ_m. Pressure from longitudinal muscle contraction was calculated using longitudinal muscle cross-sectional area (A_l) and projected coelomic area during longitudinal muscle contraction (C_l), while pressure from circumferential muscle contraction was calculated using circumferential muscle cross-sectional area (A_c) and projected coelomic area during circumferential muscle contraction (C_c) (Quillin, 1998):

$$P_{m\ (longitudinal)} = (\sigma_m A_l) C_l^{-1} \qquad P_{m\ (circumferential)} = (\sigma_m A_c) C_c^{-1} \tag{3}$$

Calculation of Mechanical Advantage and Force Output

As I describe above, the *L/D* ratio was observed to change as a function of size and thus the mechanical advantage of the musculature changes during growth. Since the mechanical advantage is the reciprocal of the distance advantage, I calculated the mechanical advantage (*MA*) of the circumferential musculature as the absolute value of the decrease in body diameter (*D*) during circumferential muscle contraction divided by the resulting increase in body length (*L*), as a function of the *L/D* ratio, for the 25% decrease body in diameter that is typical of *L. terrestris* during movement (Quillin, 1999). Likewise, the mechanical advantage of the longitudinal muscle was calculated as the absolute value of the decrease body length of the worm divided by the resulting increase in body diameter, as a function of the *L/D* ratio:

$$MA_{(\text{circumferential})} = \frac{|\Delta D|}{|\Delta L|} \quad MA_{(\text{longitudinal})} = \frac{|\Delta L|}{|\Delta D|} \tag{4}$$

These calculations thus provided estimates of the mechanical advantage of both the longitudinal and circumferential musculature as a function of size**.**

Statistical Analysis

I used the *lmodel2* package (Legendre, 2011) in R (R Development Core Team, 2013) for statistical analysis. I performed both ordinary least squares (OLS) and reduced major axis (RMA) regression on the log transformed scaling data fit to the power function $y=aM^b$, where y represents the morphological traits of interest, a is the scaling constant, M is body mass, and b is the scaling exponent. OLS regression does not account for error in the independent variable, while RMA regression does (Rayner, 1985). I calculated the 95% confidence intervals of the slope to determine if the scaling exponent b was significantly different from the expected isometric scaling exponent, b_o, as described previously (e.g. Herrel and O'Reilly, 2006; Nudds, 2007; Chi and Roth, 2010). Both OLS regression and RMA regression fit similar scaling exponents in my analysis and were consistent in distinguishing significant differences from isometry. Because of the similarity and agreement between the models, only the RMA regressions are reported.

Results

Scaling of Linear Dimensions

I found both body length and diameter across all measured segments scaled allometrically (Fig. 2.3). While body length scaled significantly greater (b=0.39) than predicted for isometry (b_o=0.33), the diameter of all measured segments scaled less than predicted (b=0.292, 0.278, 0.283 for the anterior, middle, and posterior segments, respectively). As a consequence, the *L/D* ratio increases with body size (b=0.119, 0.138, 0.140 for the anterior, middle, and posterior segments respectively) instead of remaining constant with body size as would be the case for isometry (b_o=0.00). I found the number of segments active in each peristaltic wave during crawling was independent of body size.

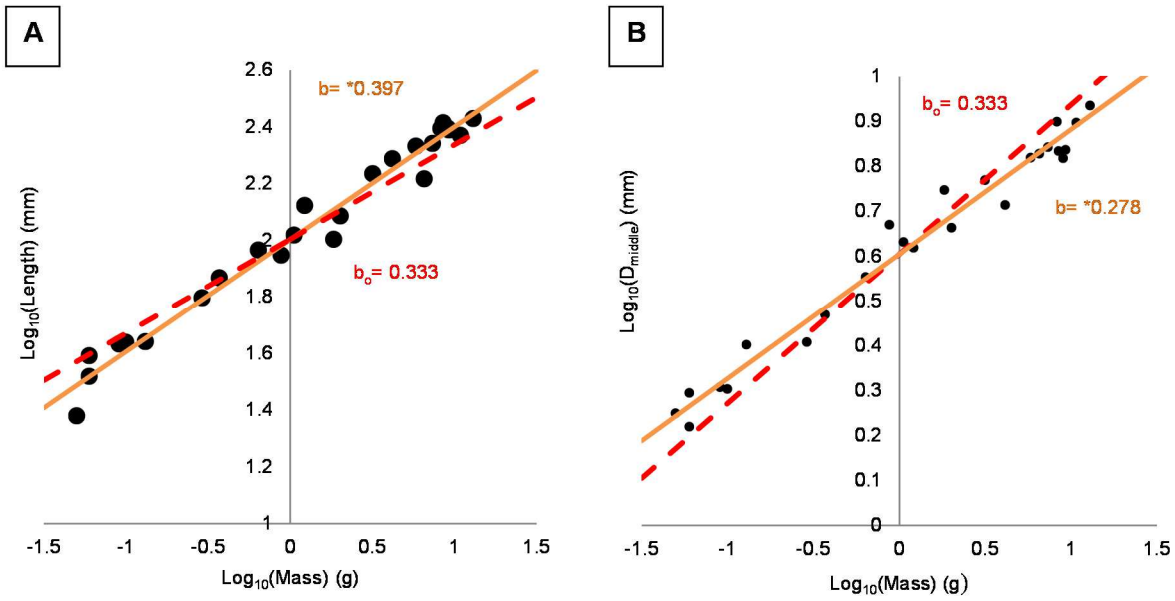

C

Linear Dimension (y)	Isometric Scaling Exponent (b_o)	RMA Scaling Exponent (b)	Lower 95% C.I.	Upper 95% C.I.	R^2
L	0.333	*0.397	0.373	0.423	0.978
$D_{anterior}$	0.333	*0.292	0.276	0.309	0.983
D_{middle}	0.333	*0.278	0.261	0.296	0.978
$D_{posterior}$	0.333	*0.283	0.257	0.312	0.952

Fig. 2.3: Scaling of linear dimensions. Length refers to body length. $D_{anterior}$, D_{middle}, and $D_{posterior}$ refer to the diameters of segments number 10, 30, and 50, respectively, from the anterior. **A**. Log transformed graph comparing body length to body mass. **B**. Log transformed graph comparing D_{middle} to body mass. The regressions on 1A and 1B depict the isometric scaling exponent (b_o, dashed line) and the scaling exponent fit to empirical data using RMA regression (b, solid line). **C**. Hypothesis testing of b using 95% confidence intervals (C.I.). * Indicates the C.I.s do not overlap with b_o. N=25

Scaling of Muscle Cross-Sectional Area

The cross-sectional area of the longitudinal musculature (Fig. 2.4A and 2.4C) scaled lower than expected (b=0.620, 0.553, 0.591 for the anterior, middle, and posterior segments, respectively) compared with isometry (b_o=0.667) for all segments measured. However, the circumferential muscle cross-sectional areas of the middle and posterior segments exhibited the

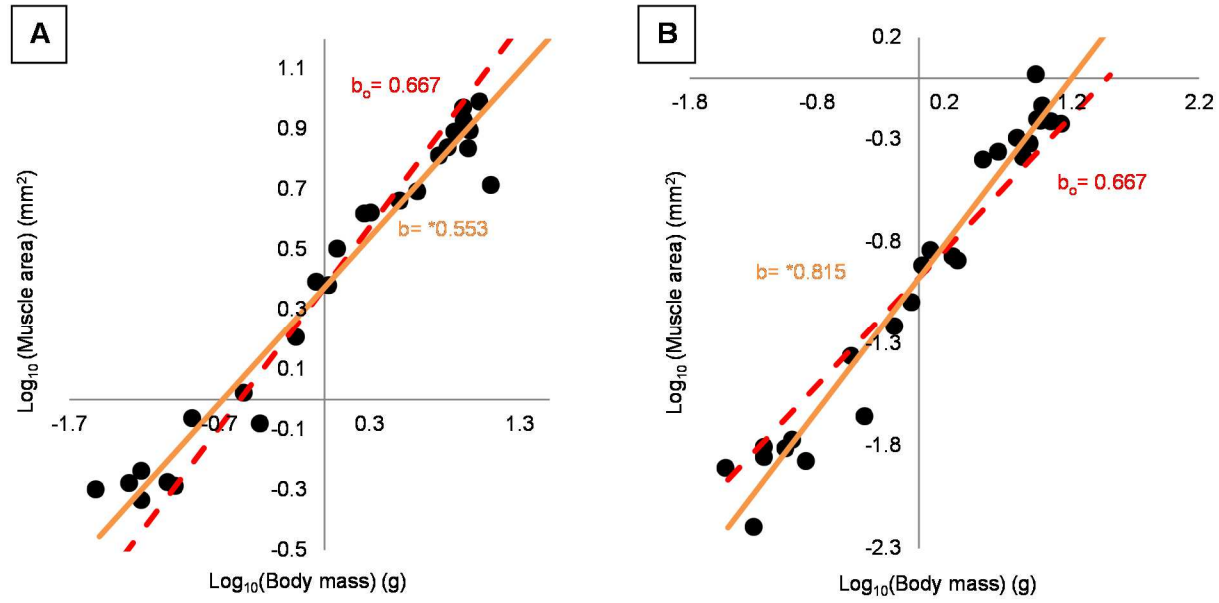

C

Muscle Area (y)	Isometric Scaling Exponent (b_o)	RMA Scaling Exponent (b)	Lower 95% C.I.	Upper 95% C.I.	R^2
$A_{l\ anterior}$	0.667	*0.620	0.580	0.662	0.976
$A_{l\ middle}$	0.667	*0.553	0.508	0.602	0.967
$A_{l\ posterior}$	0.667	*0.591	0.535	0.654	0.948
$A_{C\ anterior}$	0.667	0.690	0.630	0.757	0.955
$A_{C\ middle}$	0.667	*0.815	0.748	0.888	0.960
$A_{C\ posterior}$	0.667	*0.840	0.775	0.909	0.967

Fig. 2.4: Scaling of muscle cross-sectional areas. A_l and A_c refer to longitudinal muscle and circumferential muscle, respectively. The subscripts anterior, middle, and posterior denote the locations sampled. **A**. Log transformed graph of longitudinal muscle cross sectional area $A_{l\ middle}$ and body mass. **B**. Log transformed graph of circumferential muscle area in the middle segment $A_{c\ middle}$ and body mass. **C.** Hypothesis testing of b using 95% C.I. N=25. Refer to Fig. 2.3 for details.

opposite trend. The circumferential muscle cross-sectional area in the middle and posterior segments (Fig. 2.4B and 3C) scaled greater than expected (b=0.815, 0.840 for middle and posterior segments, respectively) compared with isometric scaling (b_o=0.667). Circumferential muscle cross-sectional area in the anterior segment did not scale significantly differently from isometry (b=0.690).

Scaling of Leverage and Force Production

Because of the increase in the *L/D* ratio with size, the mechanical advantage and distance advantage of the musculature changes with size (Fig. 2.5). I calculated that the mechanical advantage of the circumferential musculature will decrease with body size (b=-0.112) but that of the longitudinal musculature will increase. (b=0.112). Since the force output is proportional to the product of the mechanical advantage and cross-sectional area of the musculature, I calculated that the force output (Table 2.1) from the longitudinal muscle scales greater than isometry in the anterior segments (b= 0.724) and near isometry for the middle and posterior segments (b=0.653, 0.680 for the middle and posterior segments, respectively). Force output from the circumferential muscle of the anterior segments scales less than expected (b=0.561) for isometry, but the force output of the circumferential muscle of the middle and posterior segments scales near isometry (b=0.687, 0.696 for the middle and posterior segments, respectively).

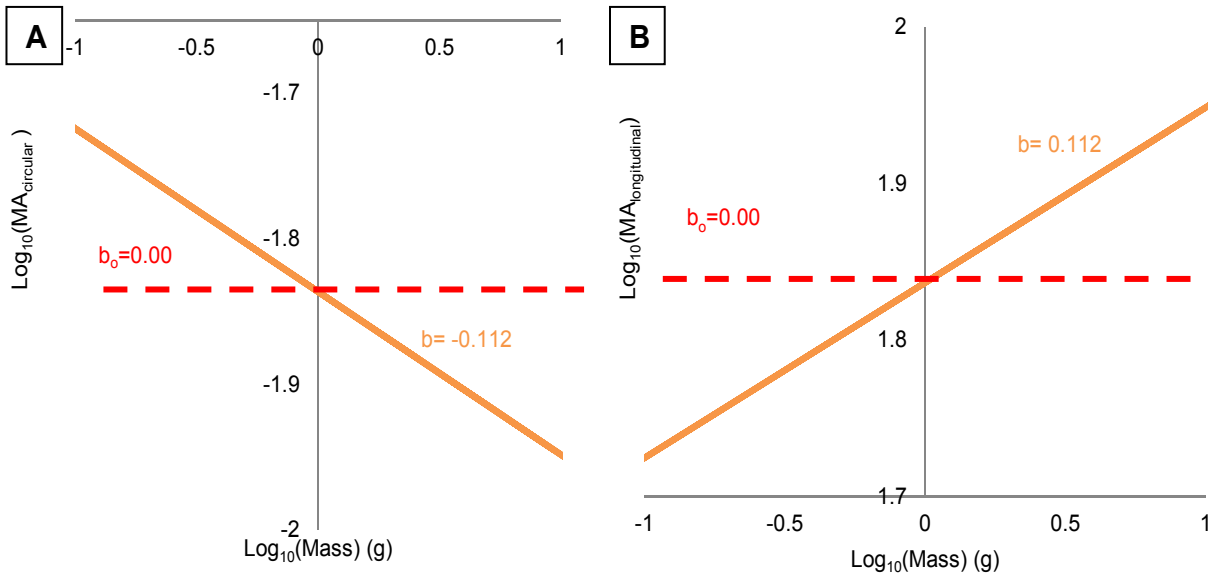

Fig. 2.5: Predictive model comparing mechanical advantage with body mass. A. Mechanical advantage from circumferential muscle contraction and ($MA_{\text{circumferential}}$) **B**. mechanical advantage from longitudinal muscle contraction ($MA_{\text{longitudinal}}$) a function of earthworm body mass.

Linear Dimension (y)	*L. terrestris*' Intercept (Log a_1)	*E. fetida*'s Intercept (Log a)	*L. terrestris*' Scaling Exponent (b_1)	*E. fetida*'s Scaling Exponent (b)
$F_{\text{l anterior}}$	2.348	2.003	0.724	0.625
$F_{\text{l middle}}$	2.215	2.085	0.676	0.725
$F_{\text{l posterior}}$	2.209	2.194	0.688	0.783
$F_{\text{c anterior}}$	-2.549	-2.289	0.562	0.457
$F_{\text{c middle}}$	-2.811	-2.379	0.687	0.542
$F_{\text{c posterior}}$	-2.893	-2.229	0.696	0.694

Table 2.2: **Model predicting the scaling of force output**. The RMA regression scaling exponents for each muscle cross-sectional area was multiplied with the scaling exponent of mechanical advantage. Mechanical advantage was calculated by normalizing the changes in *L/D* ratios with mass and calculating the reciprocal of distance advantage over 25% radial strain. F_{l} and F_{C} refer to longitudinal muscle and circumferential muscle force output, respectively. The subscripts $_{\text{anterior}}$, $_{\text{middle,}}$ and $_{\text{posterior}}$ denote the locations sampled.

Scaling of Pressure

I did not observe a difference from isometry (b=0.00) in the ratio of the areas of the muscle and coelom (*A/C*) for the anterior and middle segments for both the longitudinal muscles (b=0.021, 0.060 for the anterior and middle segments, respectively) and circumferential muscles (b= 0.044, 0.049 for anterior and middle segments, respectively) (Fig. 2.6). The posterior segments, however, showed significant differences in the ratio of *A/C* with body size for both the longitudinal (b=0.146) and circumferential (b=0.378) muscle.

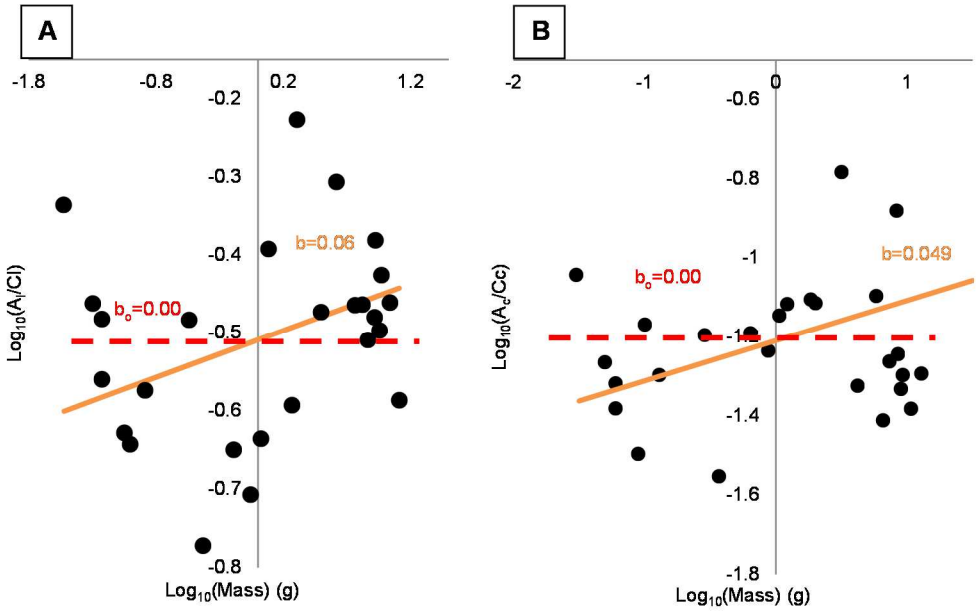

C

Ratio A/ C (y)	Isometric Scaling Exponent (b_o)	Measured Scaling Exponent (b)	Lower 95% C.I.	Upper 95% C.I.	R^2
$A_l/C_{l\ anterior}$	0.000	0.021	-0.004	0.050	0.105
$A_l/C_{l\ middle}$	0.000	0.060	-0.043	0.200	0.055
$A_l/C_{l\ posterior}$	0.000	*0.146	0.061	0.265	0.305
$A_c/C_{c\ anterior}$	0.000	0.044	-0.126	0.269	0.014
$A_c/C_{c\ middle}$	0.000	0.049	-0.100	0.228	0.020
$A_c/C_{c\ posterior}$	0.000	*0.378	0.253	0.560	0.556

Fig. 2.6: Scaling of the ratio of muscle cross-sectional areas (*A*) to projected coelomic area (*C*) where muscle contraction is applied. The subscripts $_l$ and $_c$ refer to longitudinal and circumferential muscles, respectively. The subscripts $_{anterior}$, $_{middle}$, and $_{posterior}$ denote the locations sampled. **A**. Plot of $A_l/C_{l(middle)}$ relative to body mass. **B**. Plot of $A_c/C_{c(middle)}$ relative to body mass. **C**. Hypothesis testing of b using 95% confidence intervals (C.I.). N=25.

Discussion

Scaling Trends

Although previous work (Quillin, 1998) had suggested that scaling of the hydrostatic skeleton should be isometric, my results show that a number of mechanically important dimensions of *L. terrestris* grow allometrically. I suspect that these differences reflect the methods used. Quillin 1998 used frozen sections, which tend to be subject to much greater distortion and artefact, and are significantly thicker than the sections I obtained using glycol

methacrylate embedding. Glycol methacrylate embedding procedures have the advantage of causing little distortion and shrinkage, compared with other histological methods, and thinner sections allow better resolution of detail. In addition, her sections were unstained, which makes identification of the components of the tissues challenging, in particular in the smallest specimens. Instead, I employed selective stains that allowed clear differentiation of muscle and connective tissues. Finally, I used serial sections in both sagittal and transverse planes, while Quillin 1998 sectioned in the sagittal plane only, which complicates the measurement of the cross-sectional area of the longitudinal muscle in particular.

Mechanical and Distance Advantage

I found that *L. terrestris* grows disproportionately long ($L \propto M^{0.397}$) and thin ($D \propto M^{<0.30}$), and thus the length-to-diameter ratio increases with body size ($L/D \propto M^{>0.10}$). This trend was also observed by Piearce 1983, who measured formalin fixed *L. terrestris* earthworms and noted an increase in the *L/D* ratio with mass. This increase in the *L/D* ratio impacts the mechanics of the musculature. I estimated the effect of this allometry on the scaling of distance advantage and mechanical advantage of the musculature during elongation and shortening. From the standpoint of the circumferential musculature that elongates the animal, adult worms (10g body mass) have an approximately 117% greater distance advantage compared with 0.01g hatchlings. This increase in distance advantage during elongation is consistent with the observations of Quillin, 1999, who found that *L. terrestris'* stride length (i.e. distance traveled during one peristaltic wave) during crawling increased allometrically with size. From the standpoint of the longitudinal musculature that shortens the animal and thereby causes radial expansion, I estimate that adults have 117% greater mechanical advantage compared with 0.01g hatchlings.

Force Output

Force output to the environment is a function of the forces generated by the muscles and the transmission of those forces by the skeleton. In order to predict the scaling of force output, I multiplied the scaling of the muscle cross-sectional area and the scaling of mechanical advantage of the skeleton. Although the longitudinal muscle cross-sectional area increases less than predicted by isometry ($A_l \propto M^{0.553\text{-}0.620}$), it gains mechanical advantage with size ($MA \propto M^{0.112)}$ due to the increase in *L/D*. The increase in mechanical advantage compensates for the allometric scaling of the muscle cross-sectional area, and the force output is thus nearly isometric ($F_l \propto M^{0.653\text{-}0.724}$). The circumferential musculature shows a similar trend; in the middle and posterior segments, the circumferential muscle cross-sectional area increases at a rate that is greater than predicted by isometry ($Ac \propto M^{0.69\text{-}0.840}$), but its mechanical advantage decreases with size ($MA \propto M^{-0.112}$). The force output is thus nearly isometric ($F_c \propto M^{0.561\text{-}0.696}$).

While my findings on the scaling of circumferential muscle cross-sectional area are in agreement with prior research by Quillin 2000, my force calculations do not resolve the disproportionately low scaling of force measured by Quillin 2000 in earthworms crawling through force transducers. In the present study, I was able to address several of the factors that she suggested might be responsible for the discrepancy, including scaling of muscle area and of mechanical advantage. In addition, she suggested that muscle stress might vary with body size, the kinematics of burrowing might change with size, and the resistance to soil deformation might depend on the scale of the deformation, issues that are the focus of my current investigations. An additional possibility may be the relative dimensions of the force transducers used in her experiments, which may not have measured an equivalent number of segments in the seven size classes of worms analyzed.

Pressure from Muscle Contraction

I found no significant trend with size of the ratio between muscle cross-sectional area and area of the coelom (Pm α A/C α M^0). Although the contractile properties of the developing muscle have not been measured, if I assume that the peak isometric stress of the muscle is independent of body size, then these results predict that the pressure produced by the musculature will be independent of body size. Internal pressure measurements of *L. terrestris* on the surface are consistent with this prediction and exhibit no trend with body size (Quillin, 1998).

Intersegmental Differences

Several of the allometric trends differed between segments, which may reflect the relative importance of different portions of the body in burrowing. Because the peristaltic wave often dissipates as it travels down the length of the body, segments closer to the tail are likely of less importance in burrowing than those near the head (Yapp, 1956). My data are consistent with this proposal as longitudinal force production of the anterior segments increased at a greater rate (F_l α $M^{0.724}$) than expected from isometry, while the middle and posterior segments scaled close to isometry. The longitudinal muscles are thought to be important in moving soil laterally to enlarge the burrow, anchor the worm, and break up soil articles ahead of the worm (Gray and Lissman, 1938; Keudel and Schrader, 1999).

I also found that circumferential muscle force production scaled disproportionately low in the anterior segments (F_c α $M^{0.561}$), but scaled near isometry for the middle and posterior segments. The circumferential musculature plays an important role when the animal crawls on the surface by causing the segments to elongate and move forward. Indeed, in contrast to burrowing, the highest pressures recorded during crawling result from circumferential muscle contraction (Seymour, 1969). Thus, the allometric trends I observed in the anterior segments may

reflect the increased importance of burrowing locomotion as *L. terrestris* grow since only adult worms are found to make deep burrows.

Potential Selective Pressures for Allometric growth

Because I identified several significant allometric growth patterns in *L. terrestris*, it is of interest to consider the potential selective pressures that may be acting on these animals in the environment, especially since previous research had predicted that growth would be isometric. I briefly outline below two hypotheses for the allometric trends observed. These hypotheses are not mutually exclusive and testing them is a focus of my ongoing research.

As an earthworm grows, selection might favor a thinner body in order to reduce "strain hardening" during burrow formation (Piearce, 1983). Many soils, including loose granular soils and consolidated clays, exhibit this phenomenon, in which the modulus of compression or stiffness of the soil increases with increasing strain (Chen, 1975; Yong et al., 2012; Holtz et al., 2010). As an earthworm grows in cross-section, it must displace more soil radially, with a resulting increase in the stiffness of the soil surrounding the burrow. Small worms (including the hatchlings of burrowing earthworm species) are often found near the soil surface and have been hypothesized to squeeze through existing cracks and pores as "crevice burrowers" (Arthur, 1965; Gerard, 1967). If small worms can indeed exploit these small crevices, they may avoid displacing the soil and thereby avoid the strain hardening effect. As a burrower grows and exceeds the size of the crevices, there could be a selective advantage in becoming relatively thinner to reduce this effect. This may explain why I found that *L. terrestris* grew disproportionately long and thin during ontogeny. My results indicate that the relative reduction in diameter was achieved by reducing both the longitudinal muscle cross section ($A_l \propto M^{0.553-}$

$^{0.620}$) and the cross-sectional area of the coelom; the ratio of longitudinal muscle area to coelomic area did not change with body size ($A_l/C_l \propto M^0$).

The increase in the length to diameter ratio I observed may also be the result of selective pressures associated with burrowing using a mechanism termed "crack propagation", which has been demonstrated in numerous burrowers in marine muds (Dorgan et al., 2005; Dorgan et al., 2007; Dorgan et al., 2008). Che and Dorgan (2010) found that small marine worms that use this mechanism, which involves lateral expansion of the anterior portion of the body to fracture the mud, are relatively thicker when burrowing and exert relatively higher forces in order to apply the required stress to propagate a crack ahead of the worm. Thus, they show similar allometry in body dimensions to that observed here for *L. terrestris,* with small worms being relatively thicker than large worms. Dorgan et al. (2006) propose that terrestrial soils may fracture based on a review of earthworm and root growth literature, but the possibility of crack propagation by terrestrial worms has not yet been investigated. This is an important area for future research since a variety of terrestrial soil environments possess mechanical properties amenable to this burrowing mechanism (Molles, 2009).

Conclusions

My analysis indicates that, contrary to expectations from previous work, the hydrostatic skeleton of *L. terrestris* does not exhibit isometric scaling during growth. A number of functionally relevant aspects of the morphology scale allometrically including the overall shape of the animal and the cross-sectional area of the musculature. Additional work is needed to investigate the selective pressures responsible for the increase in the *L/D* ratio and allometry in the force production of the anterior segments. I hypothesize that changes in soil properties and burrowing mechanics with size are important. I tested these hypotheses and also explored the

scaling of hydrostatic skeletons in other taxa, taking advantage of the taxonomic diversity and range of habitats and ecology of soft-bodied invertebrates. Using this approach, I identified general principles of scaling in hydrostatic skeletons and burrowing mechanics.

CHAPTER 3: DIFFERENCES IN THE SCALING AND MORPHOLOGY BETWEEN LUMBRICID EARTHWORM ECOTYPES

Summary

Many soft-bodied invertebrates use a flexible, fluid-filled hydrostatic skeleton for burrowing. The aim of my study was to compare the ontogenetic scaling and body morphology between surface-dwelling and burrowing earthworm ecotypes to explore the specializations of non-rigid musculoskeletal systems for burrowing locomotion. I compared the scaling of adult lumbricid earthworms across species and ecotypes to determine if linear dimensions were significantly associated with ecotype. I also compared the ontogenetic scaling of a burrowing species, *Lumbricus terrestris*, and a surface-dwelling species, *Eisenia fetida*, using glycol methacrylate histology. I found that burrowing species were longer, thinner, and had higher length-to-diameter ratios than non-burrowers, and that *L. terrestris* was thinner for any given body mass compared to *E. fetida*. I also found differences in the size of the musculature between the two species that may correlate with surface crawling or burrowing. My results suggest that adaptations to burrowing for soft-bodied animals include a disproportionately thin body, small body volume, and strong longitudinal muscles.

Introduction

Burrowing is a difficult form of locomotion due to the abrasive, heterogeneous, and dense nature of many substrates. Despite the challenges, many vertebrates and invertebrates ranging from micrometers to meters in length burrow effectively in a variety of substrates. Their burrowing actions alter the soil environment and aid in nutrient recycling, air and water infiltration, and soil decompaction.

Many invertebrate burrowers lack rigid skeletal elements, relying instead on a hydrostatic skeleton consisting of a liquid-filled internal cavity surrounded by a muscular body wall (Chapman, 1958; Kier, 2012). When the muscles in the body wall contract, the internal fluid is pressurized, allowing for skeletal support, muscle antagonism, skeletal leverage, locomotion, and other skeletal functions (Chapman, 1950, 1958; Alexander, 1995). The hydrostatic skeleton can also accommodate deformation in the body due to muscle contraction. Earthworms, for example, possess two predominant muscle orientations, circumferential and longitudinal. Circumferential muscle contraction elongates the worm, allowing it to move forward and excavate a new burrow; the longitudinal muscles shorten and expand the worm laterally, allowing for anchorage and burrow consolidation (Trueman, 1975). In addition, the radial straining of the soil by the longitudinal muscles breaks up soil particles ahead of the worm, reducing the pressure required for axial elongation (Abdalla et al., 1969; Whalley and Dexter, 1994; Keudel and Schrader, 1999; Dorgan et al., 2008).

Soft-bodied burrowing invertebrates range in size from several hundred micrometers in length (e.g. nematodes) to several meters in length (e.g. earthworms), and burrow in a variety of terrestrial and marine environments. The effects of size on burrowing mechanics has not, however, been studied in detail (e.g. Piearce, 1983; Quillin, 2000; Chi and Dorgan 2010). In

addition, the impacts on subterranean organisms of anthropogenic changes in soil properties from chemicals and heavy machinery have been investigated previously, yet we do not know if there are size-dependent effects on burrowers (e.g. Ehlers, 1975; Roberts and Dorough, 1985; Chan and Barchia, 2007). This research may also provide insights important for the design of burrowing soft robots (e.g. Trimmer, 2008; Trivedi et al., 2008; Daltorio et al., 2013).

The physical characteristics of soil may impose size-dependent constraints on burrowers (Dorgan et al., 2008; Che and Dorgan, 2010; Kurth and Kier, 2014). For example, many soils exhibit strain hardening, in which the modulus of compression (stiffness) of the soil increases with increasing strain (Chen, 1975; Yong et al., 2012; Holtz et al., 2010). As an earthworm grows in cross-section, it must displace more soil radially as it burrows, which may result in an increase in the stiffness of the soil surrounding the burrow. Small worms may avoid the strain hardening effect due to the relatively small volume of soil they must displace during burrowing. Thus, as a burrower grows there may be a selective advantage to becoming relatively thinner and reducing the volume of the body to mitigate the strain hardening effect (Piearce, 1983; Kurth and Kier, 2014).

In Chapter 2 I showed that the burrowing earthworm *Lumbricus terrestris* becomes relatively thinner during growth and shows additional allometric changes in the musculature (Kurth and Kier 2014). I hypothesized that these allometries may help to compensate for changes in burrowing mechanics with growth. In order to examine this issue, in this study I compared the linear dimensions of earthworms across ecotypes, as well as the ontogenetic scaling of a non-burrowing, surface-dwelling earthworm, *Eisenia fetida*. Not all earthworms burrow; there are three main ecotypes of earthworms that are largely differentiated by their burrowing patterns or lack thereof (Bouché, 1977). Surface-dwelling species like *E. fetida* are known as epigeic

worms, which do not burrow and are instead found under leaf litter, in manure, and under debris. There are also endogeic worms, which create ephemeral horizontal burrows in the upper 10-15cm of soil and are geophagus (Edwards and Bohlen, 1977). Lastly, there are anecic worms, like *L. terrestris*, that build deep permanent/semi-permanent vertical burrows and feed on surface litter (Keudel and Schrader, 1999). I refer to these three ecotypes as surface-dwellers, horizontal burrowers, and vertical burrowers, respectively.

I hypothesized that there would be both ontogenetic and interspecific differences between earthworm ecotypes. To mitigate strain hardening, I predicted that the burrowing species would be thinner for any given body mass during development compared with surface-dwellers, resulting in higher length-to-diameter ratios and smaller body volumes in the burrowing species. I also hypothesized that forces from the longitudinal musculature, which radially expand the worm during contraction, would be relatively larger in the burrowers compared with the surface-dwellers. These muscles are believed to be important in burrowing by anchoring the worm, consolidating the burrow, relieving soil compaction ahead of the worm, and pulling posterior segments into the burrow (Seymour, 1969; McKenzie and Dexter, 1988; Keudel and Schrader, 1999; Barnett et al., 2009). These muscles also move the bulk of soil during burrow formation, and must generate sufficient force to overcome potential strain hardening effects in the soil (Barnett et al., 2009).

In contrast to the longitudinal muscles, I predicted forces from the circumferential muscles, which thin and elongate the worm, would be larger in the surface-dwellers. The circumferential muscles are particularly important in surface crawling, extending the worm forward during each peristaltic wave of contraction and aiding penetration into litter and under

debris; in fact, the largest pressures exerted in surface crawling earthworms occur during circumferential muscle contraction (Gray and Lissman, 1938; Arthur, 1965; Seymour, 1969).

I found significant differences in the length-to-diameter ratio and scaling between ecotypes and significant ontogenetic differences in scaling between *E. fetida* and *L. terrestris*, consistent with my hypotheses (Kurth and Kier, 2014). My results demonstrate that many aspects of the hydrostatic skeleton of earthworms develop in different ways between species, reflecting the ecological context of the organism.

Scaling of Functionally Relevant Morphological Features

A variety of organisms including *L. terrestris* exhibit allometric growth, in which the relative proportions change with body size rather than remaining constant, as in isometric growth (Huxley and Tessier, 1936; Schmidt-Nielsen, 1997). Since the density of an animal typically does not change with size, the mass (M) is proportional to the volume (V). If an organism scales isometrically, linear dimensions such as length (L) or diameter (D) are predicted to scale to the animal's $V^{1/3}$ and thus $M^{1/3}$ and any area, such as surface area or muscle cross-sectional area, will scale as $V^{2/3}$ and thus $M^{2/3}$.

Scaling of Linear Dimensions

In an isometrically scaling vermiform animal, the L/D ratio will not change with size. This is because both L and D are linear dimensions and should scale as $M^{1/3}$. Kurth and Kier (2014) found allometry in the overall dimensions of *L. terrestris*, however, which changes the relative force and displacement of the musculature during growth (Kier and Smith, 1985; Vogel, 2013). An increase in the L/D ratio during growth, as is found in *L. terrestris*, increases the distance advantage (the ratio of distance output/distance input) for the circumferential muscles and increases the mechanical advantage (the ratio of force output/ force input) for the

longitudinal muscles (Kurth and Kier, 2014). Since mechanical advantage and distance advantage are reciprocal, an increase in the *L/D* ratio decreases the mechanical advantage of the circumferential musculature and decreases the distance advantage of the longitudinal musculature.

For any given body mass, I predict that *E. fetida* will have a lower *L/D* than *L. terrestris* because *E. fetida* is not under selective pressure to minimize its diameter for burrowing. A smaller *L/D* means that *E. fetida* will have lower mechanical advantage during longitudinal muscle contraction and higher mechanical advantage during circumferential muscle contraction for a given size than *L. terrestris*.

Scaling of Body Volume

Body volume likely scales proportionally with mass in *E. fetida* and *L. terrestris* since the density of earthworms probably does not change with size. However, there may be interspecific differences in the magnitude of body volumes across ecotypes. If burrowers are thinner than surface-dwellers, they may also have smaller body volumes as a consequence. Small body volumes would allow burrowers to displace a lower volume of soil during burrowing and may mitigate strain hardening.

Scaling of Muscle Cross-Sectional Areas and Force Output

The scaling of muscle physiological cross-sectional area (*A*) determines how relative force production by the musculature changes with size, because force due to muscle contraction is proportional to cross-sectional area. If the circumferential and the longitudinal musculature scales isometrically, the cross-sectional area of each will be proportional to $M^{2/3}$. The final force output the animal exerts on the environment, however, is a product both of the force generated by the muscles and the mechanical advantage produced by the skeleton itself:

$$F \alpha A(Mechanical\ Advantage) \quad (1)$$

Where F is the force output to the environment and A is the muscle cross-sectional area (Kurth and Kier, 2014). I predict that the scaling of force output for *E. fetida* will be lower during longitudinal muscle contraction but higher during circumferential muscle contraction than *L. terrestris*.

Materials and Methods

Interspecific Measurements and Phylogenetic Reconstruction

I used sexually mature earthworm specimens preserved in 70-95% ethanol in the collections of the Smithsonian Institution Museum of Natural History (Washington, DC). A phylogeny is available of species in the Lumbricidae family (Pérez-Losada et al., 2012), so I focused my analysis on genera from this family to avoid pseudo-replication (Felsenstein, 1985). I further narrowed the study by only comparing lumbricid species whose ecotypes are well documented (Bouché, 1977; Sims and Gerard, 1985; Edwards and Bohlen, 1996). I used calipers to measure the length and anterior diameter of three adult specimens per species and calculated an average length and diameter, which was then used to calculate the length-to-diameter ratio. I was also able to compare the interspecific scaling of linear dimensions in burrowing and surface dwelling ecotypes. Because many specimens I measured had been dissected and were missing inner organs, I used body volume as a proxy for body mass. I also pooled horizontal and vertical burrowers together for the scaling study due to the low availability of vertically burrowing lumbricid species. No *Hormogaster elisae* specimens were available for analysis, so it was only used to root the phylogenetic tree as discussed below.

I used TreeGraph2^{TM} (Stöver and Müller, 2010) to construct a simplified phylogeny based on the lumbricid earthworm phylogeny by Pérez-Losada et al. 2012. Pérez-Losada et al.

2012 used molecular data from multiple specimens of each species, which resulted in significant variation in branch length and branch placement between specimens within a species. The authors attributed this variation to the sampling of cryptic species. Because I do not know which specimens were misidentified, I simplified the phylogeny by placing each species in the clade where most specimens per species appeared. Due to the high variation and uncertainty in branch length I also made all branch lengths equal in my simplified tree. Although this reduced my statistical power, the reduction is relatively minor and tends to produce only false negative results (Grafen, 1989; Martins and Garland, 1991; Swenson, 2009).

E. fetida Collection and Maintenance

E. fetida earthworms were supplied by Uncle Jim's Worm Farm (Spring Grove, PA USA) as well as raised from hatchlings bred in a colony maintained in the laboratory. Adult worms (~0.1-0.7g) were purchased, raised from purchased juveniles, and raised from colony hatchlings. Hatchlings were raised from cocoons deposited by adults bred in the laboratory colony. All worms were housed in plastic bins filled with moist peat moss (Inouye et al., 2006) at 15ºC (Presley et al., 1996) and were fed dried infant oatmeal (Ownby et al., 2005).

Histology and Morphometrics

The measurements and calculations follow those described in Kurth and Kier, 2014 for *L. terrestris* in order to allow consistent comparisons between *E. fetida* and *L. terrestris*. See Chapter 2 for details on the measurements and calculations of *L. terrestris*

Each *E. fetida* worm was anesthetized in a 10% ethanol solution in distilled water (v/v) until quiescent, patted dry, and weighed. The length was obtained after dragging the worm by the anterior end along the lab bench to straighten the body and extend the segments to a consistent resting length. Because *E. fetida* does not add segments with growth, I measured the length of

the entire body. The worm was then sacrificed and three blocks of tissue containing 20 segments each were removed (segments 1-20, 21-40, and 41-60, numbering from anterior).

The tissue blocks were fixed in 10% formalin in distilled water (v/v) for 24-48 hours. After fixation, the blocks were further dissected for embedding (segments 9-14, 29-34, and 49-54). I refer to segments 9-14 as "anterior", segments 29-34 as "middle", and segments 49-54 as "posterior". The anterior, middle, and posterior segments were then cut so that both transverse and sagittal sections could be obtained from each location. The tissue blocks were partially dehydrated in 95% ethanol and embedded in glycol methacrylate plastic (Technovit 7100, Heraeus Kulzer GmbH, Wehrheim, Germany). Sections of 3-7 μm thickness were cut with a glass knife. I used a Picrosirius/Fast Green stain in order to differentiate muscle from connective tissue (López-DeLeón and Rojkind, 1985) as described previously in Kurth and Kier, 2014. I used Sigma Scan (Systat Software, Inc., San Jose, CA, USA) to make morphological measurements on micrographs. Longitudinal muscle cross-sectional area (A_l) and diameter (D) were measured from transverse sections, whereas circumferential muscle cross-sectional area (A_c) was measured from sagittal sections (Fig. 3.1). The earthworms prepared in this way were flattened slightly and thus had an elliptical cross-sections. To determine an equivalent diameter of a circular cylinder, I measured the major and minor axes, calculated the area of the ellipse and then calculated the diameter of a circle of the same area.

Calculation of Body Volume

Corrected diameter (D) and elongated body length (L) were used to calculate body volume. Since earthworms are approximately cylindrical in shape, body volume was calculated as the volume of a cylinder:

$$V = \pi \left(\frac{D}{2}\right)^2 L \qquad (2)$$

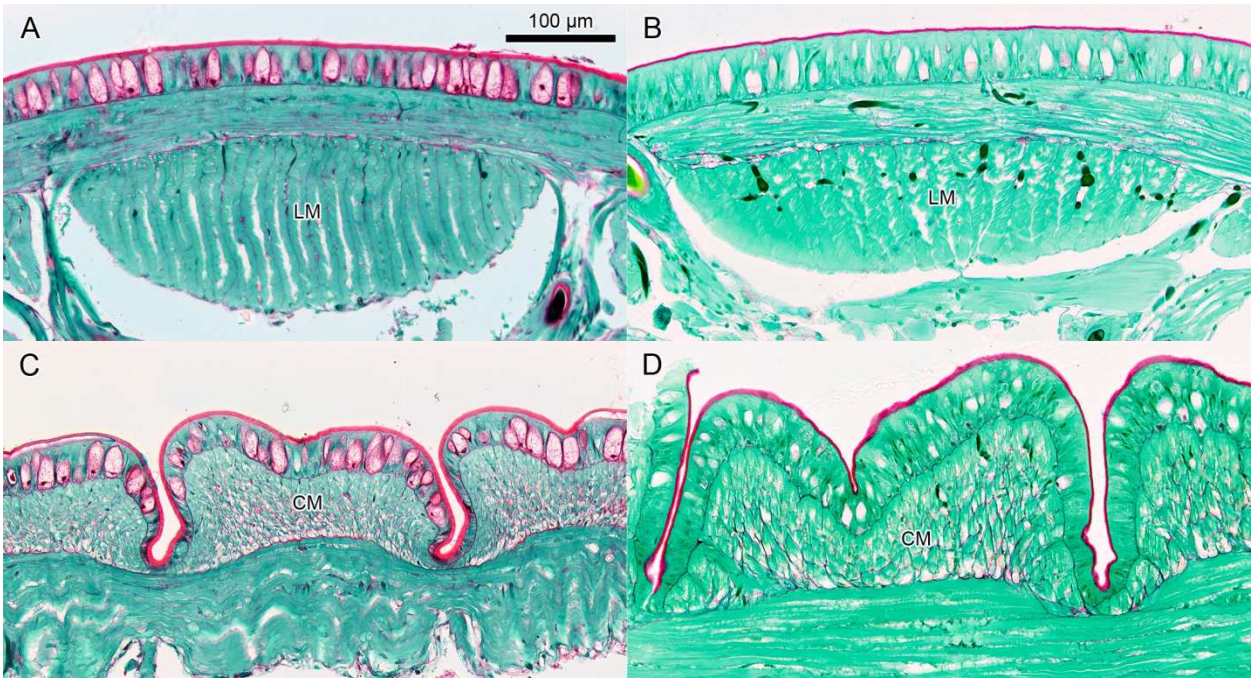

Fig. 3.1: **Photomicrographs (bright field microscopy) of 0.1g *Eisenia fetida* and *Lumbricus terrestris* specimens stained with Picrosirius/Fast Green**. All sections were 7µm in thickness. A. Transverse section of *L. terrestris* showing the cross-sectional area of the longitudinal musculature. B. Transverse section of *E. fetida* showing the cross-sectional area of the longitudinal musculature. C. Parasagittal section of *L. terrestris* showing the cross-sectional area of the circumferential musculature. D. Parasagittal section of *E. fetida* showing the cross-sectional area of the circumferential musculature. L M, longitudinal muscle; C M, circumferential muscle.

Calculation of Mechanical Advantage and Force Output

The scaling of mechanical advantage and force production was calculated for each worm using its average *L/D* ratio across segments and its muscle cross-sectional areas. The average *L/D* ratio was observed to change as a function of size and thus the mechanical advantage of the musculature changes during growth (Kier and Smith, 1985; Kurth and Kier, 2014). Since the mechanical advantage is the reciprocal of the distance advantage, I calculated the mechanical advantage of the circumferential musculature as the absolute value of the decrease in body diameter (*D*) during circumferential muscle contraction divided by the resulting increase in body length (*L*), as a function of the *L/D* ratio, for a 25% decrease body in diameter. Kinematic data for *E. fetida* is unavailable but a 25% change in body diameter has been empirically recorded in

L. terrestris during crawling (Quillin, 1999). Since *L. terrestris* and *E. fetida* are closely related phylogenetically, a 25% change in diameter is a reasonable assumption for both species. (Quillin, 1999; Kurth and Kier, 2014). Likewise, the mechanical advantage of the longitudinal muscle was calculated as the absolute value of the decrease body length of the worm divided by the resulting increase in body diameter, as a function of the *L/D* ratio:

$$Mechanical\ Adv_{\text{(circumferential)}} = \frac{|\Delta D|}{|\Delta L|}\ Mechanical\ Adv_{\text{(longitudinal)}} = \frac{|\Delta L|}{|\Delta D|} \tag{3}$$

These calculations thus provided estimates of the mechanical advantage of both the longitudinal and circumferential musculature as a function of size**.**

Force production was calculated in each worm as the product of mechanical advantage and muscle cross-sectional area in both the circumferential and longitudinal muscles. I made the assumption that stress in the muscle does not change with ontogeny, though this assumption has not been empirically tested in obliquely striated muscle.

Statistical Analysis

I used R statistical software for both the phylogenetic and ontogenetic analyses (R Development Core Team, 2014). We used the *ape* package in R (Paradis et al., 2004) to perform independent contrasts on the phylogeny. This approach allowed me to test for correlations between ecotype and *L/D* ratio while avoiding pesudoreplication (Felsenstein, 1985). I treated ecotype as a continuous variable to allow for transitional/intermediate ecotypes in ancestral nodes.

I also used linear regression on log transformed interspecific and ontogenetic scaling data. I fit both sets of scaling data to the power function $y=aM^b$, where y represents the

morphological traits of interest, a is the scaling constant, M is body mass, and b is the scaling exponent. Log transforming these data allowed me to perform regression analyses, as b becomes the slope of the line and $\log(a)$ becomes the intercept.

I used the *caper* function (Orme et al., 2012) in R (R Development Core Team, 2014) to perform phylogenetically corrected regression on the interspecific scaling data. I pooled horizontal and vertical burrowers together for this analysis because only three vertical burrowing species were measured, and all three were similar in body size. To test for differences in slope and intercept between burrowing and surface-dwelling ecotypes, I performed an ANCOVA analysis on the phylogenetically corrected regression data. Although there may be error in the x-variable (i.e. volume) that is not accounted for in a standard ANCOVA, ANCOVAs using model II regression and reduced major axis techniques are not well developed or commonly used (Sokal and Rolhf, 1985). Thus, standard ANCOVAs are still commonly used in scaling studies (e.g. Niven and Scharlemann, 2005; Davies and Moyes, 2007; Snelling et al., 2011).

I used the *lmodel2* package (Legendre, 2011) in R to perform ordinary least squares and reduced major axis regression on the ontogenetic scaling data. In my ontogenetic analysis, the symbols b_{Lt} and $\log(a_{Lt})$ denote the slopes and intercepts of *L. terrestris*, while the symbols b_{Ef} and $\log(a_{Ef})$ denote the slopes and intercepts of *E. fetida*. To determine differences in slope and intercept between the two species, I used a standard ANCOVA. I also compared RMA scaling exponent b_{Lt} and constant a_{Lt} for *L. terrestris* against the corresponding 95% confidence intervals for *E. fetida* (Heins et al., 2004). My data generally showed high coefficients of determination ($R^2 > 0.85$), and both OLS regression and RMA regression fit similar scaling exponents in my analysis and were consistent in distinguishing significant scaling differences between species. Because of the similarity and agreement between the models, only the ANCOVA and OLS

results for both species are reported to remain consistent with the statistical reporting from the interspecific scaling study.

To account for multiple comparisons, a Bonferroni correction was used on the p-value outputs from the ANCOVAs. Only two comparisons (length and diameter) were used to calculate the Bonferroni correction in the interspecific scaling study. However, 18 comparisons were used to calculate the Bonferroni correction for the ontogenetic scaling study. These 18 comparisons distinguished different measurements as separate comparisons (e.g. length, diameter, longitudinal muscle cross-sectional area, circumferential muscle cross-sectional area, mechanical advantage during longitudinal muscle contraction, etc.) and distinguished measurements across segments as additional separate comparisons (e.g. anterior diameter, middle diameter, posterior diameter). Most p-values remained significant.

Results

Interspecific Scaling of Linear Dimensions

Because *L/D* is dimensionless, I first compared this value across species regardless of body size. I found a significant relationship between *L/D* and ecotype across species and clades ($p<0.05$; Fig. 3.2). Surface-dwelling worms generally had the lowest *L/D* of the three ecotypes. This low *L/D* indicates that surface-dwellers were relatively wider and/or shorter for a given body mass than the burrowers. Vertical burrowers had the highest *L/D* ratios of the three ecotypes, indicating that they were relatively thin and/or long for a given body mass. Horizontal burrowers had moderate *L/D*, which were significantly higher than surface-dwellers and significantly lower than vertical burrowers ($p<0.05$). I did not, however, find a significant difference between body length and ecotype or diameter and ecotype ($p>0.05$) with the exception of vertical burrowers which were significantly longer than the two other ecotypes ($p<0.05$).

These results indicate that differences in *L/D* between surface-dwellers and horizontal burrowers result from differences in both length and diameter, at a given body mass.

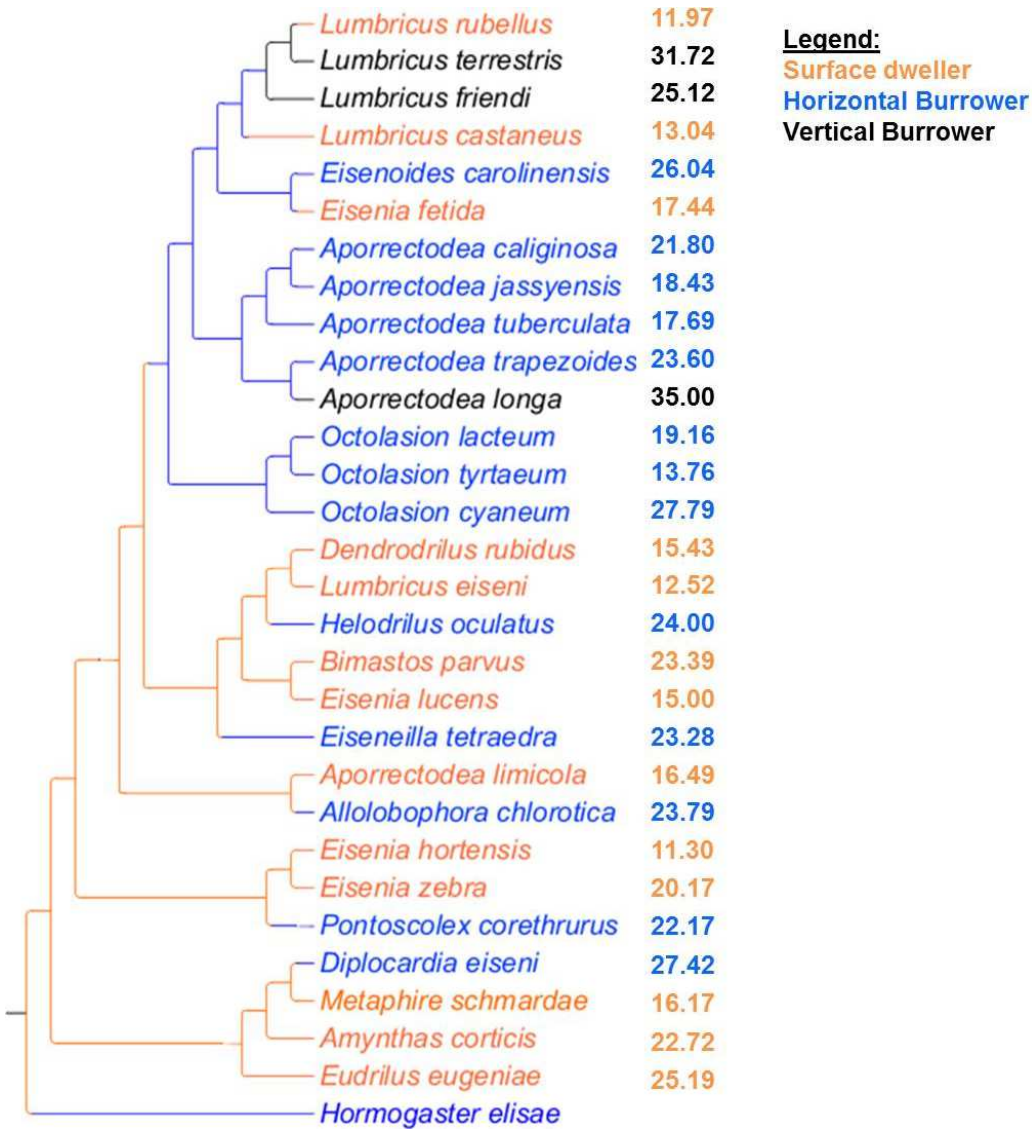

Fig. 3.2: Simplified phylogenetic tree comparing *L/D* and ecotype. The phylogeny was based on a tree built by Pérez-Losada et al. 2012. . No *Hormogaster elisae* specimens were available for analysis, so it was only used to root the phylogenetic tree. Text colors indicate ecotype. The numbers adjacent to the phylogeny indicate each species' *L/D* value. Each *L/D* value is an average from three adult specimens per species.

These *L/D* results were also reflected when comparing the scaling of surface dwelling and burrowing species (Fig. 3.3). I found that while both burrowing and surface dwelling species increased in length with similar scaling exponents (b= 0.410 and 0.401 for burrowers and surface dwellers, respectively), burrowing species were significantly longer for a given body volume than surface dwellers (a= 0.737 and 0.686 for burrowers and surface dwellers, respectively). Anterior diameter, however, showed a different scaling trend. While both burrowers and surface dwellers also increased in diameter at similar rates (b= 0.295 and 0.300 for burrowers and surface dwellers, respectively), burrowers were thinner for a given body volume (a=-0.291 and -0.316 for burrowers and surface dwellers, respectively).

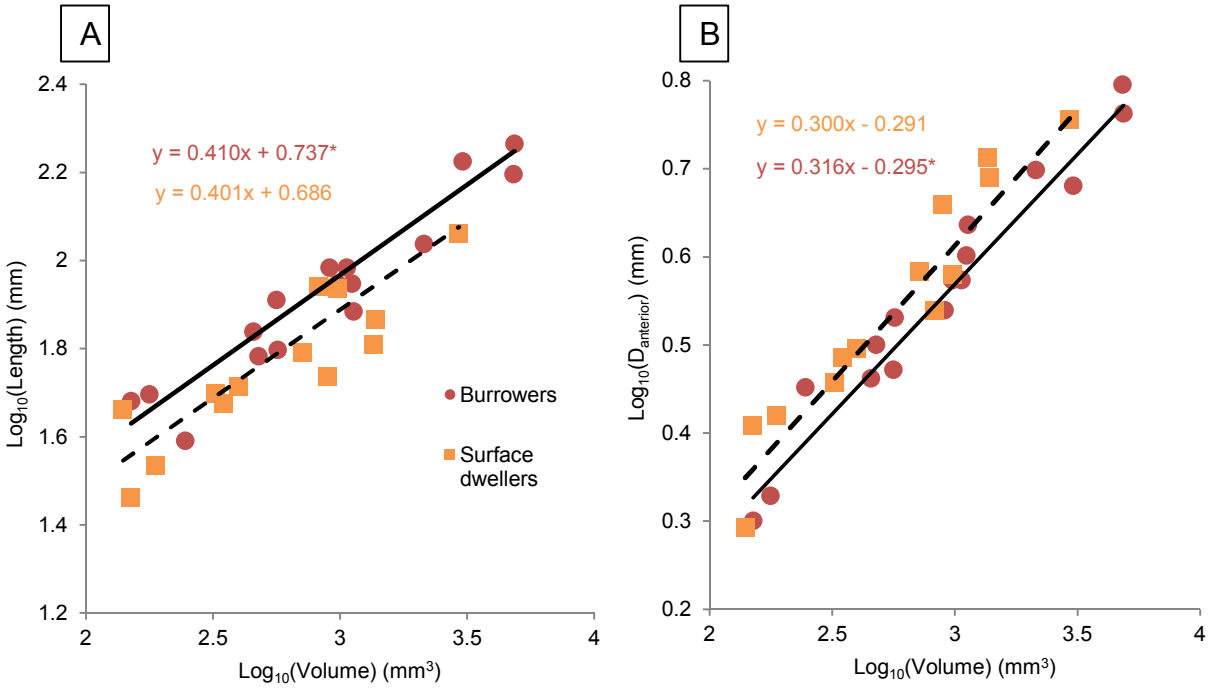

Fig. 3.3: Interspecific differences in the scaling of linear dimensions. **A**. Log transformed graph comparing body length to body volume between burrowing and surface dwelling adult lumbricid species. **B**. Log transformed graph comparing anterior diameter, $D_{anterior}$, to body volume between burrowing and surface dwelling lumbricid species. The regressions shown in 2A and 2B were fit to empirical data using OLS regression (solid line for burrowers, dashed line for surface-dwellers), and the regression equations for both ecotypes are shown. * Indicates a significant difference between species with the Bonferroni correction. N=29.

Ontogenetic Scaling of Linear Dimensions

I found a significant difference between the scaling of *L/D* between the two species (Fig. 3.4). While both *L. terrestris* and *E. fetida* grew disproportionately long (b_{Lt}=0.393, b_{Ef}=0.383) and disproportionately thin (b_{Lt} =0.290, b_{Ef}=0.293) at similar rates, *E. fetida* was always significantly wider at a given body mass than *L. terrestris,* as shown by the differences in log(*a*), the y-intercept of the log-transformed graph (log a_{Lt}= 0.630, 0.605, 0.550; log a_{Ef}=0.861, 0.883, 0.850 for anterior, middle, and posterior segments, respectively) (Table 3.1). Due to these differences in diameter, *E. fetida* had a lower *L/D* for any given body mass compared to *L. terrestris* (log a_{Lt}=1.407, log a_{Ef}= 1.202; averaged across segments) despite a similar increase in *L/D* with size for both species (b_{Lt}= 0.114, b_{Ef}=0.087; averaged across segments).

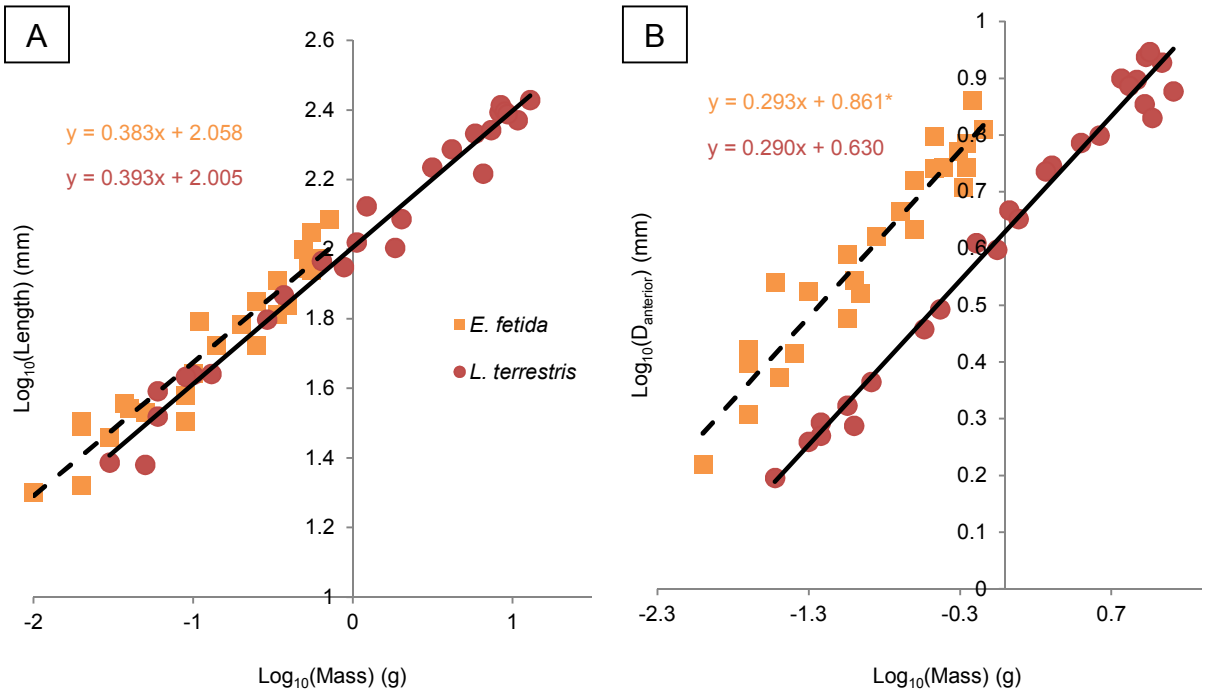

Fig. 3.4: Ontogenetic scaling of linear dimensions. A. Log transformed graph comparing body length to body mass for *L. terrestris* and *E. fetida*. **B**. Log transformed graph comparing anterior diameter, $D_{anterior}$, to body mass for *L. terrestris* and *E. fetida*. The regressions shown in 3A and 3B were fit to empirical data using OLS regression (solid line for *L. terrestris*, dashed line for *E. fetida*), and the regression equations for both species are shown. * Indicates a significant difference between species with the Bonferroni correction. N=25 per species.

Linear Dimensions (y)	*L. terrestris'* Intercept (Log a_{Lt})	*E. fetida's* Intercept (Log a_{Ef})	P-value	*L. terrestris'* Scaling Exponent (b_{Lt})	E. fetida's Scaling Exponent (b_{Ef})	P- value	R^2
L	2.005	2.058	**0.005**	0.393	0.383	0.646	0.912
$D_{anterior}$	0.630	0.861	**$2.0 \cdot 10^{-16}$***	0.290	0.293	0.849	0.911
D_{middle}	0.605	0.883	**$2.0 \cdot 10^{-16}$***	0.275	0.300	0.215	0.909
$D_{posterior}$	0.550	0.850	**$2.0 \cdot 10^{-16}$***	0.277	0.308	0.134	0.958

Table 3.1: Scaling of linear dimensions in *L. terrestris* (vertical burrower) *E. fetida* (surface-dweller). Length refers to body length. $D_{anterior}$, D_{middle}, and $D_{posterior}$ refer to the diameters of segments number 10, 30, and 50, respectively, from the anterior. An ANCOVA was used on empirical data fit by OLS to compare the intercepts (log a_{Lt} and log a_{Ef}) and slopes (b_{Lt} and b_{Ef}) between the two species. * Indicates a significant difference between species with the Bonferroni correction. N=25 per species.]

Because *E. fetida* was similar in length to *L. terrestris* but larger in diameter, *E. fetida* also had larger body volume for a given size than *L. terrestris* (a_{Lt} =3.096, a_{Ef}=3.665) (Fig. 3.5). Both species, however, had a nearly proportional relationship between the scaling of body mass and body volume (b_{Lt} =0.951, b_{Ef}=0.967), which is expected since both species likely maintain constant body density with changes in body size.

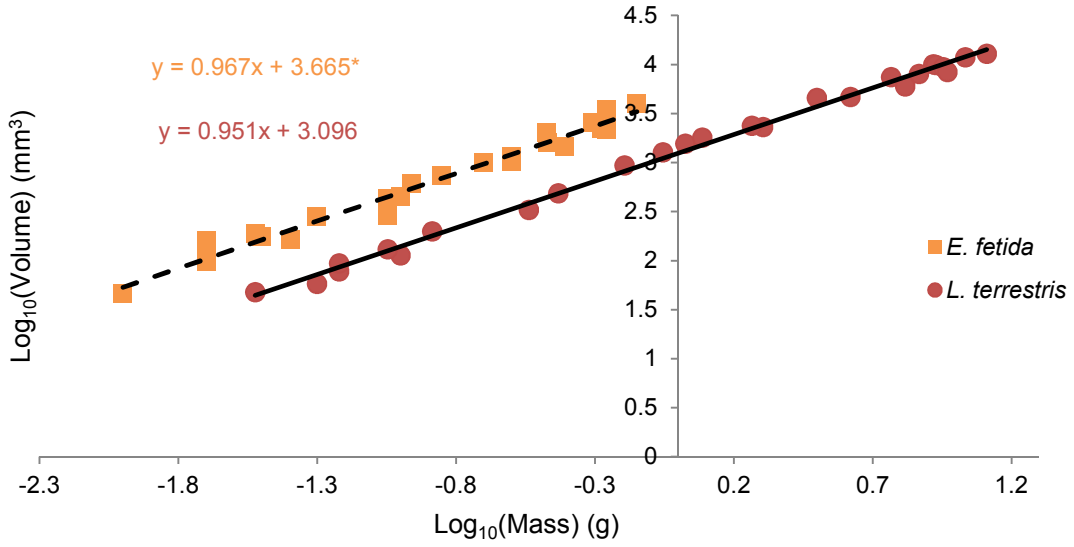

Fig. 3.5: Ontogenetic scaling of volume. Log transformed graph comparing body volume to body mass for *L. terrestris* and *E. fetida*. The regressions shown were fit to empirical data using OLS regression (solid line for *L. terrestris*, dashed line for *E. fetida*), and the regression equations for both species are shown. * Indicates a significant difference between species with the Bonferroni correction. N=25 per species.

Ontogenetic Scaling of Muscle Cross-Sectional Area

I found differences in muscle cross-sectional area between species (Fig. 3.6; Table 3.2). In the anterior segments, *L. terrestris* had larger longitudinal muscles for a given body mass than *E. fetida* (log a_{Lt}= 0.512; log a_{Ef}=0.354) and its longitudinal muscles grew at faster rates than those of *E. fetida* (b_{Lt} = 0.612; b_{Ef}=0.539), but these differences were not statistically significant (Fig. 3.5). Conversely, *E. fetida* had larger anterior circumferential muscles at a given body mass than *L. terrestris* (log a_{Lt}= -0.713; log a_{Ef}= -0.640), despite faster growth of these muscles in *L. terrestris* (b_{Lt} =0.674; b_{Ef}=0.543).

Muscles in the middle and posterior segments were similar in the two species (Table 3.2). The longitudinal muscles from the middle segments scaled similarly (b_{Lt}=0.541; b_{Ef}=0.552) and were similar in cross-sectional area at a given body mass (log a_{Lt}= 0.375; log a_{Ef}=0.392), while the circumferential muscles grew at a faster rate in *L. terrestris* (b_{Lt} = 0.800; b_{Ef}=0.627) but were larger at a given body mass in *E. fetida* (log a_{Lt}= -0.974; log a_{Ef}=-0.731). The posterior longitudinal segments showed the opposite scaling trend from the anterior segments; the longitudinal muscle of *E. fetida* increased in cross-sectional area at a faster rate (b_{Lt} =0.564; b_{Ef}=0.640) and was larger at a given body mass (log a_{Lt}=0.379; log a_{Ef}=0.437), though these differences were not statistically significant. The posterior circumferential muscles showed no significant difference in scaling exponents between the two species (b_{Lt} = 0.792; b_{Ef}=0.743), though the circumferential muscle cross-sectional area of *E. fetida* was larger at a given body mass than that of *L. terrestris* (log a_{Lt}= -1.048; log a_{Ef}=-0.609).

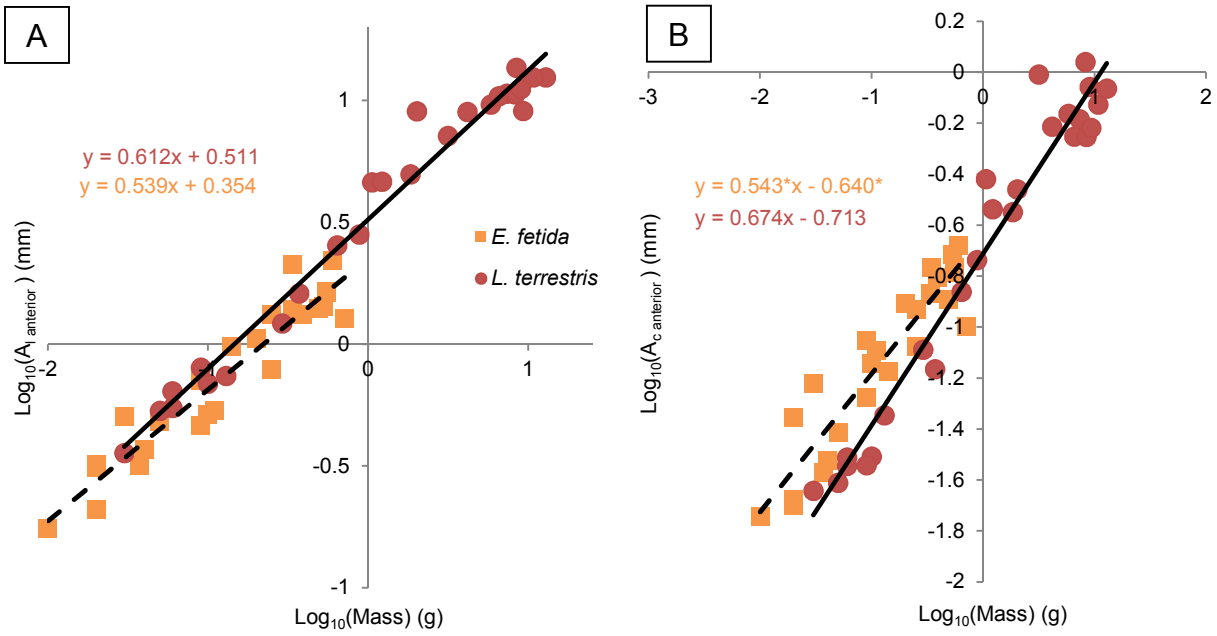

Fig. 3.6: Ontogenetic scaling of muscle cross-sectional areas. A_l and A_c refer to longitudinal muscle and circumferential muscle cross sectional areas, respectively. **A**. Log transformed graph comparing A_l to body mass for *L. terrestris* and *E. fetida*. **B**. Log transformed graph comparing A_c to body mass for *L. terrestris* and *E. fetida*. The subscripts $_{anterior}$, $_{middle}$, and $_{posterior}$ refer to the locations sampled. The regressions shown in 1A and 1B were fit to empirical data using OLS regression (solid line for *L. terrestris*, dashed line for *E. fetida*), and the regression equations for both species are shown. * Indicates a significant difference between species with the Bonferroni correction. N=25 per species.

Muscle Area (y)	*L. terrestris'* Intercept (Log a_{Lt})	*E. fetida's* Intercept (Log a_{Ef})	P-value	*L. terrestris'* Scaling Exponent (b_{Lt})	*E. fetida's* Scaling Exponent (b_{Ef})	P- value	R^2
$A_{l\ anterior}$	0.512	0.354	**0.034**	0.612	0.539	0.084	0.903
$A_{l\ middle}$	0.375	0.392	0.514	0.541	0.552	0.595	0.930
$A_{l\ posterior}$	0.379	0.437	0.511	0.564	0.640	0.472	0.962
$A_{c\ anterior}$	-0.713	-0.640	**0.001***	0.674	0.543	**0.002***	0.862
$A_{c\ middle}$	-0.974	-0.731	**$6.4 \cdot 10^{-9}$***	0.800	0.627	**0.002***	0.853
$A_{c\ posterior}$	-1.048	-0.609	**$7.2 \cdot 10^{-12}$***	0.792	0.743	0.090	0.838

Table 3.2: Scaling of muscle cross-sectional area in *L. terrestris* (vertical burrower) *E. fetida* (surface-dweller). A_l refers to longitudinal muscle cross-sectional area, while A_c refers to circumferential muscle cross-sectional area. The subscripts $_{anterior}$, $_{middle}$, and $_{posterior}$ refer to the diameters of segments number 10, 30, and 50, respectively, from the anterior. An ANCOVA was used on empirical data fit by OLS to compare the intercepts (log a_{Lt} and log a_{Ef}) and slopes (b_{Lt} and b_{Ef}) between the two species. * Indicates a significant difference between species with the Bonferroni correction. N=25.

Ontogenetic Scaling of Mechanical Advantage and Force Production

Because the *L/D* ratio increased in both *E. fetida* and *L. terrestris,* both had similar trends in the scaling of mechanical advantage (Fig. 3.7). I calculated increases in mechanical advantage during longitudinal muscle contraction for both species (b_{Lt} =0.104; b_{Ef}=0.078), though *L. terrestris* had higher mechanical advantage for a given body mass than *E. fetida* (a_{Lt} = 1.872; a_{Ef}=1.650). The calculated mechanical advantage of the circumferential muscle decreased with growth in both species (b_{Lt} =-0.104; b_{Ef}=-0.078), but *L. terrestris* exhibited lower mechanical advantage at a given body mass (log a_{Lt}=-1.872; log a_{Ef}=1.650).

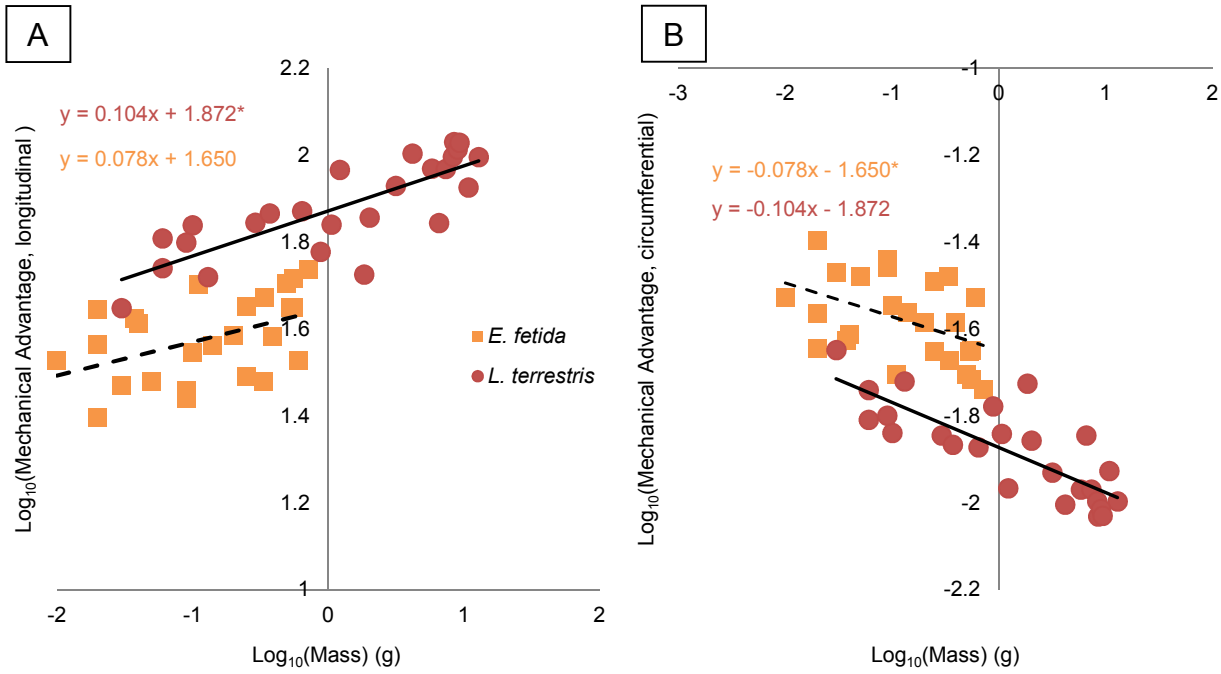

Fig. 3.7: Comparison of calculated mechanical advantage with body mass. Mechanical advantage was calculated by normalizing each worm's average *L/D* across segments with mass and calculating the reciprocal of distance advantage over 25% radial strain. (A) Mechanical advantage of longitudinal muscle contraction and (B) mechanical advantage of circumferential muscle contraction as a function of earthworm body mass. * Indicates a significant difference between species with the Bonferroni correction. N=25 per species.

I also observed significant differences in the scaling of calculated force production between the two species (Fig. 3.8; Table 3.3). In the anterior segments (Fig. 3.7), I found calculated force output during longitudinal muscle contraction at any given body mass was

greater for *L. terrestris* than for *E. fetid*a (log a_{Lt}=2.383; a_{Ef}=2.003). In addition, longitudinal muscle force production increased at a greater rate with mass in *L. terrestris* than *E. fetida* (log b_{Lt}=0.716; b_{Ef}=0.617) though this difference was not statistically significant with the Bonferroni correction. In the case of calculated circumferential muscle force production, however, *E. fetida* had a greater circumferential force output at a given body mass than did *L. terrestris* (log a_{Lt}=-2.584; log a_{Ef}=-2.288), but similar growth rates (b_{Lt}=0.568; b_{Ef}=0.465).

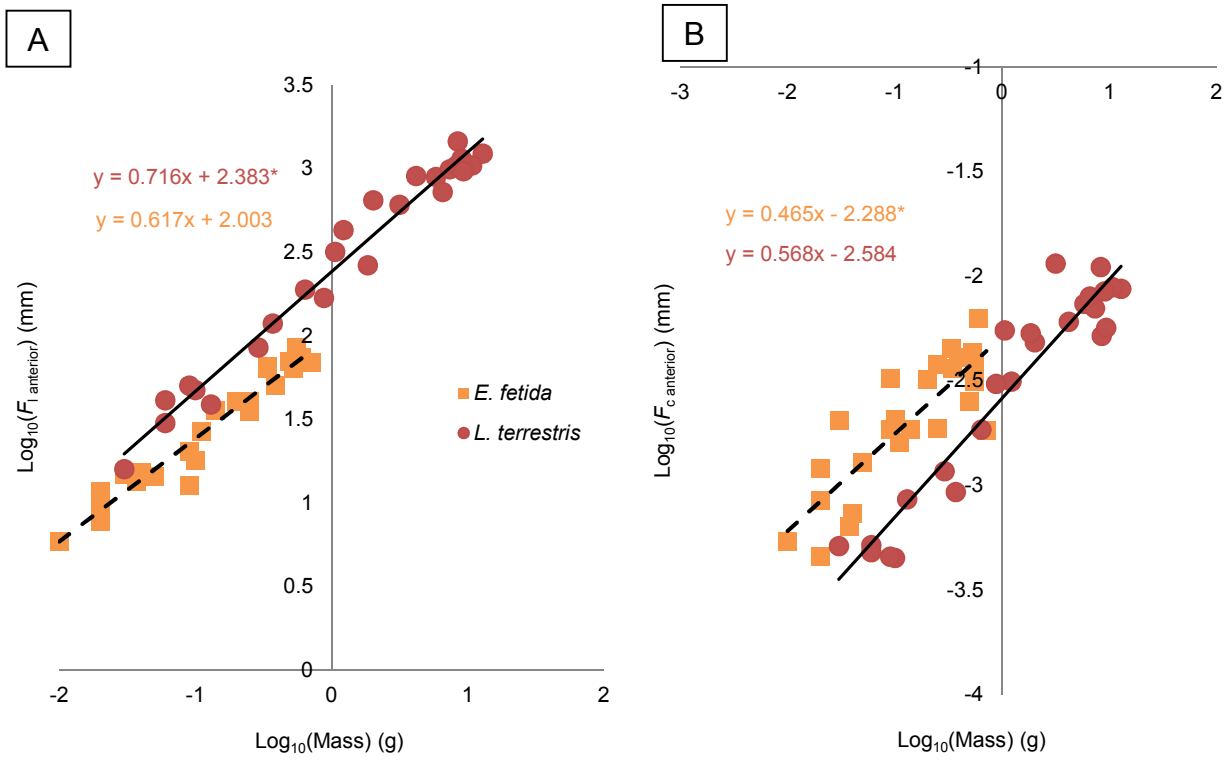

Fig. 3.8: Comparison of calculated force production with body mass. Force production was estimated for each worm using its mechanical advantage and muscle cross-sectional area. Mechanical advantage was calculated by normalizing each worm's *L*/*D* ratio with mass and calculating the reciprocal of distance advantage over 25% radial strain (A) Force production during anterior longitudinal muscle contraction and (B) force production during anterior circumferential muscle contraction as a function of earthworm body mass. * Indicates a significant difference between species with the Bonferroni correction. N=25 per species.

I found that most of the differences in force production between *E. fetida* and *L. terrestris* were consistent across segments (Table 3.3). Longitudinal muscle force production in the middle and posterior segments was greater for a given mass in *L. terrestris* than *E. fetida* (log a_{Lt}=

2.245; log a_{Ef}=2.041 in middle segments; log a_{Lt}= 2.251; log a_{Ef}=2.086 in posterior segments), though these segments did not show significant inter-specific differences in the rates of longitudinal force production with size (b_{Lt} =0.649, b_{Ef}=0.630 in middle segments; log b_{Lt}= 0.668, log b_{Ef}=0.717 in posterior segments). Circumferential muscle force production also exhibited similar trends to the anterior segments, with higher intercepts in *E. fetida* (log a_{Lt}= -2.838, log a_{Ef} -2.380 in the middle segments; log a_{Lt}= -2.920, log a_{Ef} -2.258 in the posterior segments) and similar scaling exponents between the two species (b_{Lt} =0.681; b=0.550 in the middle segments; b_{Lt} =0.688; b=0.665 in the posterior segments).

Linear Dimension (y)	*L. terrestris*' Intercept (Log a_{Lt})	*E. fetida*'s Intercept (Log a_{Ef})	P- value	*L. terrestris*' Scaling Exponent (b_{Lt})	*E. fetida*'s Scaling Exponent (b_{Ef})	P- value	R^2
$F_{l\ anterior}$	2.383	2.003	**$9.13 \cdot 10^{-13}$***	0.716	0.617	**0.02**	0.946
$F_{l\ middle}$	2.245	2.041	**$2.11 \cdot 10^{-7}$***	0.649	0.630	0.633	0.946
$F_{l\ posterior}$	2.251	2.086	**$1.39 \cdot 10^{-5}$***	0.668	0.717	0.334	0.916
$F_{c\ anterior}$	-2.584	-2.288	**$9.59 \cdot 10^{-8}$***	0.568	0.465	0.154	0.703
$F_{c\ middle}$	-2.838	-2.380	**$1.08 \cdot 10^{-12}$***	0.681	0.550	0.066	0.759
$F_{c\ posterior}$	-2.920	-2.258	**$3.43 \cdot 10^{-15}$***	0.688	0.665	0.759	0.783

Table 3.3: Scaling of calculated force production in *L. terrestris* (vertical burrower) *E. fetida* (surface-dweller). Calculated force production was estimated for each worm using its mechanical advantage and muscle cross-sectional area. Mechanical advantage was calculated by normalizing each worm's *L/D* ratio with mass and calculating the reciprocal of distance advantage over 25% radial strain. F_l and F_c refer to longitudinal muscle and circumferential muscle force output, respectively. The subscripts anterior, middle and posterior denote the locations sampled. * Indicates a significant difference between species with the Bonferroni correction. N=25.

Discussion

Previous studies found that the hydrostatic skeleton in *L. terrestris* scales allometrically but the reasons for these growth patterns remain unclear (Quillin, 2000; Kurth and Kier, 2014). I hypothesized that one important factor may be compensation for the effects of soil strain hardening as the animal becomes larger. I compared the hydrostatic skeleton across ecotypes in earthworms using interspecific and ontogenetic methods. My results are consistent with the

strain hardening hypothesis, and suggest that a disproportionately thin diameter, small volume, and large forces during longitudinal muscle contractions are key burrowing adaptations in soft-bodied animals.

Linear Dimensions and Volume

I found burrowing species across clades to have higher *L/D* ratios than surface-dwellers, consistent with previous research by Piearce, 1983. These *L/D* differences were reflected in both the interspecific and ontogenetic scaling of linear dimensions. The interspecific scaling analysis revealed that both ecotypes grew disproportionately long and thin, but burrowing species were significantly longer and thinner than surface-dwelling species. Ontogenetically, both the burrowing *L. terrestris* and surface-dwelling *E. fetida* grew disproportionately long and thin. At any given body mass, however, *L. terrestris* was significantly thinner than *E. fetida*. As a result, burrowers have higher *L/D* ratios and smaller body volumes than surface dwellers. Since burrowers would experience greater selective pressures for thin, small bodies than surface dwellers in order to alleviate strain hardening underground, the results are consistent with the strain hardening hypothesis.

Mechanical Advantage

Ontogenetic changes in mechanical advantage showed similar trends between species since the *L/D* ratio increased in both during growth. For both species, mechanical advantage increased with body size for longitudinal muscle contraction and decreased with body size for circumferential muscle contraction. The magnitudes of mechanical advantage, however, differed slightly between the two species due to differences in *L/D* ratios. *L. terrestris* had greater mechanical advantage during longitudinal muscle contraction, while *E. fetida* had greater mechanical advantage during circumferential muscle contraction. I believe these differences in

mechanical advantage highlight the relative importance of the longitudinal and circumferential muscles in burrowing and crawling, respectively, as discussed below.

I found it surprising that for *E. fetida* the mechanical advantage during circumferential muscle contraction decreased with growth, given the importance of circumferential muscles in surface crawling (Gray and Lissman, 1938; Seymour, 1969). As I discuss below, however, an increase in circumferential cross-sectional area appears to compensate for the loss of mechanical advantage; the circumferential muscles in *E. fetida* are significantly larger than those in *L. terrestris*.

Differences in Calculated Force Production

The segments measured in *E. fetida* are estimated to produce significantly higher circumferential force and significantly lower longitudinal muscle force along the length of the body when compared with similar segments in *L. terrestris.* These differences agree with previous research that suggested that circumferential muscles are of great importance for crawling while the longitudinal muscles are essential for burrowing (Chapman, 1950; Seymour, 1969). Powerful circumferential muscle forces would permit surface dwelling worms to squeeze in-between rocks, litter, and debris on the surface and potentially escape predation and desiccation. Conversely, robust longitudinal muscle forces would allow burrowing earthworms to overcome strain hardening in soil by exerting sufficient force to laterally displace soil, expand the burrow walls, break up soil particles ahead of the burrow, anchor the worm, and pull posterior segments into the burrow (Seymour, 1969; McKenzie and Dexter, 1988; Keudel and Schrader, 1999; Barnett et al., 2009).

Scaling Similarities

Although my results showed significant differences in the magnitude of musculoskeletal dimensions and calculated forces (i.e. different intercepts) between surface-dwellers and burrowers, it is unclear why both burrowers and surface-dwellers exhibit scaling similarities (i.e. similar scaling exponents). For example, both burrowing and surface-dwelling ecotypes grow disproportionately long and thin and are predicted to exhibit similar increases in circumferential and longitudinal muscle forces with size. These shared scaling trends may be the result of ecological, physiological, or functional similarities between the species.

For instance, both ecotypes may growth disproportionately thin because the relative surface area for gas exchange would be enhanced in larger individuals. Since the burrowing earthworms are more likely to encounter hypoxic regions than surface-dwellers, there may be increased selection pressure for a high *L/D* ratio in burrowing species.

Similar increases in the rates of force production with size may result from the shared functions of these muscles across ecotypes. The circumferential muscles in all earthworms must grow sufficiently powerful to push the animal forward and excavate through debris or soil. The longitudinal muscles in all species must provide sufficient forces to anchor the earthworm, prevent backslip, pull posterior segments forward, and dilate away constrictive soil or debris.

CHAPTER 4: ANALYSIS OF THE SCALING OF BURROWING MECHANICS USING X-RAY CINEMATOGRAPHY AND ROBOTICS

Summary

Burrowers range from micrometers to meters in length, and act as important ecosystem engineers in a variety of habitats. Despite the ecological importance of burrowing, little is known about the effects of body size on soil/animal interactions during burrowing. I studied the ontogenetic scaling of burrowing mechanics using a combination of X-ray filming and robotic modeling. I hypothesized that larger worms may be less effective at burrowing than smaller worms because larger worms must displace greater volumes of soil in order to burrow, which may cause the soil to stiffen. To test this hypothesis, I attached lead markers on specific sites on the anterior portion of *L. terrestris* worms ranging in body mass from 0.075g-7.812g. I then used bi-planar x-ray cinematography to film the marked worms burrowing through topsoil in three dimensions to analyze the scaling of burrowing kinematics. I also constructed inflatable worm-like robots varying in size from 2mm to 26.2mm in diameter to measure the relationship between radial strain and inflation pressure in soil across worm sizes. My results are consistent with my hypotheses and indicate that smaller burrowers are faster than larger burrowers, perhaps because they experience less strain hardening of the soil. I have found the scaling of burrowing kinematics to be fundamentally different from the scaling of surface crawling kinematics in soft-bodied invertebrates.

Introduction

Burrowing animals vary in body size, taxonomy, and geography, and live in a variety of aquatic and terrestrial substrates. These "ecosystem engineers" are of environmental and agricultural interest, due to their ability to break down and recycle organic matter, aerate soils, increase water infiltration, and alter soil density (Edwards and Bohlen, 1977). Despite the environmental importance of burrowing animals, many aspects of burrowing mechanics remain unexplored, including the effects of size and scale. The body length of burrowers ranges over orders of magnitude, from micrometer long nematodes to meter long earthworms. Relatively little research, however, has focused on how body size might affect a burrower's interactions with the soil (e.g. Piearce, 1983; Chi and Dorgan, 2010). Anthropogenic and ecological changes in soil could impose size-dependent effects on burrowers that can only be predicted by understanding the scaling of burrowing kinematics and mechanics.

One of the difficulties in attempting to address this question is the inability to observe burrowing animals in natural conditions. This challenge becomes exacerbated for the smallest burrowers, because they are difficult to track and can be easily lost in the substrate. Attempts by previous researchers to record animals burrowing against a glass plate or in transparent gels are problematic because they do not completely replicate the mechanics and three-dimensional structure of the native habitat (Trevor, 1976; Dorgan et al., 2005). To overcome these difficulties, I used novel methods including 3D X-ray cinematography and the construction of inflatable 'worm robots'. I was able to use X-ray cinematography to visualize lead markers placed on *Lumbricus terrestris* earthworms underground, and to determine the effects of size on burrowing kinematics (Fig. 4.1A). I also used X-ray cinematography on a size range of buried

worm robots during inflation to test for size-dependent changes in soil stiffness during lateral expansion (Fig. 4.1B).

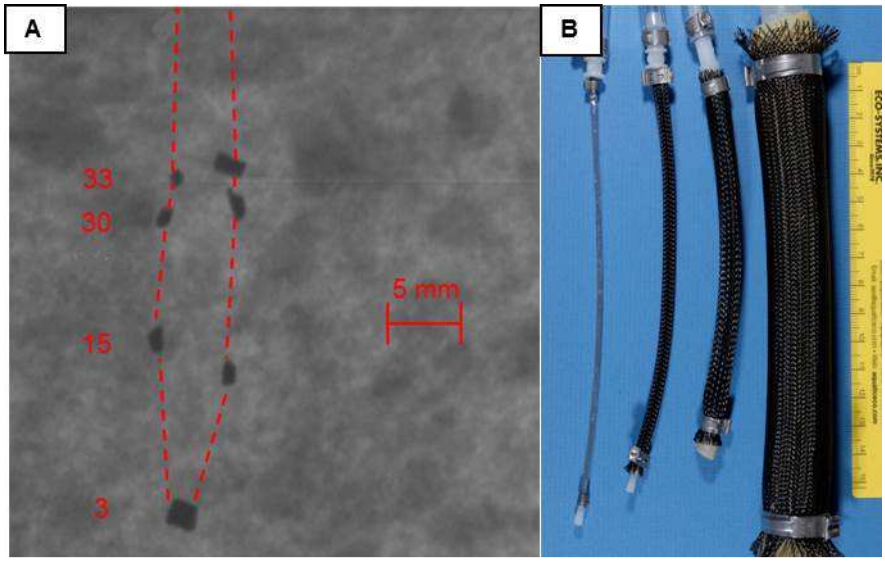

Fig. 4.1: X-ray image of head-first burrowing *L. terrestris* earthworm and a size range of worm robots. A. The grey medium is commercial grade topsoil, while the black markers are the lead chips attached to the earthworm. The numbers beside the lead markers indicate the worm's segment number where the marker was attached. The red dashed lines show an approximate outline of the earthworm's body based on the position of the lead markers. **B.** The various sizes of uninflated worm robots from smallest to largest. I refer to these as small, medium, large, and extra-large from left to right, respectively.

I used *L. terrestris* earthworms for the kinematic study because this species is a robust burrower and grows up to three orders of magnitude in body mass during development (Quillin, 1998). *L. terrestris* burrows using peristaltic waves that travel backwards from the anterior end. Two orientations of muscle fibers, circumferential and longitudinal, are responsible for this peristalsis. Circumferential muscle contraction elongates the worm, allowing it to move forward and excavate a new burrow; the longitudinal muscles expand the worm laterally, and are responsible for the majority of soil displacement and burrow enlargement (Barnett et al., 2009). In addition, the radial straining of the soil by the longitudinal muscles breaks up soil particles ahead of the worm, reducing the pressure required for axial elongation (Abdalla et al., 1969;

Whalley and Dexter, 1994; Keudel and Schrader, 1999; Dorgan et al., 2008).There are typically 1 to 2 simultaneous waves of circumferential and longitudinal muscle contraction along the length of the worm during locomotion (Gray and Lissman, 1938; Quillin, 1999).

The kinematics experiment tested for the effects of scaling on burrowing locomotion, while the robotics experiments tested for the presence of strain hardening in soils. Strain hardening occurs when granular soils become increasingly stiff (i.e. the modulus of compression increases) with increases in strain (Chen, 1975; Yong et al., 2012; Holtz et al., 2010). This phenomenon could become a significant problem for worms as they increase in body size. As a worm grows, it must strain a greater volume of soil in order to burrow, thus strain hardening effects are expected to increase with body size (Kurth and Kier, 2014).

I first measured the ontogenetic changes in *L. terrestris* burrowing kinematics in natural topsoil. On the surface, larger worms crawl faster than smaller worms (Quillin, 1999); if the opposite trend occurs during burrowing, then larger worms could be experiencing greater resistance to burrowing, which would support the strain hardening hypothesis. I also investigated strain hardening in soils using inflatable worm robots constructed from Mckibben actuators. These robots shorten and expand laterally during inflation, mimicking the actions of the longitudinal muscle in earthworms. I constructed a variety of robot sizes that encompassed the diameters of hatchling, juvenile, and adult *L. terrestris* earthworms (Fig. 4.1B). I also constructed a robot with a similar diameter to some of the largest earthworm species (Lang et al., 2012). By determining the relationship between inflation pressure and diameter for each size class of robot, I was able to test if larger robots experienced stiffer soil than smaller robots.

If the strain hardening hypothesis is supported, the results would indicate a special case in animal locomotion in which smaller animals prove faster and more effective at moving than

larger animals. This would be a stark contrast to scaling effects in many other forms of locomotion, including surface crawling in the same earthworm species (*L. terrestris*). Strain hardening also has the potential to challenge many other burrowing species and may be present in a range of additional soil types (Yong et al., 2011).

Materials and Methods

X-Ray Kinematics

Juvenile (1-3g) *L. terrestris* worms were supplied by Knutson's Live Bait (Brooklyn, MI USA) as well as raised from hatchlings bred in a colony maintained in the laboratory. Adult worms (3-10g) were purchased locally, raised from purchased juveniles, and raised from colony hatchlings. Hatchlings were raised from cocoons deposited by adults bred in the laboratory colony. All worms were housed in plastic bins filled with moist topsoil (composed of organic humus and peat moss) at 17ºC (Berry and Jordan, 2001) and were fed dried infant oatmeal (Burch et al., 1999).

To begin each kinematic experiment, I selected an earthworm, patted it dry to remove soil particles and mucus, and weighed it on a mass balance. I then glued X-ray opaque lead markers onto its body for tracking. Biological glue (Vetbond™) was not secure, so I used cyanoacrylate glue (Crazy Glue®, Westerville, Ohio) instead. One lead marker was attached dorsally on the worm's anterior end (~segment 3; counting from anterior to posterior). I also attached pairs of lateral markers on segments 15, 30, and 33 (Fig. 4.1A). Worms under 0.5g, however, only had markers attached to segments 3 and 15. The hatchlings were sensitive to excessive handling, and would become inactive if additional markers were attached. Most juveniles and adults, however, resumed normal peristaltic crawling once all of the markers were attached. If the earthworm appeared to be active and behaving normally after the attachment of lead markers, (i.e.

undergoing peristalsis; not writhing or displaying escape reflexes), it was then used in the experiments. Worms that did not display normal behavior were not used.

I used two X-ray systems linked to cameras for burrowing filming. One X-ray system consisted of a flat panel detector, while the other system used a C-arm apparatus and image intensifier. All of the X-ray experiments conducted were in accordance with the Georgia Institute of Technology's radiation protocols. The X-ray systems were set to 95 kV and 20 mA. I placed the two X-ray sources orthogonally to one another, and placed X-ray detectors linked to cameras opposite of the X-ray sources (Fig. 4.2). I then placed a one-gallon cylindrical glass container filled with commercial topsoil (Scotts ® Premium Topsoil) in-between both x-ray sources and the two detectors. The topsoil within the container was first dried and weighed, and was then wetted and patted down to a bulk density of 0.83g/cm^3 and moisture content of 0.23 g H_2O/g soil. I settled on this combination of bulk density and moisture content because the earthworms were willing to burrow in it, and it represented reasonable estimates for soil conditions in grasslands and forest topsoils (Adams and Froehlich, 1981; Chanasyk and Naeth, 1995; Davidson et al., 1998; Davidson et al., 2000). The soil was also cooled and mixed in-between trials to approximately 15°C to minimize heat induced stress to the earthworms (Berry and Jordan, 2001) and to prevent soil compaction. In-between trials, the soil was stored in a closed container to minimize evaporative water loss from the soil that would alter moisture content.

Once the soil was prepared and placed in-between the x-rays, I inserted a ball point pen approximately 2.5cm into the soil to create a divot. I then inserted a worm head-first into the divot and covered the worm with topsoil. Once the worm was covered, I patted the soil down to the desired bulk density. Creating this divot stimulated the earthworms to begin burrowing;

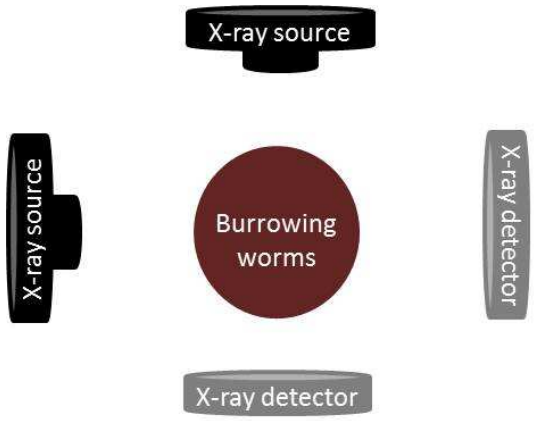

Fig. 4.2: Experimental setup for x-ray kinematics experiment. A one gallon glass container filled with topsoil and lead marked earthworms was placed in-between two X-ray sources and their corresponding X-ray detectors and cameras. One detector was a flat panel system, while the other detector was a C-arm apparatus with an image intensifier.

simply placing the earthworm into the container motivated the worm to crawl but not to burrow. To motivate the worms to burrow as quickly as possible, I placed a drop of liquid detergent on the tail as an irritant. If I observed the worm beginning to undergo peristalsis into the soil I would then turn on the x-rays and begin recording. If the worm remained still or backed out of the burrow, I would remove it and use another worm.

I tracked the progression of the lead marked earthworm into the topsoil using MATLAB tracking software (Serrano et al., in prep.) on the x-ray recordings. I measured several aspects of the burrowing kinematics in relation to body size, including: stride length, stride frequency, duty factor, burrowing speed, burrowing direction, and longitudinal/radial strain in the hydrostatic skeleton. I measured stride length as the distance moved per peristaltic wave, stride frequency as the number of peristaltic waves per second, and duty factor as the ratio of the time the worm was stationary over the sum of the time the worm spends active and stationary. Longitudinal strain was calculated as the change in body length during peristalsis over the elongated length during peristalsis, while radial strain was calculated as the change in width during peristalsis over the

expanded width during peristalsis. My calculations follow the analysis of earthworm crawling kinematics in Quillin, 1999. See Quillin, 1999 for details.

Since earthworms burrow headfirst, I tracked the progression of anterior-most marker on segment 3 in order to determine the scaling of burrowing speed, stride length, stride frequency, and duty factor. I calculated axial strain by measuring the changes in length between segments 3 and 15. I calculated radial strain by measuring the changes in width between the paired markers on segment 15.

Robotics Construction and Testing

The worm robots were designed to ensure there would be no aneurysms in the tubing during inflation. The smallest robot was made from a McKibben actuator provided by C. Rahn, Pennsylvania State University, University Park, PA USA, while the remaining robots were constructed from latex tubing inside double braided expandable fray-resistant polyester mesh sleeving. All robots were approximately 30 cm long but varied significantly in diameter. I called the smallest diameter tubing the "small" size, which mimicked hatchling *L. terrestris* earthworms in diameter and was approximately 2mm wide uninflated. The "medium" tubing mimicked juvenile earthworms and was approximately 5 mm wide, while the "large" size tubing was 7 mm wide, and mimicked adult earthworms. As an extreme example, I also constructed an "extra-large" size robot whose diameter mimicked that of the Amazonian Earthworm, *Rhinodrilus priollii,* and was 26.2mm wide. (Lang et al., 2012). Each robot was horizontally placed in a 1.5 gallon plastic rectangular container which was halfway filled with topsoil. The soil used was sifted through a 5 mm^2 mesh to minimize differences in soil properties between trials. The soil was also wetted to the same moisture content as the soil from kinematics experiment (discussed

above), and was stored in a closed container between trials to minimize water loss from evaporation.

Once the robot was placed on top of the soil, I covered the robot with additional soil until the container was completely filled. The soil was then patted down to the same bulk density used in the kinematics experiment. The robots were inflated using house air in the lab, which generated sufficient pressures to inflate all robots in air and in soil (0 PSI-120 PSI). Because the robots were air-filled and hollow, they were easily visible in the X-ray image. Consequentially, I was able to simultaneously measure changes in inflation pressure and robot diameter using pressure transducers (Omega® PX309-100G 5V, Stamford, CT) and X-ray filming. I also simultaneously recorded changes in inflation pressure and robot diameter in air to determine the resistance of the robot itself to inflation (see Strain Hardening Calculations below for details).

Strain Hardening Calculations

I manually measured changes in worm diameter from the X-ray videos at 3-6 different pressures during inflation. I was unable to distinguish changes in robot diameters at additional pressures because of the low resolution of the robot's body in the X-ray videos. To determine changes in stiffness during robot inflation, I plotted the relationships between inflation pressure and radial strain for each robot size in both air and soil. Radial strain was calculated as:

$$\frac{Inflated\ Diameter - Uninflated\ Diameter}{Uninflated\ Diameter} \quad (1)$$

I was then able to deduct the pressure at any given strain in air from the pressure at that given strain in soil. This allowed me to subtract out the resistance of the robot to inflation and determine the resistance of the soil alone to inflation. I call this subtracted pressure the "corrected pressure" in my figures and discussion. Changes in stiffness were determined by the presence of non-linearity in the slopes of strain/corrected pressure curves (Vogel, 2003).

I also mapped changes in "corrected pressure" against changes in robot diameter to directly compare the inflation behavior of the robots to one another. Change in diameter was calculated as:

$$Inflated\ Diameter - Uninflated\ Diameter \quad (2)$$

I performed static tests by manually inflating the robots with house air, as well as dynamic tests using a function generator and pressure control valve to control the frequency, number, and rate of inflation. Both sets of tests showed similar behavior and minimal hysteresis in the loading and unloading curves (Fig. 4.3) so I pooled the data from both tests. I only measured the pressure/diameter characteristics of the first inflation in each trial, because the burrow was visibly formed after only one inflation cycle.

Statistical Analysis

I used R statistical software (R Development Core Team, 2014) for analysis of both the kinematics and robotics experiments. I fit my kinematic scaling data to the power function $y=aM^b$, where y represents the morphological traits of interest, a is the scaling constant, M is body mass, and b is the scaling exponent. Pressure/strain curves and a pressure/diameter change curve generated by the robotics experiments were fit to several potential functions and tested for goodness of fit via the Akaike Information Criterion (AIC) and residuals plots (Burnham and Anderson 2004). I ultimately fit power functions ($y=aX^b$) to pressure/strain curves and a third-order polynomial function to the pressure/ diameter change curve.

All power functions were subsequently $\log_{10}$ transformed to perform linear regression on the data. I chose RMA regression over OLS regression because OLS regression does not account for error in the independent variable, while RMA regression does (Rayner, 1985).

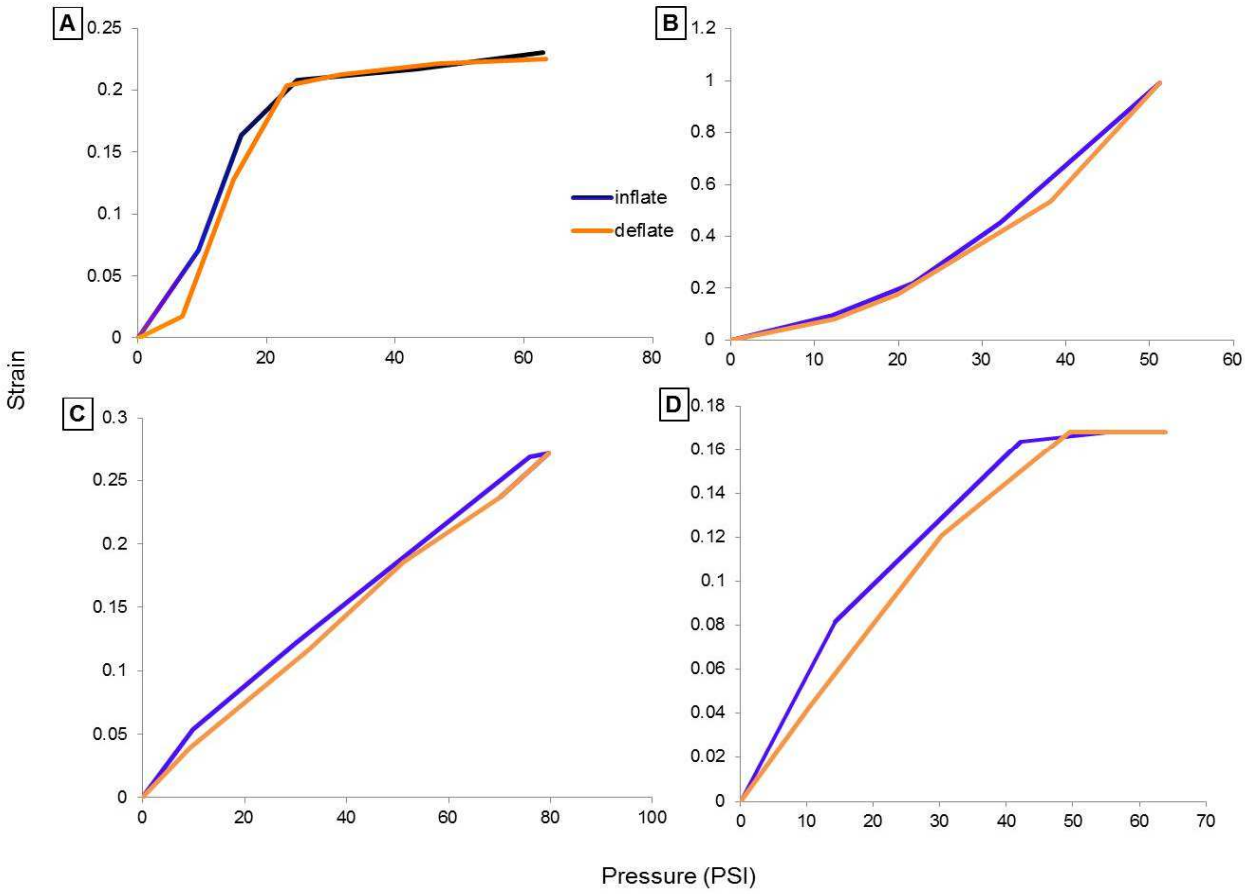

Fig. 4.3: Viscoelasticity and hysteresis testing in the worm robots. Comparison of pressure/strain curve during inflation and deflation in air for **A.** extra-large, **B.** large, **C.** medium, and **D.** small diameter robots.

I used the lmodel2 package (Legendre, 2011) in R to perform RMA regression and calculated the 95% confidence intervals of the slope to determine if the scaling exponent *b* was significantly different from other exponents (different from linearity in the robotics experiment and different from the scaling of crawling kinematics in the burrowing kinematics experiment).

Results

I found the scaling of *L. terrestris* burrowing kinematics to be significantly different than the scaling of surface crawling in this species. I found that burrowing speed decreased with body size (b=-0.34), indicating that smaller worms were able to burrow faster than larger worms (Figs 4.4 and 4.5A).

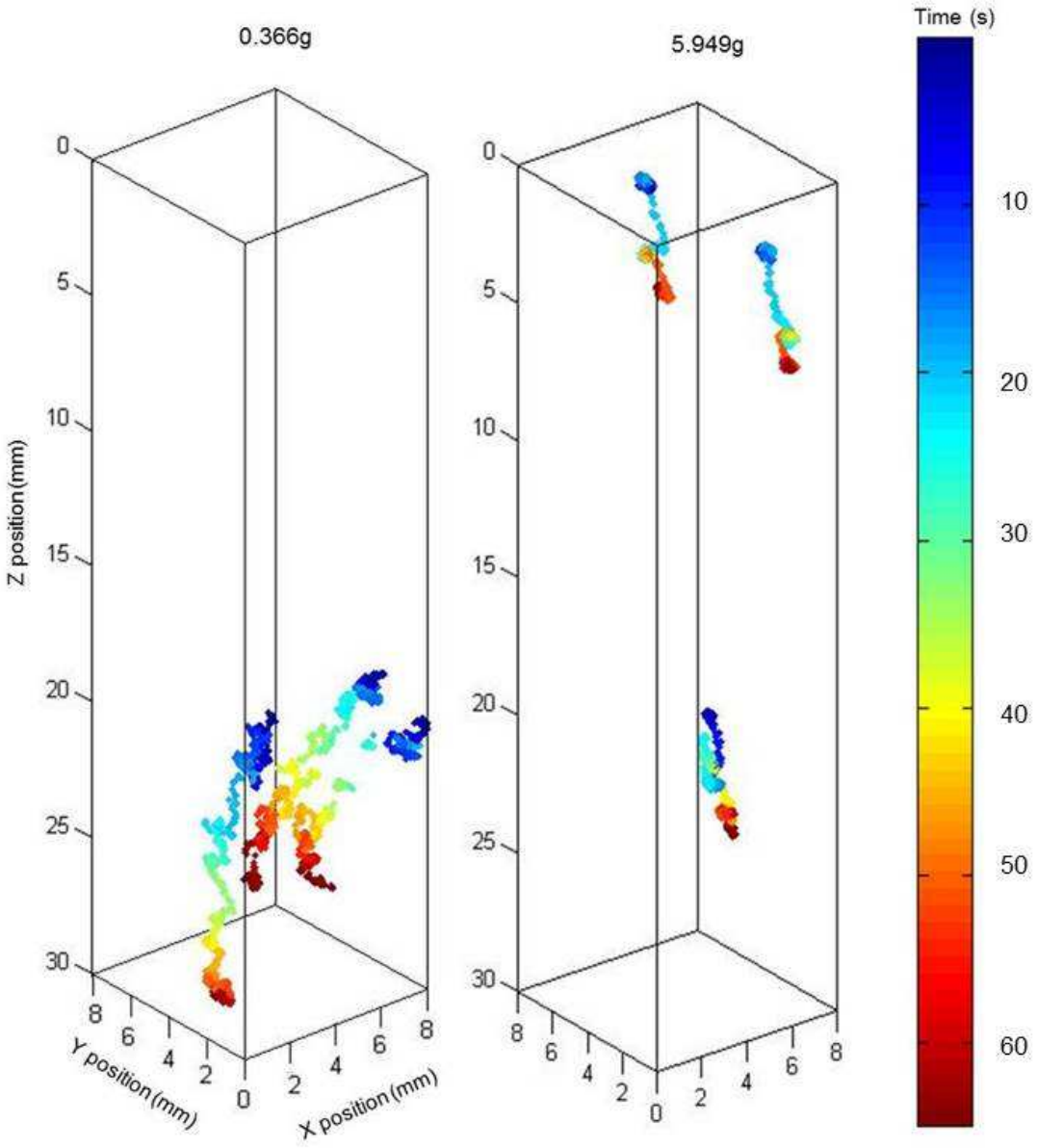

Fig. 4.4: Marker tracking of burrowing juvenile (left) and adult (right) *L. terrestris* earthworms. One marker was attached to segment 3 (bottom-most marker), and two markers were attached laterally on segment 15. Changes in color depict the progression of the earthworm through time after approximately 65 seconds.

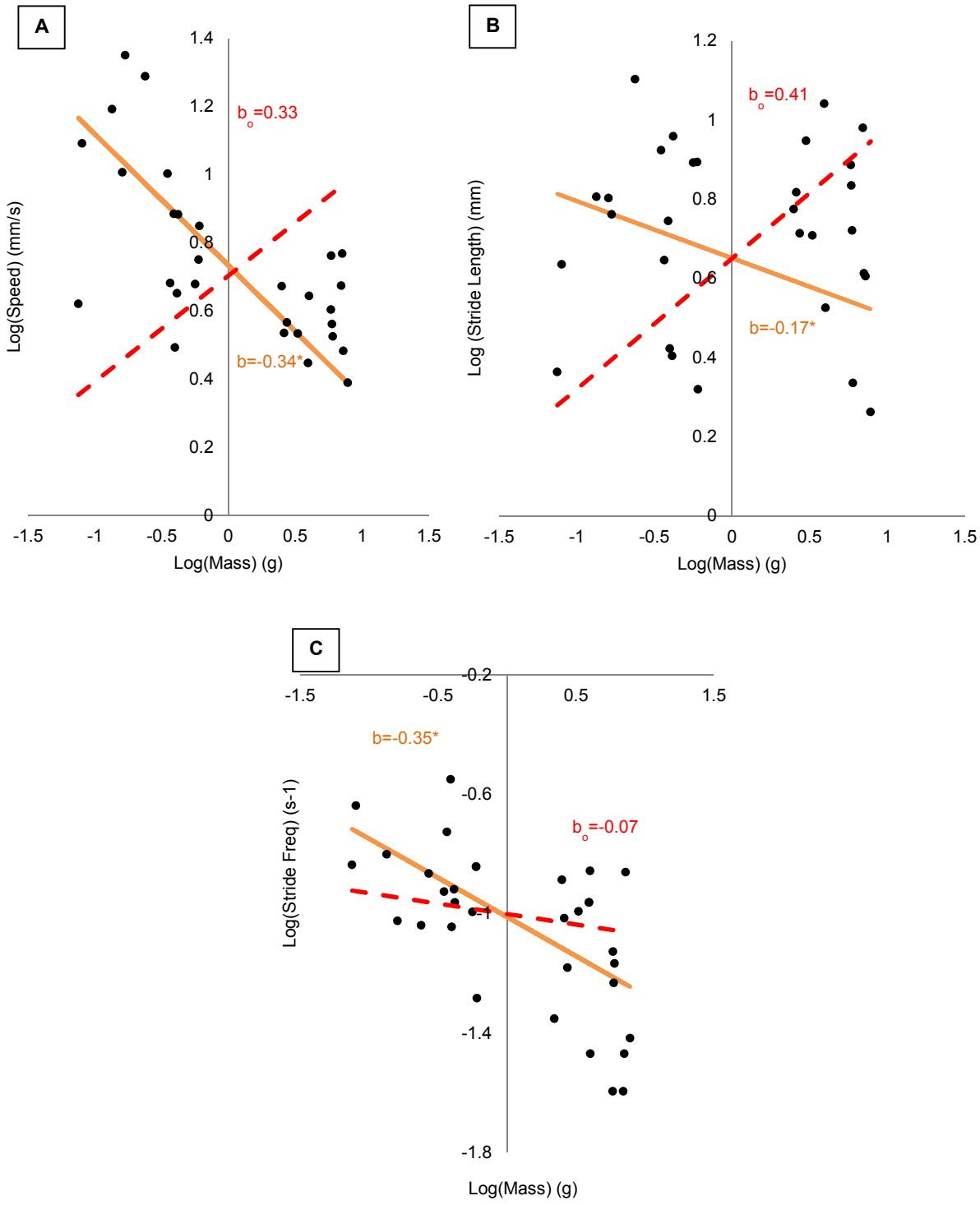

Fig. 4.5: The effects of body size on burrowing speed in topsoil. Plots depict $\log_{10}$ transformed data. The expected scaling (b_o) exponent from Quillin 1999's crawling kinematic study is the dashed line. The measured scaling exponent (b) fit to data with RMA regression is shown as the solid line. *Indicates non-overlapping 95% confidence with b_o. **A**. Burrowing speed plotted against body mass. **B**. Stride length during burrowing plotted against body mass. **C**. Stride frequency during burrowing plotted against body mass. N=29.

Smaller worms were able to burrow faster using higher stride frequencies (b=-0.35) and similar larger stride lengths (b=-0.17) compared with larger worms (Fig. 4.5B & 4.5C). The scaling of stride frequency and stride length during burrowing was also significantly different than the scaling of these variables during crawling (Quillin, 1999). In crawling, stride length increases with body size (b_o= 0.41), which is the opposite trend from burrowing. Stride frequency also decreases with body size during crawling (b_o= -0.07), but the size-related differences are greater in burrowing than in crawling.

I also found several other kinematic changes in burrowing locomotion, including changes in duty factor and skeletal strain. Duty factor (the ratio of time the worm is stationary relative to its total burrowing time) decreased with body size (b=-0.08), indicating that smaller worms were spending a smaller fraction of their time underground actively moving compared to larger worms (Fig. 4.6A), despite ultimately burrowing slower than the smaller worms. This difference was not, however, significantly different from the scaling of duty factor during crawling (b_o=-0.03) (Quillin, 1999). Strain in the body during elongation and expansion also exhibited negative scaling trends. Small worms were able to undergo greater bodily strains than larger worms during both elongation (b=-0.30) and expansion (b=-0.28) (Fig. 4.6B & 4.6C). These decreases in skeletal strain with increases in body size are not found in crawling earthworms (b_o=0.00 during elongation and expansion while crawling) (Quillin, 1999).

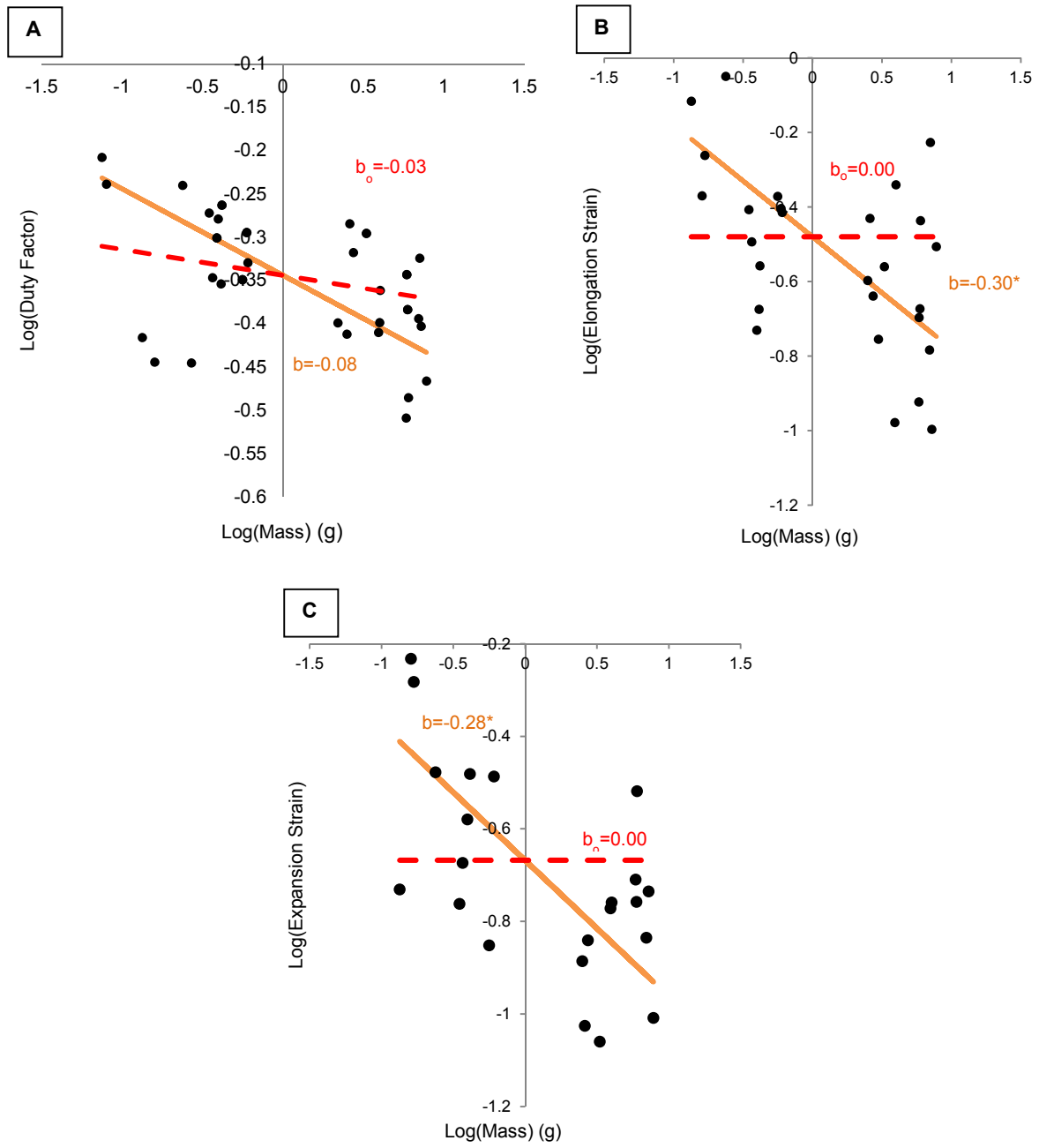

Fig. 4.6: The effects of body size on duty factor and skeletal strain. Plots depict $\log_{10}$ transformed data. The expected scaling (b_o) exponent is shown as the dashed line. The measured scaling exponent (b) fit to data with RMA regression is the solid line. *Indicates non-overlapping 95% confidence with b_o. **A.** Duty factor during burrowing plotted against body mass. N=29. **B.** Longitudinal strain during burrowing plotted against body mass. N=28. **C.** Radial strain during burrowing plotted against body mass. N=22.

In addition to kinematic differences, I found differences in soil behavior that were a function of robot size. Pressure/strain inflation curves were significantly different from linearity (b=1.00) in the extra-large and large worm robots (b=3.30 and 4.04 for extra-large and large robots, respectively) (Figs. 4.7A & 4.6B) but not in the medium and small robots (b=1.17 and 0.77 for the medium and small robots, respectively) (Figs. 4.7C & 4.7D).

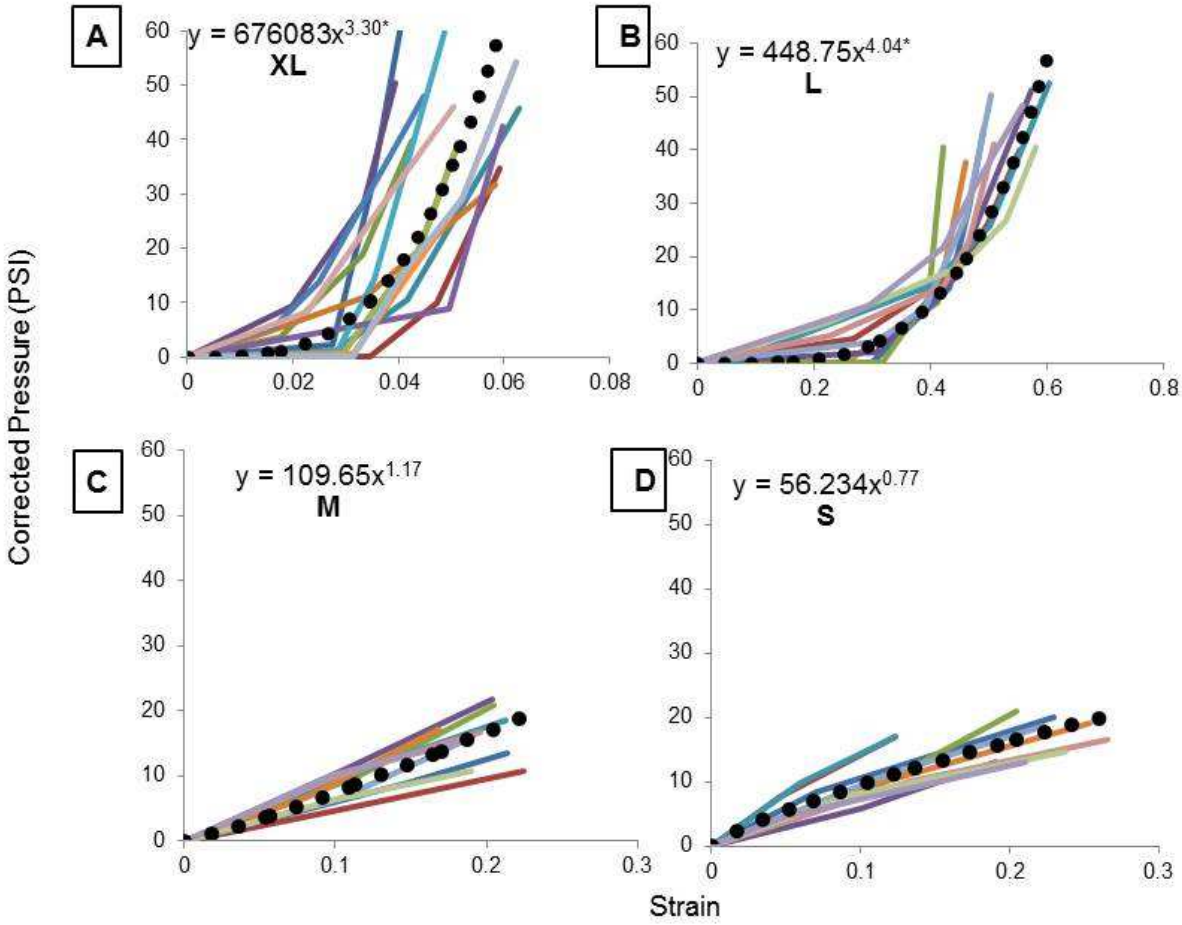

Fig. 4.7: **The effects of robot size on soil resistance to inflation**. Each colored line represents a single trial. 3-6 pressure and strain measurements were taken during inflation at for each trial. The black dotted lines and equations display log back-transformed coefficients fit from RMA regression. * Indicates a difference from linearity using 95% RMA confidence intervals. N=10. Plots **A-D** show the relationship between inflation strain and corrected inflation pressure in sifted topsoil (i.e. pressure to inflate in air subtracted out) in the: **A**. extra-large (XL), **B.** large (L), **C.** medium (M), and **D.** small (S) robots.

The inflation behavior of the robots appears to be tied the magnitude of diameter changes the robot undergoes in soil (Fig. 4.8). The pressures needed to inflate robots underground disproportionately increase once robots undergo sufficiently large diameter changes. Large and extra-large robots were capable of greater changes in diameter than medium and small robots but also required greater inflation pressures once large diameter changes had been achieved. (Figs 4.7 &4.8).

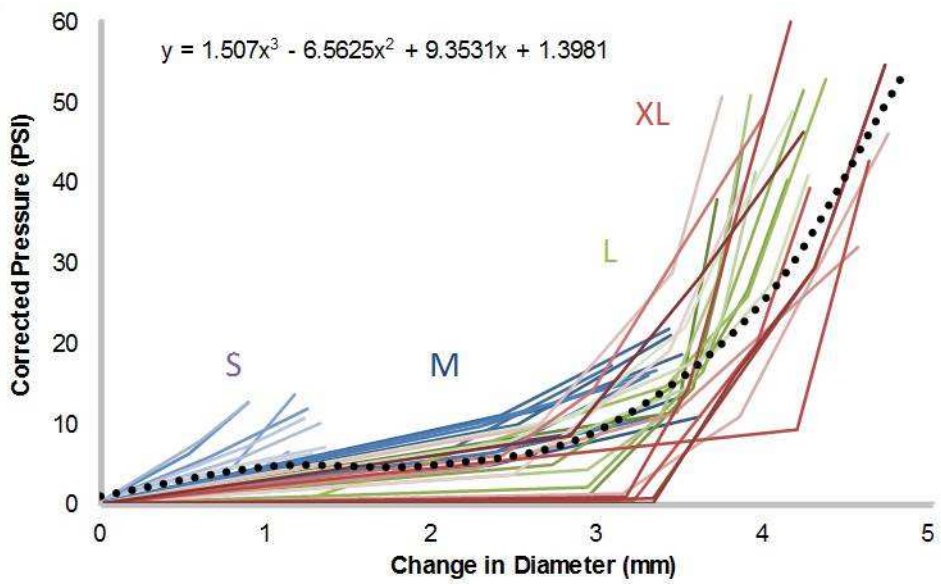

Fig 4.8: The relationship between changes in robot diameter and soil resistance to inflation. Each line represents a single trial. 3-6 pressure and strain measurements were taken during inflation at for each trial. N=10 trials per robot size. Light blue lines depict small robot (S) trials. Dark blue lines depict medium robot (M) trials. Green lines depict large robot (L) trials. Red lines depict extra-large (XL) trials. The black dotted line and equation displays the best-fit model fit for all of the trials across robot sizes pooled together.

Discussion

This study has uncovered an interesting exception in animal locomotion; smaller animals are faster at movement than larger animals (Alexander, 1995). In this case, smaller worms burrowed at faster absolute speeds than larger worms by taking similar stride lengths forward while undergoing peristalsis more frequently. This is a stark difference from the scaling of

surface crawling speed in this same species; during crawling, large worms are significantly faster than smaller worms as they take significantly longer strides forward (Quillin, 1999; Quillin, 2000). These unusual ontogenetic trends in burrowing kinematics may be linked to strain hardening in the soil, which causes larger burrowers to experience stiffer, more resistant soil than smaller burrowers.

I was able to support the strain hardening hypothesis using two novel experiments, 3D X-ray kinematics and inflatable worm robotics. The burrowing kinematics study found several ontogenetic trends consistent with strain hardening, including burrowing speed, stride length, duty factor, and body strain. These data indicated that large burrowers did not elongate and expand their bodies far underground, and spent a larger portion of the burrowing cycle actively attempting to progress forward into the soil. Despite the greater activity of the large worms, they were ultimately slower burrowers compared to their smaller counterparts. These kinematic data support a disproportionate increase in burrowing difficulty with increases in body size.

The robotics experiment also supported the strain hardening hypothesis by directly recording increases in soil stiffness during the inflation of the large and extra-large robot sizes, whose diameters were similar to adult *L. terrestris* earthworms and adult giant Amazonian earthworms (*Rhinodrilus priollii*), respectively (Lang et al., 2012; Kurth and Kier, 2014). The relationship between radial inflation strain and inflation pressure was positive and non-linear in these robots, indicating an increase in soil stiffness and the presence of strain hardening. Unlike the two largest robots, the medium and small robots' strain/pressure curves remained linear throughout inflation in soil, indicating no change in soil stiffness during inflation and the absence of strain hardening. The small and medium robots mimicked the diameters of the hatchling and juvenile *L. terrestris* earthworms, respectively. These results reflect the conclusions made in the

burrowing kinematics experiment; larger worms appear to experience greater difficulty burrowing compared with smaller worms due to strain hardening.

The presence or absence of strain hardening during burrowing may be related to the quantity of soil that must be displaced to make room for the burrower's body. In the large and extra-large robots, strain hardening began to occur once the robot had expanded sufficiently in diameter, causing larger and larger volumes of soil to be displaced by the increasing radial expansion of the robot. The small and medium robots, however, were incapable of large diameter changes due to their relatively small radial expansions and, consequently, neither experienced strain hardening. Why strain hardening occurs once the robots have expanded to sufficiently large diameters is likely due to the granular properties of topsoil. As the robots increase in diameter, soil particles must be compressed and rearranged to make room for the expanding robot. Soil stiffness likely increases due to changes in soil packing and a reduction in void space; the result is an increase in the number of contact points between particles and increasing rigidity (Lambe and Whitman, 1969; Hagerty et al., 1993; Dorgan et al., 2006).

My experiments provide evidence for repeatable, size-dependent and significant differences in soil behavior using inflatable robots that likely represent the actions of burrowers in a more meaningful way than previous penetrometer experiments and oedometer experiments. Penetrometers are rod-like devices used to determine soil strength via resistance to penetrometer insertion. Penetrometers of varying diameters do not show consistent differences in penetration resistance (i.e. stress). Some data indicate smaller penetrometers experience greater penetration resistance, while other studies do not find significant differences in penetration resistance across penetrometer sizes (Smith, 2000). The reason our robots did find size-related differences in soil resistance while penetrometers do not are likely due to experimental differences. Penetrometers

are driven into the soil axially do not radially expand once underground, whereas our robots only expand radially. As a consequence, resistance from the soil to penetrometers is largely due to friction, which is minimized in mucus-covered earthworms through lubrication of the skin (Edwards and Bohlen, 1996; Smith, 2000). In contrast, it is likely that soil resistance to the worm-like robots primarily results from compression of the soil during radial expansion.

The behavior of granular media during oedometer experiments is consistent with my robotics results in granular soil. Oedometer experiments are one-dimensional confined compression tests of soil; since many burrowing species compress soil during burrowing, oedometer tests may show soil behaviors relevant to burrowing animals (Trueman, 1975; Barnett et al., 2009). Odeometer tests on granular media show that increasing compressive pressure from 0-100PSI (the pressure range used in this study) results in higher soil stiffness (Lambe and Whitman, 1969). This is consistent with my findings, which showed increases in soil stiffness with increases in robotic inflation pressure.

These size-dependent differences in burrowing kinematics and mechanics have interesting implications for burrowing adaptations and constraints. My strain hardening results, for example, may explain why earthworms grow disproportionately thin and disproportionately increase longitudinal muscle force production during ontogeny (Kurth and Kier, 2014). Thin bodies would allow larger worms to radially displace less soil than a worm maintaining its relative proportions, which would reduce strain hardening. Robust longitudinal musculature would assist large worms in generating sufficient forces to counteract soil stiffening due to strain hardening.

Strain hardening may also impact a plethora of other burrowers and soil types. Many soft-bodied burrowers move using a similar dual anchoring mechanism to earthworms,

including: polychaetes, anemones, gastropods, and holothurians (Trueman, 1975), and size-dependent decreases in burrowing speed have also been documented in the burrowing marine worm, *Cirriformia moorei* (Che and Dorgan, 2010). These species interact with many types of granular soils, including: sands, silts, gravels, loams, and clays. Because strain hardening is characteristic of loose granular soils and consolidated clays, many soft-bodied burrowing species could potentially experience strain hardening (Yong et al., 2011). It is also possible that strain hardening imposes constraints on hard-bodied burrowers, but no research has investigated this issue.

More research is needed in burrowing biomechanics in order to elucidate the physical and biological interactions and constraints occurring underground. New methods, such as X-ray cinematography and robotics, may assist in resolving these issues by visualizing and mimicking the actions of burrowers. Burrowers play important biomechanical, physical, and ecological roles in the soil. This study has highlighted several important aspects of burrowing mechanics and raises additional questions for future research.

CHAPTER 5: THE SCALING OF PRESSURES AND FORCES DURING BURROWING IN THE EARTHWORM *LUMBRICUS TERRESTRIS*

Summary

Changes in body size alter and constrain many characteristics in organisms, including numerous aspects of locomotion. It is currently unclear, however, how changes in body size alter burrowing mechanics despite burrowers' taxonomic diversity, ecological importance, and vast size range. To explore this issue, I measured the scaling of pressure generation, force production, and locomotory costs during burrowing using an ontogenetic size range of *Lumbricus terrestris* earthworms. I measured pressure in the coelomic cavity of earthworms ranging in body mass from 0.12g-10.39g. In each trial, I stimulated worms to burrow against the sides of a transparent tank filled with topsoil so that the body was visible. Once the worm began to burrow I measured coelomic pressure during muscle contraction and calculated its force production and burrowing costs based on this pressure. I found both pressures and forces increased with body size at rates greater than predicted by the scaling of morphology alone. I also discovered that burrowing costs may rise rapidly as burrowers grow. These data suggest that burrowing becomes disproportionately more difficult as *L. terrestris* grows, possibly due to increases in soil stiffness with body size.

Introduction

Size affects how organisms interact with and move through the environment, yet the effects of size on burrowing locomotion are poorly understood (Piearce 1983; Quillin, 2000; Che and Dorgan, 2010). This is surprising considering that burrowers span orders of magnitude in body size, and their interactions with the soil are beneficial in maintaining soil and plant quality (Darwin, 1881; Whalley and Dexter, 1994). It seems unlikely that, for example, a microscopic nematode and a two meter long earthworm manipulate soil particles in a similar manner. What aspects of burrowing change when burrowers become larger or smaller?

The goal of this study was to understand how changes in body size alter burrowing forces and pressures. To address this issue, I used an ontogenetic size range of *Lumbricus terrestris* earthworms. This species is an ideal system for study because it is an adept terrestrial burrower and grows approximately three orders of magnitude during ontogeny. *L. terrestris* also burrows throughout its development, and readily exhibits burrowing behavior in a laboratory setting. Using internal pressure recordings during burrowing, I was able to calculate the scaling of burrowing pressures, forces, and costs.

I hypothesized that burrowing forces, pressures, and costs would disproportionately increase with body size due to strain hardening in soils. Strain hardening is an increase in the compressive modulus of soil due to increasing strain, such that soils become disproportionately stiffer the more they are compressed (Yong et al., 2012). Strain hardening is characteristic of loose granular soils and consolidated clays, and could pose a significant challenge for growing terrestrial burrowers that must strain and compress increasingly large volumes of soil (Chen, 1975).

If strain hardening occurs, then large worms would be forced to use significantly higher forces and pressures than smaller worms to overcome the increase in soil stiffness with body size. This steep increase in force production with body size would, in turn, contribute to sharp size-related increases in burrowing costs. My results would be consistent with the strain hardening hypothesis if the forces and pressures measured increase with body size at greater rates than predicted by the scaling of the musculoskeletal system ($Force \propto M^{>0.69}$ during longitudinal muscle contraction; $Force \propto M^{>0.62}$ for circumferential muscle contraction; $Pressure \propto M^{>0}$ during circumferential and longitudinal muscle contraction) and burrowing costs will increase at greater rates than other forms of locomotion ($Cost\ per\ distance \propto M^{>0.62\text{-}0.69}$) (Alexander, 1995; Vogel, 2003; Kurth and Kier, 2014).

Materials and Methods

Pressure Recordings

I used an ontogenetic range of *Lumbricus terrestris* earthworms ranging from 0.12g - 10.39g in body mass. Each worm was placed in a transparent plastic tank containing commercial grade topsoil (Scotts® Premium Topsoil). I attempted to keep a constant soil density of 0.82 g/cm^3, moisture content of 0.23 g water/g soil, and temperature of 15°C. Such soil conditions are representative of forest topsoils and are sufficiently cool to minimize heat-induced stress in *L. terrestris* (Adams and Froehlich, 1981; Chanasyk and Naeth, 1995; Davidson et al., 1998; Davidson et al., 2000; Berry and Jordan, 2001). I achieved consistent bulk density and moisture content by drying the soil in a 60°C oven overnight then adding the appropriate volume of water and mixing the soil thoroughly. I then patted the soil down to a consistent volume inside the plastic container. I refrigerated the tank (27cm x 17cm x 17cm) with soil between trials to keep the soil at approximately 15°C. I also mixed and patted the soil down between trials to prevent

increases in soil bulk density due to soil compaction and to keep the surface soil moist. To prevent water evaporation from the soil, I covered the top of the container with masking tape.

I connected a pressure transducer (BLPR, World Precision Instruments®, Sarasota, Florida) to polyethylene tubing with a needle (23-30G) at its end. I inserted the needles into the body cavities of earthworms to measure pressure while burrowing. I inserted the needle in approximately segment 20 of the earthworm, counting from the anterior end backwards. This segment was sufficiently anterior to be involved in burrow formation (personal observation), but was sufficiently posterior that the worm resumed peristaltic crawling once the needle was inserted. If the needle was inserted too near the anterior end, the worm would writhe and refuse to resume peristaltic crawling. Once the needle was inserted, each worm was placed "head first" into a 3cm divot in the soil against the wall of the tank (Fig. 5.1). The divot was then covered with soil and patted down to a consistent volume and bulk density. Creating this divot stimulated the earthworms to begin burrowing instead of crawling around the surface of the container. To motivate the worms to burrow as quickly as possible, I placed a drop of liquid detergent on the tail as an irritant. If I observed the worm beginning to undergo peristalsis into the soil I began recording; if the worms remained stationary or backed out of the soil I used another worm. I allowed earthworms to burrow for two minutes before removing them and prepping the soil for a new trial; earthworms were used for one burrowing trial only.

I recorded simultaneous pressure and video of the worm burrowing using LabVIEW© software (National Instruments™, Austin, TX). Simultaneous pressure and video recordings allowed me to differentiate between pressure peaks due to circumferential muscle contraction and pressure peaks due to longitudinal muscle contraction. I could also estimate the area over

which pressure was being applied using the video footage, and indirectly calculate the scaling of force production (see "calculations" below for force calculations).

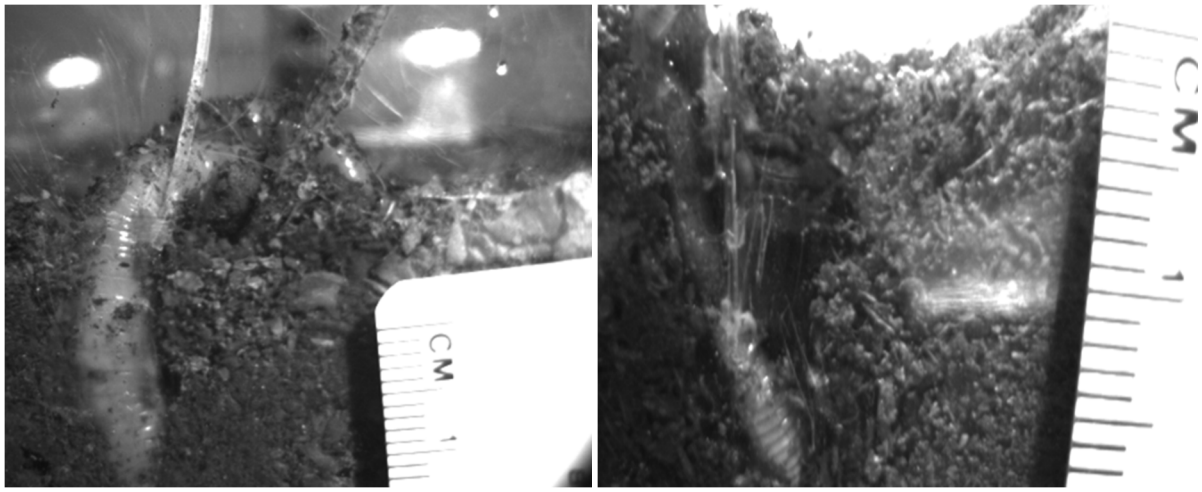

Figure 5.1: Images of burrowing adult (left) and hatchling (right) earthworms connected to pressure transducers. Worms burrowing against transparent plastic tank wall. Commercial topsoil used for substrate.

Calculations

I calculated force production as the product of the pressure in segment 20 and the area over which the pressure was applied. Force production during circumferential muscle contraction (F_{CM}) was calculated as the product of pressure production during circumferential muscle contraction (P_{CM}) and the area of application during circumferential muscle contraction (A_{CM}). Likewise, force production during longitudinal muscle contraction (F_{LM}) was calculated as the product of pressure production during longitudinal muscle contraction (P_{LM}) and the area of application during longitudinal muscle contraction (A_{LM}):

$$F_{CM} = P_{CM} \cdot A_{CM} \qquad F_{LM} = P_{LM} \cdot A_{LM} \tag{1}$$

Because contraction of the circumferential muscles causes axial elongation, A_{CM} is the cross-sectional area of segment 20. Conversely, contraction of the longitudinal muscles causes radial expansion, so A_{LM} is the surface area of segment 20 (Fig. 5.2; see Quillin, 2000 for details).

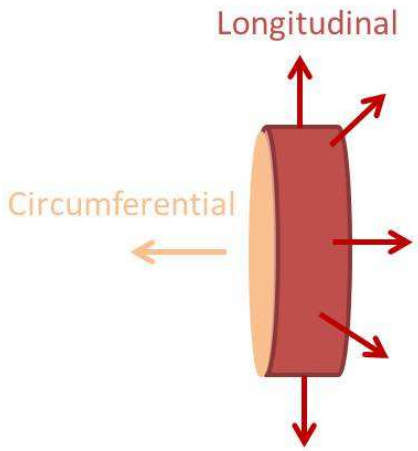

Figure 5.2: Area of application during muscle contraction. Schematic comparing the area of application in an earthworm segment during circumferential muscle contraction (orange) and longitudinal muscle contraction (red). The arrows show the direction the forces will be applied to the enviornment.

I calculated average and maximum pressure and force production for both circumferential and longitudinal muscle contractions. Average pressure and force were calculated from five pressure/area recordings in a single bout of burrowing; maximal pressure and force were taken from the largest recorded pressure peak.

I also used these force data to calculate the cost of burrowing locomotion in combination with with kinematic data from Chapter 4. In order to pool the data from both experiments, I matched up earthworms with similar body masses, thereby providing both force and kinematic data for a given earthworm size.

To estimate burrowing cost, I first determined the work per stride for each earthworm. For the purpose of these calculations, I counted a single stride as the combination of one peristaltic wave of circumferential muscle contraction (i.e. elongation) plus one peristaltic wave of longitudinal muscle contraction (i.e. expansion). I calculated work per stride as the product of force production and axial displacement of the body during one wave of circumferential muscle

contraction plus the product of force production and radial displacement of the body during one wave of longitudinal muscle contraction:

$$Work\ /Stride = F_{CM} \cdot d_{CM} + F_{LM} \cdot d_{LM} \quad (2)$$

Where d_{CM} is the axial displacement of the body during circumferential muscle contraction; d_{LM} is the radial displacement of the body during longitudinal muscle contraction.

Once work per stride was calculated I then determined the number of strides needed to move each worm 1cm forward into the soil. Forward movement of the earthworm only occurs during circumferential muscle contraction, so I only used d_{CM} for this calculation. I arbitrarily picked 1cm as the distance of interest since it is a distance earthworms can easily achieve underground in only several strides (Fig. 4.3B). Because d_{cm} was recorded in cm units, I divided 1 cm by d_{cm} to determine the number of strides needed to move 1cm forward:

$$Strides/cm = 1/d_{CM} \quad (3)$$

Once I determined the number of strides per 1cm distance, I multiplied this value by work per stride (Eq. 2) to determine work per cm distance for each earthworms:

$$Work\ /Distance = Work\ /Stride \cdot Strides/cm = Work/cm \quad (4)$$

By comparing work per cm distance with body mass, I was able to detemine how burrowing costs change with earthworm size. In addition, dividing work per distance by body mass allowed me to estimate cost of transport despite a lack of calorimetry data:

$$Work/\ (Distance \cdot Mass)\ \alpha\ Cost\ of\ transport \quad (5)$$

Statistical Analysis

I used R (R Development Core Team, 2014) for statistical analysis. I performed ordinary least squares (OLS) regression on the log transformed scaling data fit to the power function $y=aM^b$, where y represents the morphological traits of interest, a is the scaling constant, M is body mass, and b is the scaling exponent. I calculated the 95% confidence intervals of the slope to determine if the scaling exponent b was significantly different from the expected scaling exponent, b_o (e.g. Herrel and O'Reilly, 2006; Nudds, 2007; Chi and Roth, 2010). In this case, the expected scaling exponents were the changes in pressure and forces due to scaling of the hydrostatic skeleton.

Results

During burrowing, recorded pressures increased with body size at a greater rate than expected by the scaling of the skeleton alone (Fig. 5.3 and 5.4). Average pressure increased with body size during both the circumferential and longitudinal muscle contraction (b=0.22 and 0.18 for the longitudinal and circumferential muscles, respectively) (Fig. 5.3). This trend is not explained by the scaling of the hydrostatic skeleton, which is predicted to maintain constant coelomic pressure (b_o=0.00) with growth (Kurth and Kier, 2014). A similar trend was also found for the scaling of maximal pressure production. Again, the largest pressures exerted in the coelomic cavity occurred in the largest earthworms during circumferential and longitudinal muscle contraction (b=0.213 and 0.166 for circumferential and longitudinal muscles, respectively, b_o=0.00). (Fig. 5.4)

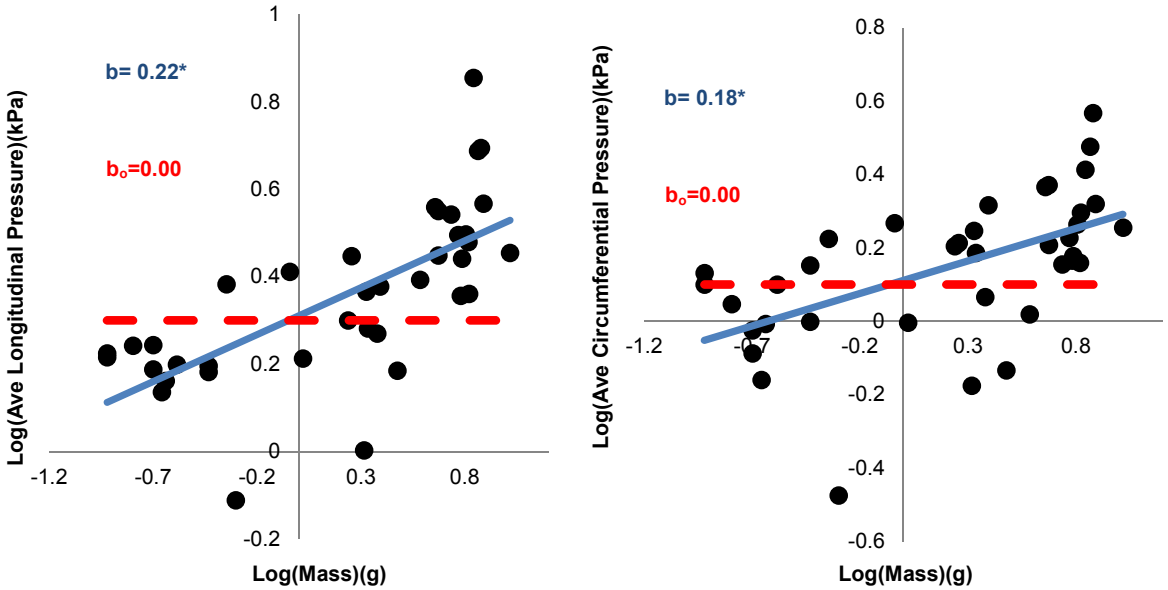

Figure 5.3: Scaling of average pressures from longitudinal muscle (left) and circumferential muscle (right) contractions. The expected scaling exponent (b_o) is the dashed line. The measured scaling exponent (b) fit to data with OLS regression is the solid line N=38. *Indicates non-overlapping 95% confidence with the b_o.

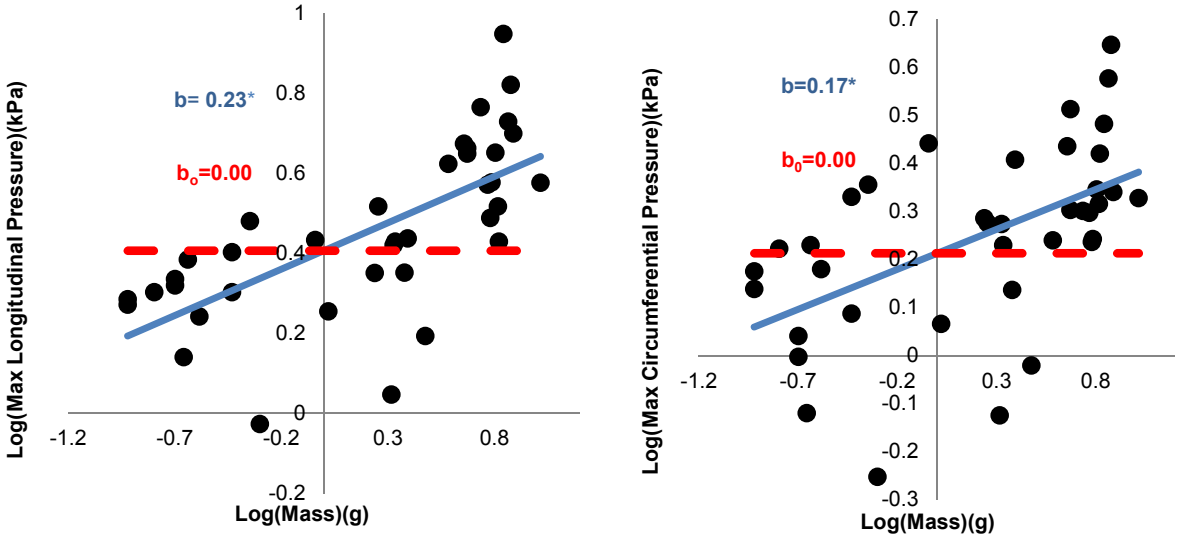

Figure 5.4: Scaling of maximal pressures from longitudinal muscle (left) and circumferential muscle (right) contractions. The expected scaling exponent (b_o) is the dashed line. The measured scaling exponent (b) fit to data with OLS regression is the solid line N=38. *Indicates non-overlapping 95% confidence with the b_o.

I also found average and maximal forces scaled differently than expected (Fig. 5.5). Average longitudinal muscle forces increased at a greater rate than predicted (b=0.76, b_o=0.69), but the differences were not significant. Average circumferential muscle force production also increased at a greater rate than predicted, and this difference was statistically significant (b=0.78, b_o=0.62).

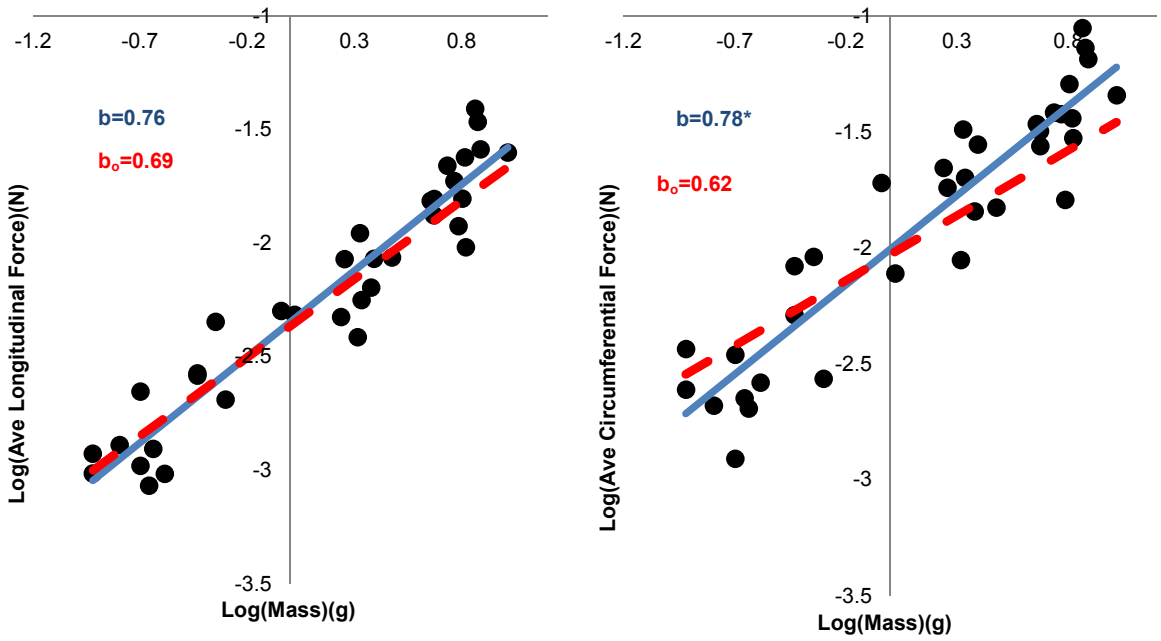

Figure 5.5: Scaling of average force production from longitudinal muscle (left) and circumferential muscle (right) contractions. The expected scaling (b_o) exponent is the dashed line. The measured scaling exponent (b) fit to data with RMA regression is the solid line. N=35. *Indicates non-overlapping 95% confidence with b_o.

Likewise, the scaling of maximal forces were significantly higher than predicted for both muscle sets (Fig. 5.6) (b=0.77 and b_o=0.69 for the longitudinal muscles; b=0.76 and b_o=0.62 for the circumferential muscles), and showed similar scaling exponents to the scaling of average force production (b=0.76 and 0.77 for average and maximal longitudinal muscle forces, respectively; 0.78 and 0.76 for average and maximal circumferential muscle forces, respectively).

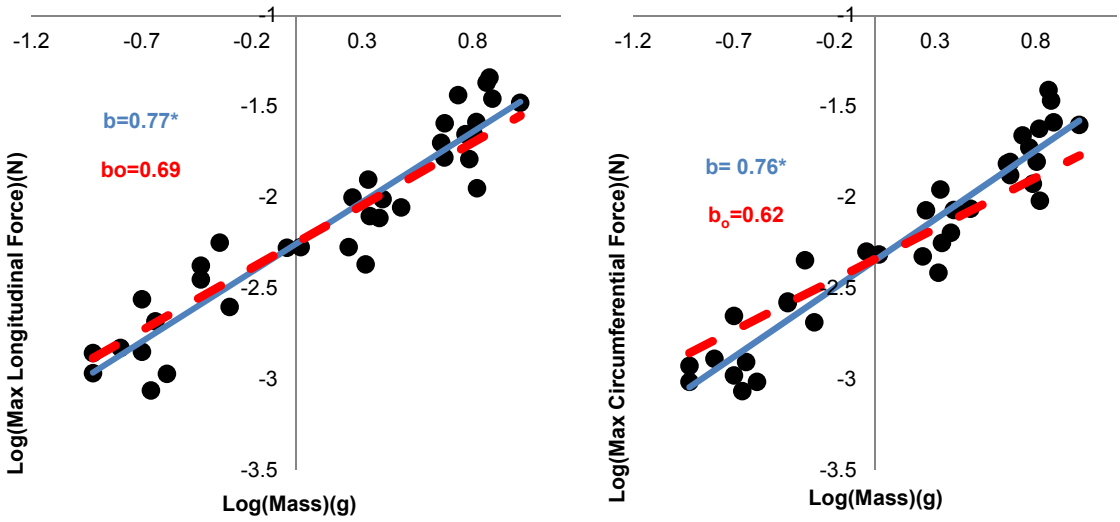

Figure 5.6: Scaling of maximal force production from longitudinal muscle (left) and circumferential muscle (right) contractions. The expected scaling (b_o) exponent is the dashed line. The measured scaling exponent (b) fit to data with RMA regression is the solid line. N=35. *Indicates non-overlapping 95% confidence with b_o.

Burrowing costs also exhibited unusual trends. Like other forms of locomotion, cost of transport decreased with body size, though the rate of decrease differs from running, swimming, and flying (Fig.5.7). The difference in cost of transport between small and large burrowers was smaller in magnitude (b=-0.29) relative to running, swimming, and flying (b=-0.32, -0.38, and -0.31) (Alexander, 1995; Vogel 2003). The scaling of burrowing cost of transport, however, was not significantly different from running, swimming, or flying due to large variation in the data.

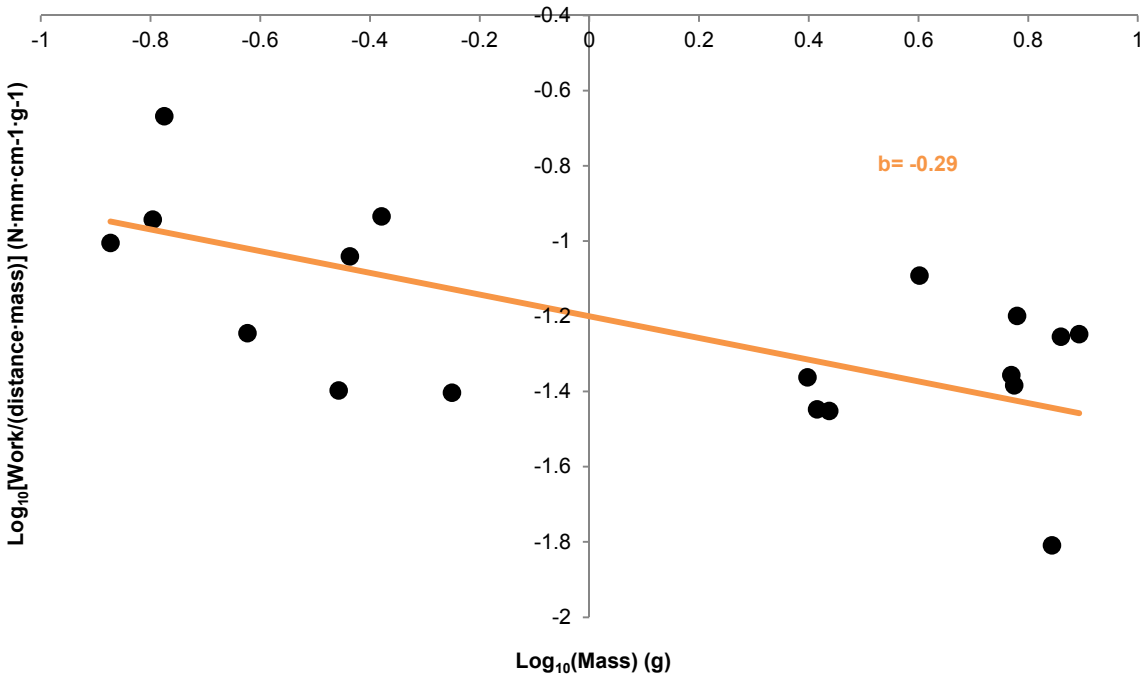

Fig. 5.7: The effects of body size on the cost of burrowing locomotion. **A.** The effect of body size on burrowing cost per distance using work during burrowing. **B.** The effect of size on burrowing cost of transport using work output per distance per mass. N=18.

Discussion

While crawling *L. terrestris* exert similar pressures throughout ontogeny (Quillin, 1998) but the scaling of burrowing pressures changes with body size. As *L. terrestris* worms increase in size, they exert greater burrowing forces and pressures than expected from the scaling of the hydrostatic skeleton alone. These size-related increases in pressures and forces occur during average and maximal pressure and force production. Size-related increases in soil stiffness could explain why larger worms must exert greater pressures during burrowing. If strain hardening occurs in soil, then large worms may experience stiffer soil than small worms simply because large worms must displace a greater volume of soil in order to form a burrow (Chen, 1975; Yong et al., 2012; Holtz et al., 2010). As a result, large worms may need to exert disproportionately high forces and pressures to overcome increases in soil stiffness.

Strain hardening may also explain why the scaling of burrowing forces from this study are much higher than the forces recorded in Quillin, 2000 from *L. terrestris* worms moving through pre-made burrows (b=0.76-0.78 in current study; b=0.43-0.47 in Quillin, 2000). The earthworms in Quillin 2000 did not form burrows, and instead crawled through artificial burrows that had been formed prior to the placement of earthworms. Thus, the earthworms in Quillin 2000 did not displace soil and could not have experienced strain hardening. In comparison, earthworms in this study displaced soil, formed burrows, and could experience strain hardening. Discrepancies in methods could explain the conflicting force data.

In addition to burrowing forces and pressure increasing disproportionately with size, my analysis also suggests that burrowing costs increase with body size at a greater rate than other locomotory forms. Using work as a proxy for metabolic cost, I found that burrowing costs per distance increase with mass at a significantly greater rate than flying and swimming costs. Burrowing costs appear to increase rapidly as burrowers grow, consistent with increases in soil stiffness with burrower size. This preliminary estimate is not ideal, however, as direct measurements of metabolic costs are needed to estimate cost of transport in a manner comparable to previous studies of animal locomotion. In addition the pressure recording experiments and the kinematics experiments were done independently using different earthworms. I combined data from earthworms with similar body masses, but using a single earthworm to collect force and distance data simultaneously would have been preferable to reduce error and variation in the data. Indeed, my cost of transport analysis showed great variation in the data, and despite its lower scaling exponent it was not found to be statistically different than the scaling of other locomotory forms. A more refined cost of transport experiment may reduce such variation and show more definitive results.

Another interesting trend found was related to the relative magnitude of the circumferential and longitudinal muscle forces. Chapman, 1950 had noted the longitudinal musculature in earthworms appeared far larger and more robust than the circumferential muscles. He calculated that the longitudinal muscles were capable of exerting pressures several times larger than that of the circumferential muscles. Yet my data and those data from Quillin 2000 show similar magnitudes of force production during circumferential and longitudinal muscle contraction. While maximal longitudinal pressure and force production was higher than maximal circumferential force production, the difference was not nearly as great as Chapman 1950 suggested. While it is not clear why this discrepancy exists, one possibility is simply that the longitudinal muscles rarely produce maximal force; if they did and were not supported radially by a well consolidated burrow, the animal would risk rupturing its body (Chapman, 1950). In my experiments the worms burrowed in soil with bulk densities similar to those typically found in the first few centimeters of forest soil, but *L. terrestris* is capable of burrowing as deep as 1-2 meters below the soil's surface (Gerard, 1969). It is possible that the longitudinal muscles play an increasingly important role with increase in burrowing depth and soil compaction and density. It has been noted that the longitudinal muscles are vital for burrowing in order to displace soil away, anchor the worm during burrowing, and break up soil particles ahead of the worm (Seymour, 1969; Keudel and Schrader, 1999). Thus, as the worm burrows further down, the longitudinal muscles may be required to exert greater and greater forces in order to successfully displace soil. Additional experiments with soil of greater density would be helpful in exploring this possibility.

My results highlight the potential complexities and constraints of burrowing behavior. The fact that larger worms exert higher pressures and forces than predicted by the morphology

alone suggest they must overcome a disproportionately larger increase in soil resistance relative to their smaller counterparts. Considering the vast array of burrowing animals, the question arises: Do other burrowing animals show similar size-dependent changes in burrowing mechanics? If strain hardening is responsible for the trends observed in this study, it would likely affect other soft-bodied burrowers because most use a similar burrowing mechanism that employs a dual anchoring system (Trueman, 1975). Strain hardening could also affect hard-bodied burrowers as well, since larger hard-bodied burrowers must push, pull, and scrape away a larger volume of soil in order to excavate a burrow relative to their smaller counterparts. At the least, strain hardening may make it more difficult for larger hard-bodied burrowers to insert their bulkier limbs into the soil. Additional studies would be useful to determine if larger burrowers across taxa and soil types consistently exert disproportionately larger pressures, forces, and burrowing costs relative to their smaller counterparts. More research would also be useful to explore the presence and propensity of strain hardening in soils and more directly link burrowing mechanics to soil properties.

CHAPTER 6: CONCLUSIONS AND FUTURE DIRECTIONS

Major Findings

My studies have several overarching findings with broad significance to biomechanics, ecology, and evolution. First, I found that the hydrostatic skeleton of earthworms does not maintain isometry during growth. Instead, I found the length, diameter and muscle cross-sectional area of *L. terrestris* to grow allometrically throughout ontogeny. These changes in skeletal proportions with body size alter mechanical advantage and force production as the animal grows. I also found that the scaling of the hydrostatic skeleton differs based on ecological context. Surface-dwelling earthworms exhibited differences in the scaling of the hydrostatic skeleton relative to burrowing earthworms. Differences in selective pressures and musculoskeletal adaptations are likely causes of the morphological differences between the two ecotypes.

One selective pressure that may influence the scaling of burrowing earthworms is strain hardening in terrestrial soils. Strain hardening can occur in loose granular soils and consolidated clays, and causes the stiffness of the soil to increase with increasing strain (Chen, 1975; Yong et al., 2012; Holtz et al., 2010). This phenomenon poses a problem for growing earthworms. As an earthworm grows it must radially displace greater volumes of soil, and will experience progressively stiffer soil as a consequence. I documented the effects of strain hardening in large but not small earthworms using inflatable robotic worms, and I discovered that burrowers become relatively thinner and exert disproportionately larger radial forces as they grow, perhaps in response to this effect.

Strain hardening may also be responsible for the size-related differences found in burrowing kinematic and mechanics. I found adult earthworms to exert disproportionately larger forces while burrowing yet they burrow more slowly than their smaller counterparts. In the case of burrowing earthworms, being bigger may be detrimental to locomotion.

Significance

My results have academic and practical implications in several major scientific fields. I have extended knowledge in the field of locomotion by documenting an exception to the general rule that larger animals are faster than smaller animals (Schmidt-Nielsen, 1984; Alexander, 2003). I found that the positive trend between speed and body size can be negated by the scaling of physical constraints. In this particular case, soil resistance increases with burrower size, which caused earthworms that exhibited a typical positive size/speed trend during crawling to display a trend reversal underground. It is possible that these aforementioned results reflect a larger pattern in burrowing locomotion whereby smaller burrowers are faster and more effective, but additional research is needed (Che and Dorgan, 2010).

These results also have interesting morphological implications. I found that, contrary to prior studies (Quillin, 1998; Quillin, 1999), the hydrostatic skeleton of soft-bodied invertebrates exhibits allometry. The reasons for such allometry are likely linked to the ecological context of the animal, as well as physical and evolutionary pressures. For example, surface dwelling and burrowing earthworms both exhibit allometry, but the patterns of allometry differ between the two ecotypes. Since burrowers and surface-dwellers likely experience different physical constraints and environmental pressures, it is perhaps not surprising their skeletons have adapted and developed in different ways. It is not known how other soft-bodied invertebrates scale (e.g.

anemones, holothurians, hirudineans, etc.) and studying these scaling effects further may provide important insight into the challenges these animals face and their adaptations.

The field of robotics may also benefit from this research. The creation of soft-bodied robots has shown great potential in terms of navigating confined and/or variable environments (Kim et al., 2013). Soft-bodied invertebrates such as earthworms and caterpillars have provided an important source of biomimetic inspiration for the design and construction of these soft robots (Trimmer, 2008; Trivedi et al., 2008). One capability that has not yet been attempted, however, is burrowing. This is surprising considering the multitude of soft invertebrates that are capable of burrowing. Soft burrowing robots may be advantageous over current burrowing machinery for several reasons. For example, thin worm-like robots may burrow with less resistance than current digging equipment by minimizing strain hardening effects in soil. Another such advantage of an 'earthworm-like' burrowing machine is that it negates the need to bring soil to the surface during burrow excavation. Earthworm-like robots would simply need to displace the soil away radially in order to form a burrow. Soft burrowing robots also would not require the replacement of hard parts over time, since components such as drills or spades would not be required in order to burrow. It also may be easier to alter burrowing directions underground due to the flexible nature of the robot.

There also may be ecological and evolutionary interest in this work. According to the phylogeny presented in Chapter 4, burrowing has evolved independently multiple times. It appears the switch from surface dwelling to burrowing, and vice versa, has occurred often. This may indicate that the adaptations required to switch between ecotypes are not mechanistically complex and can be reversed. I also found evidence for ecotype differences in other environmental pressures not explicitly studied in this thesis (e.g. dessication, predation,

respiration, reproduction). Since earthworms are of agricultural interest, further work is needed to understand what ecological pressures exert the greatest influence on earthworm abundance across species and ecotypes.

Future Directions

Key aspects of this research (e.g. strain hardening, the effects of body size on burrowing mechanics, the scaling of the hydrostatic skeleton) may impact a wide array of organisms. For example, strain hardening in soils may impact numerous soft-bodied and hard-bodied burrowers over a range of body size. It is also possible burrowing animals have evolved various features to mitigate strain hardening effects beyond those traits discussed here.

It would also be interesting to explore the characteristics of the soil that are responsible for strain hardening during burrowing. Strain hardening has classically been reported in loose granular soils and consolidated clays (Yong et al., 2011). This means environments with substrates like sand, silt, gravel, clay, and clayey loam may also exhibit strain hardening. I only focused my research on loamy terrestrial soils with bulk densities and moisture contents typical of forest topsoils (Adams and Froehlich, 1981; Chanasyk and Naeth, 1995; Davidson et al., 1998; Davidson et al., 2000). There are a diversity of other terrestrial and aquatic environments in which burrowers occur; do they also experience strain hardening? If so, under what conditions?

The construction of a burrowing worm-like robot has not yet occurred, yet such a robot may have a variety of interesting applications. The actions of burrowing earthworms in nature improve a variety soil properties, including: water infiltration, soil aeration, and soil de-compaction. In addition to the benefits mentioned above (see “Significance”), the construction of

burrowing worm-like robots may prove far more effective at maintaining soil quality than current tillage and aeration equipment. Soil tillage, for example, is used indiscriminately on soil plots and has been detrimental to native soil-dwelling creatures (Chan, 2001). A single worm-like robot could target specific areas in the soil while minimizing detrimental effects on soil-dwelling creatures. Soil aerating equipment tends to impact the first few inches of soil, while earthworms' burrows can extend up to two meters below the soil surface (Edwards and Bohlen, 1996). If a biomimetic burrowing worm robot can effectively match the burrowing actions of their biological counterparts, water infiltration, soil tillage, and soil aeration could become much more effective.

Studying the scaling of other burrowing organisms may also be useful in uncovering additional size-related changes in burrowing mechanics, burrowing adaptations and soil constraints. Most scaling studies on burrowing have focused on soft invertebrates (e.g. Quillin, 2000; Che and Dorgan 2010; Kurth and Kier, 2014), yet many hard-bodied invertebrates and vertebrates burrow as well. The scaling studies that have been performed on hard-bodied burrowing animals (e.g. McNab, 1979; De La Huz t al., 2002; Xu et al., 2014) have not linked the scaling of the musculoskeletal system to changes in burrowing mechanics /soil constraints with body size. It is currently unclear what, if any, allometries in growing hard-bodied burrowers exist as size-related burrowing adaptations. We may glean additional information on burrowing biomechanics by taking size into account in a wider array of burrowing animals.

It may also be useful to compare the scaling of the hydrostatic skeleton in other animals. Doing so could uncover additional physical constraints that hydrostatic skeletons encounter in other environments, and reveal how the skeleton compensates for these constraints. It is likely that the hydrostatic skeletons of marine invertebrates scale in significantly different ways than

terrestrial hydrostatic skeletons. For example, marine hydrostats are physically supported by buoyancy in the surrounding water, whereas terrestrial hydrostats are not. Because of this, marine hydrostats may grow much larger than terrestrial hydrostats. Marine hydrostats also must contend with greater viscosity and drag forces than terrestrial burrowers. As a result, only marine burrowers may alter body shapes with growth to minimize size-induced increases in drag. Within marine animals, marine burrowers may scale differently from swimmers, and swimmers may scale differently from surface crawlers. Even within burrowers, there may be scaling differences that are dependent on the substrate experienced by a given burrower. A great deal is known about how hard skeletons scale (e.g. Schmidt-Nielsen, 1984; Vogel, 2003; Biewener, 2005), but much additional work is needed on the scaling of the hydrostatic skeletons that many invertebrates species employ.

REFERENCES

Abdalla, A. M., Hettiaratchi, D. R. P., and Reece, A. R. (1969). The mechanics of root growth in granular media. *J. Agr. Eng. Res.*, **14**, 236-248.

Adams PW, Froehlich HA (1981). *Compaction of Forest Soils*. USDA Pacific Northwest Ext Pub PNW 217. Corvallis: Oregon State University

Alexander, R. McN.(1995). Hydraulic mechanisms in locomotion. *Body Cavities: Function and Phylogeny. Selected Symposia and Monographs UZI* **8,** 187-198.

Alexander, R. McNeill. (2003). *Principles of animal locomotion*. New Jersey: Princeton University Press.

Anqi, L., Bingcong, R. L. C., and Xangxu, C. (1990). Constitution and mechanism analysis of reducing soil adhesion for the body surface liquid of earthworms. *Transactions of the Chinese Society of Agricultural Engineering*, **3**, 001.

Arthur, D. (1965). Form and function in the interpretation of feeding in lumbricid worms. *View. Biol.* **4,** 204-251.

Barnett, C. M., Bengough, A. G., & McKenzie, B. M. (2009). Quantitative image analysis of earthworm-mediated soil displacement. *Biol. Fert. Soils*. **45**, 821-828.

Berry, E. and Jordan, D. (2001). Temperature and soil moisture content effects on the growth of *Lumbricus terrestris* (Oligochaeta: Lumbricidae) under laboratory conditions. *Soil. Biol. Biochem.* **33,** 133-136.

Biewener, A. A. (2005). Biomechanical consequences of scaling. *J. Exp. Biol.* **208,** 1665-1676.

Bouché, M. B. (1977). Strategies lombriciennes. *Ecol. Bull*. 122-132.

Burch, S. W., Fitzpatrick, L. C., Goven, A. J., Venables, B. J. and Giggleman, M. A. (1999). In vitro earthworm *Lumbricus terrestris* coelomocyte assay for use in terrestrial toxicity identification evaluation. *Bull. Environ. Contam. Toxicol.* **62,** 547-554.

Chan, K. Y. (2001). An overview of some tillage impacts on earthworm population abundance and diversity—implications for functioning in soils. *Soil Till. Res*. **57**, 179-191.

Chan, K. Y., and Barchia, I. (2007). Soil compaction controls the abundance, biomass and distribution of earthworms in a single dairy farm in south-eastern Australia. *Soil Till. Res.* **94**, 75-82.

Chapman, G. (1950). Of the movement of worms. *J. Exp. Biol.* **27,** 29-39.

Chapman, G. (1958). The hydrostatic skeleton in the invertebrates. *Biol. Rev.* **33,** 338-371.

Chanasyk, D. S. and Naeth, M. A. (1995). Grazing impacts on bulk density and soil strength in the foothills fescue grasslands of Alberta, Canada. *Can. J. Soil Sci*. **75,** 551-557.

Che, J. and K. M. Dorgan. (2010). It's tough to be small: dependence of burrowing kinematics on body size. *J. Exp. Biol.* **213,** 1241-1250.

Chen, W. (1975). Limit analysis and soil plasticity, Development in Geotechnical Engineering.

Chi, K. J. and Roth, V. L. (2010). Scaling and mechanics of carnivoran footpads reveal the principles of footpad design. *J. R. Soc. Interface* **49**, 1145-55

Clark, R. B. (1967). *Dynamics in metazoan evolution: the origin of the coelom and segments.* Clarendon Press.

Daltorio, K. A., Boxerbaum, A. S., Horchler, A. D., Shaw, K. M., Chiel, H. J. and Quinn, R. D. (2013). Efficient worm-like locomotion: slip and control of soft-bodied peristaltic robots. *Bioinspir. Biomim.* **8**, 1-23.

Darwin, C. (1881). *The formation of vegetable mould: through the action of worms, with observations on their habits***.** London: John Murray**.**

Davidson, E., Belk, E., and Boone, R. D. (1998). Soil water content and temperature as independent or confounded factors controlling soil respiration in a temperate mixed hardwood forest. *Global change biology* **4**, 217-227.

Davidson, E. A., Verchot, L. V., Cattânio, J. H., Ackerman, I. L. and Carvalho, J. (2000). Effects of soil water content on soil respiration in forests and cattle pastures of eastern Amazonia. *Biogeochemistry* **48**, 53-69.

Davies, R., & Moyes, C. D. (2007). Allometric scaling in centrarchid fish: origins of intra-and inter-specific variation in oxidative and glycolytic enzyme levels in muscle. *J. Exp. Biol*. **21**, 3798-3804.

De la Huz, R., Lastra, M., & López, J. (2002). The influence of sediment grain size on burrowing, growth and metabolism of *Donax trunculus* L.(Bivalvia: Donacidae). *Journal of Sea Research*. **47**, 85-95.

Dorgan, K. M., Jumars, P. A., Johnson, B., Boudreau, B. and Landis, E. (2005). Burrowing mechanics: Burrow extension by crack propagation. *Nature* **433,** 475-475.

Dorgan, K. M., Arwade, S. R. and Jumars, P. A. (2007). Burrowing in marine muds by crack propagation: kinematics and forces. *J. Exp. Biol.* **210,** 4198-4212.

Dorgan, K. M., Arwade, S. R. and Jumars, P. A. (2008). Worms as wedges: Effects of sediment mechanics on burrowing behavior. *J. Mar. Res.* **66,** 219-254.

Dorgan, K. M., Lefebvre, S., Stillman, J. H., & Koehl, M. A. R. (2011). Energetics of burrowing by the cirratulid polychaete *Cirriformia moorei*. *J. Exp. Biol*. **214**, 2202-2214.

Dorgan, K. M., Law, C. J., & Rouse, G. W. (2013). Meandering worms: mechanics of undulatory burrowing in muds. *Proceedings of the Royal Society B: Biological Sciences*. **280,** 20122948.

Edwards, C. A., and Bohlen, P. J. (1996). *Biology and ecology of earthworms*. 3rd ed. London: Chapman and Hall.

Ehlers, W. (1975). Observations on earthworm channels and infiltration on tilled and untilled loess soil. *Soil Sci*. **119**, 242-249.

Felsenstein, J. (1985). Phylogenies and the Comparative Method. *Am. Nat.* **125,** 1-15.

Gerard, B. (1967). Factors affecting earthworms in pastures. *J. Anim. Ecol.* **36**, 235-252.

Gibson, R. N., Atkinson, R. J. A., & Gordon, J. D. M. (2006). Macrofaunal burrowing: the medium is the message. *Oceanography and Marine Biology: an annual review*. **44**, 5-121.

Grafen, A. (1989). The phylogenetic regression. *Phil. T. Roy. Soc. B* **326***,* 119-157.

Gray, J. & Lissman, H. W. (1938). Studies in animal locomotion. VI I. Locomotory reflexes in the earthworm. *J. of Exp. Biol.* **15,** 506-517.

Hagerty, M. M., Hite, D. R., Ullrich, C. R., & Hagerty, D. J. (1993). One-dimensional high-pressure compression of granular media. *Journal of Geotechnical Engineering*. **119**, 1-18.

Heins, D. C., Baker, J. A. and Guill, J. M. (2004). Seasonal and interannual components of intrapopulation variation in clutch size and egg size of a darter. *Ecol. Freshwat. Fish* **13,** 258-265.

Herrel, A. and O'Reilly, J. C. (2006). Ontogenetic Scaling of Bite Force in Lizards and Turtles. *Physiol. Biochem. Zool.* **79,** 31-42.

Hill, R.W., Wyse, G.A., Anderson, M. (2008). *Animal Physiology*. 2nd Ed. Massachusetts: Sinauer Associates

Holtz, R. D., Kovacs, W. D., Sheahan, T. C. (2010). *Introduction to Geotechnical Engineering*, Upper Saddle River, New Jersey: Prentice Hall.

Hunter, R. D., & Elder, H. Y. (1989). Burrowing dynamics and energy cost of transport in the soft-bodied marine invertebrates *Polyphysia crassa* and *Priapulus caudatus*. *J. Zool*., **218**, 209-222.

Huntington, T. G., Johnson, C. E., Johnson, A. H., Siccama, T. G., and Ryan, D. F. (1989). Carbon, organic matter, and bulk density relationships in a forested Spodosol. *Soil Science*, **148,** 380-386.

Huxley, J. S. and G. Tessier. (1936). Terminology of relative growth. *Nature* **137**, 780-781.

Inouye, L. S., Jones, R. P. and Bednar, A. J. (2006). Tungsten Effects on Survival, Growth, and Reproduction in the Earthworm, *Eisenia Fetida*. *Environ. Toxicol. Chem.* **25,** 31-31.

Keudel, M. and S. Schrader. (1999). Axial and radial pressure exerted by earthworms of different ecological groups. *Biol. Fert. Soil.s* **29,** 262-269.

Kier, W. M. (2012). The diversity of hydrostatic skeletons. *J. of Exp. Biol.* **215,** 1247-1257.

Kier, W. M. and Smith, K. K. (1985). Tongues, tentacles and trunks: the biomechanics of movement in muscular-hydrostats. *Zool. J. Linn. Soc.* **83,** 307-324.

Kim, S., Laschi, C., & Trimmer, B. (2013). Soft robotics: a bioinspired evolution in robotics. *Trends in biotechnology*. **31**, 287-294.

Kurth, J. A. and Kier, W. M. (2014). Scaling of the hydrostatic skeleton in the earthworm *Lumbricus terrestris*. *J. Exp. Biol.* **217,** 1860-1867.

Lambe, T. W., & Whitman, R. V. (1969). *Soil mechanics, Series in soil engineering*. New Jersey: John Wiley & Sons.

Lang, S. A., Garcia, M. V., James, S. W., Sayers, C. W., & Shain, D. H. (2012). Phylogeny and clitellar morphology of the giant Amazonian Earthworm, *Rhinodrilus priollii* (Oligochaeta: Glossoscolecidae). *The American Midland Naturalist*. **167**, 384-395.

Legendre, P. (2011). lmodel2: Model II Regression. R package version 1.7-0. http://CRAN.R-project.org/package=lmodel2

Lin, H., Slate, D. J., Paetsch, C. R., Dorfmann, A. L. and Trimmer, B. A. (2011). Scaling of caterpillar body properties and its biomechanical implications for the use of a hydrostatic skeleton. *J. Exp. Biol.* **214,** 1194-1204.

López-DeLeón, A. and Rojkind, M. (1985). A simple micromethod for collagen and total protein determination in formalin-fixed paraffin embedded sections. *J. Histochem. Cytochem.* **33**, 737–743.

Maginnis, T. L. (2006). The costs of autotomy and regeneration in animals: a review and framework for future research. *Beh. Ecol*. **17**, 857-872.

Martins, E. P. and Garland Jr, T. (1991). Phylogenetic analyses of the correlated evolution of continuous characters: a simulation study. *Evolution* **45,** 534-557.

McKenzie, B. M. and Dexter, A. R. (1988). Radial pressures generated by the earthworm *Aporrectodea rosea*. *Biol. Fert. Soils* **5,** 328-332.

McNab, B. K. (1979). The influence of body size on the energetics and distribution of fossorial and burrowing mammals. *Ecology*. **60**, 1010-1021.

Molles, M. C. (2010). *Ecology: concepts & applications.* 5th Ed. NY: McGraw-Hill

Newell, G. E. (1950). The role of the coelomic fluid in the movements of earthworms. *J Exp Biol*. **27**, 110-122.

Niven, J. E., & Scharlemann, J. P. (2005). Do insect metabolic rates at rest and during flight scale with body mass? *Biol. Lett.* **1,** 346-349.

Nudds, R. L. (2007). Wing-bone length allometry in birds. *J. Avian Biol.* **38,** 515-519.

Paradis, E., Claude, J. and Strimmer, K. (2004). APE: analyses of phylogenetics and evolution in R language. *Bioinformatics* **20**, 289-290.

Pérez-Losada, M., Bloch, R., Breinholt, J. W., Pfenninger, M. and DomÃnguez, J. (2012). Taxonomic assessment of Lumbricidae (Oligochaeta) earthworm genera using DNA barcodes. *Eur. J. Soil Biol.* **48,** 41-47.

Piearce, T. G. (1983). **Functional morphology of lumbricid earthworms, with special reference to locomotion**. *J. Nat. Hist.* **17,** 95-111.

Presley, M. L., McElroy, T. C. and Diehl, W. J. (1996). Soil moisture and temperature interact to affect growth, survivorship, fecundity, and fitness in the earthworm *Eisenia fetida*. *Comp. Biochem. Physiol., A: Comp. Physiol.* **114,** 319-326.

Ownby, D. R., Galvan, K. A. and Lydy, M. J. (2005). Lead and zinc bioavailability to *Eisenia fetida* after phosphorus amendment to repository soils. *Environ. Pollut.* **136,** 315-321.

Quillin, K. J. (1998). Ontogenetic scaling of hydrostatic skeletons: geometric, static stress and dynamic stress scaling of the earthworm *Lumbricus terrestris*. *J. Exp. Biol.* **201,** 1871-1883.

Quillin, K. J. (1999). Kinematic scaling of locomotion by hydrostatic animals: ontogeny of peristaltic crawling by the earthworm *Lumbricus terrestris*. *J. Exp. Biol.* **202,** 661-674.

Quillin, K. J. (2000). Ontogenetic scaling of burrowing forces in the earthworm *Lumbricus terrestris*. *J. Exp. Biol.* **203,** 2757-2770.

R Development Core Team. (2013). *R: A Language and Environment for Statistical Computing*. Vienna, Austria.

Rayner, J. M. V. (1985). Linear relations in biomechanics: the statistics of scaling functions. *J. Zool.* **206,** 415-439.

Roberts, B. L., and Dorough, H. W. (1985). Hazards of chemicals to earthworms. *Environ. Toxicol. Chem.* **4**, 307-323.

Roots, B. I., and Phillips. R. R. (1960). Burrowing and the action of the pharynx of earthworms. *Medical & biological illustration* **10**, 28-31.

Schmidt-Nielsen, K. (1984). *Scaling, why is Animal Size So Important?* United Kingdom: Cambridge University Press

Schmidt-Nielsen, K. (1997). *Animal Physiology: Adaptation and Environment,* 5th Ed. Cambridge: Cambridge University Press.

Seymour, M. K. (1969). Locomotion and coelomic pressure in *Lumbricus terrestris*. *J. Exp. Biol.* **51,** 47-58.

Sims, R. W. and Gerard, B. M. (1985). *Earthworms: Keys and Notes for the Identification and Study of the Species*. London: Brill Archive.

Smith, K. A. (2000). *Soil and Environmental Analysis: Physical Methods, Revised, and Expanded,* 2nd Ed. London: CRC Press.

Snelling, E. P., Seymour, R. S., Matthews, P. G., Runciman, S., & White, C. R. (2011). Scaling of resting and maximum hopping metabolic rate throughout the life cycle of the locust *Locusta migratoria*. *J. Exp. Biol.* **214,** 3218-3224.

Stöver, B. C. and Müller, K. F. (2010). TreeGraph 2: combining and visualizing evidence from different phylogenetic analyses. *BMC Bioinformatics* **11,** 7.

Swenson, N. G. (2009). Phylogenetic resolution and quantifying the phylogenetic diversity and dispersion of communities. *PLoS One* **4,** e4390.

Trevor, J. H. (1976). The burrowing activity of *Nephtys cirrosa* Ehlers (Annelida: Polychaeta). *J. Exp. Mar. Biol. Ecol*. **24**, 307-319.

Trevor, J. H. (1978). The dynamics and mechanical energy expenditure of the polychaetes *Nephtys cirrosa*, *Nereis diversicolor* and *Arenicola marina* during burrowing. *Estuar. cstl mar. Sci*. **6**, 605–619.

Trimmer, B. A. (2008). New challenges in biorobotics: Incorporating soft tissue into control systems. *Appl Bionics Biomech* **5**, 119-126.

Trivedi, D., Rahn, C. D., Kier, W. M. and Walker, I. D. (2008). Soft robotics: Biological inspiration, state of the art, and future research. *Applied Bionics and Biomechanics* **5,** 99-117.

Trueman, E. R. (1966). Observations on the burrowing of *Arenicola marina*. *J. Exp. Biol*. **44**, 93-118.

Trueman, E.R. (1975). *The Locomotion of Soft-bodied Animals*. New York: American Elsevier Publishing Company, Inc.

Vogel, S. (1988). *Life's devices: The physical world of animals and plants*. New Jersey: Princeton University Press.

Vogel, S. (2003). *Comparative biomechanics: life's physical world*. New Jersey: Princeton

Whalley, W. R., and Dexter, A. R. (1994). Root development and earthworm movement in relation to soil strength and structure. *Arch. Agron. Soil Sci.*, **38**, 1-40.

Whiteley, G.M., and Dexter, **A. R.** (1981) The dependence of soil penetrometer pressure on penetrometer size. *Journal of Agricultural Engineering Research.* **26,** 467–476.

Xu, L., Snelling, E. P., & Seymour, R. S. (2014). Burrowing energetics of the Giant Burrowing Cockroach Macropanesthia rhinoceros: An allometric study. *Journal of insect physiology.* **70**, 81-87.

Yapp, W. B. (1956). Locomotion of worms. *Nature* **177,** 614-615.

Yong, R. N., Nakano, M. and Pusch, R. (2011). *Environmental soil properties and behavior*. Florida: CRC Press Llc.